Zhongqiang Lin

Education

2010- 2015 **Ph.D. Pharmaceutical Sciences** (GPA: 3.9, Conferred July 2015)

School of Pharmacy, University of Maryland Baltimore

- Thesis: Extended Release Formulation Investigations on Ethylcellulose curing; Thesis advisor: Prof. Stephen W Hoag
  - Developed innovative methods to tests films' vapor permeability and invented a new way to quantify the extent of film coalescence during curing process
  - Used physical properties with Near Infrared Spectroscopy (NIR) and chemometric tools to model films' physical properties
  - Prepared multiparticulate coated beads and analyzed the release mechanism with a model drug

2010 **Master in Chemistry,** (First Class Honor, GPA: 4.0 equiv.), **Oxford University, Oxford, UK**

- Masters thesis: *Using Ring Closing Metathesis to stabilize and improve bioactivity of synthetic peptides*. Advisor: Prof. Benjamin G Davis. Project used techniques: Solid Phase Peptide Synthesis (SPPS) using Liberty^{TM} system; HPLC for peptide purification; Circular Dichroism (CD) spectroscopy for determination of peptide secondary structures; organic synthesis.

2009 **BSc in Chemistry,** (First Class Honor, GPA: 4.0 equiv.), **Oxford University, Oxford, UK**

- Jesus College Scholar (Open Scholarship and Thomas William Thomas Scholarship: based on academic excellence)

2004- 2006 **Dauntsey's School, UK**

- Five A- Levels: Mathematics (A), Further Mathematics (A), Physics (A), Chemistry (A), Chinese (A)

Professional Experience

2013- 2014 **School of Pharmacy, University of Maryland, Baltimore, MD**

- Taught and demonstrated the fluid bed coating and pan coating processes for biannual short course 'Tablets & Capsules Hands-On Short Course' organized by the school of pharmacy
- Hands-on GMP manufacturing projects included: fish oil capsules; solid oral immediate release capsules; sublingual protein filmstrips; scaling- up of placebo cough syrup. Prepared GMP manufacturing and release documents. Performed stability and release tests for manufactured products.
- Assisted in preparing the CMC documents of an Investigational New Drug (IND) filing to US FDA.

May- Aug, 2013 **Intern, Oral Drug Products, Manufacturing Science and Technology, Abbvie Inc, North Chicago, IL**

- Prepared solid oral extended release dosage forms; Evaluated relationship

between in vitro dissolution and in vivo performance

- Skills acquired: Tablet preparation using wet granulation, HPLC and dissolution test

May- Aug, 2012 **Intern, Oral Drug Products, Manufacturing Science and Technology, Abbvie Inc,**

North Chicago, IL

- Developed a new solvent-free manufacturing process of a marketed extended release solid dosage formulation using Hot Melt Extrusion technique
- Skills acquired: hot melt granulation through extrusion, dissolution, ion chromatography, DSC and stability tests

Jun- Aug, 2008 **Summer Student, Institute of Cancer Therapeutics, University of Bradford, UK**

- Synthesis of tetrahydroisoquinoline analogues using transition metal catalysis (Sponsor: Merck UK)

Coursework, Knowledge and Skills

- Courses: Drug Discovery and development; Pharmaceutical Formulation and Unit Operations; Bioanalytical Methods; Transporters and Metabolism; Biostatistics; Regression Analysis Pharmacokinetics; Modern Drug Delivery; FOSS XDS NIR systems; Polymer Physics; Heat and Mass Transfer
- Process and Analytical Skills: proficient in pharmaceutical processes including: coating, wet granulation, tableting, hot melt extrusion. Analytical: NIR chemometric modeling, HPLC, GC, dissolution and disintegration tests, mechanical evaluation of products.
- IT and software skills: SAS, PLS Toolbox, Chemdraw, iMovie, Photoshop

Awards

- Excipient Graduate Student Scholarships, (International Pharmaceutical Excipient Council, Americas Foundation, 2014)
- Merit Student Award, (School of Pharmacy, University of Maryland, 2014)
- Travel Fellowship, (International Diffuse Reflectance Conference, 2014)
- President's Commendation: 'Outstanding Contribution of Student Organization', (University of Maryland Baltimore 2012)
- First Prize Abbvie Intern Business Case Competition (Abbvie Inc, 2012)

Publication

- Z. Lin, D. Zhou, S. Hoag and Y. Qiu, Understanding of In Vitro Release and Its Link with Product Design, In Vivo Performance and Biowaiver Regulations of Oral Extended Release Dosage Forms, *In Preparation.*
- Z Lin, B. Carlin, R. Choski and S. Hoag, Study of Aqueous Ethylcellulose Films Curing: Part I: Mechanism and Theory, *In Preparation*
- Z Lin, B. Carlin, R. Choski and S. Hoag, Study of Aqueous Ethylcellulose Films Curing: Part II: Practical Analysis, *In Preparation*

References Available Upon Request

Abstract

Title of Dissertation: Understanding Curing of Ethylcellulose Film Coating And *In Vitro In Vivo* Performance of Oral Dosage Forms With Scientific Regulatory Implications on Biowaiver

Zhongqiang Lin, Doctor of Philosophy, 2015

Dissertation Directed by: Stephen W. Hoag, PhD, Professor, Pharmaceutical Sciences

The aim of this study focus on the extended release formulation on two aspects: the quantification and mechanistic research on pharmaceutical coating curing with a specific focus on how the moisture affect the curing; and in vivo and in vitro release of matrix ER tablets with implications on regulatory biowaiver using marketed products as practical examples. In all cases, it was found that the relative humidity of the environments were more important to reach higher extent of coalescence for EC pseudolatex films and temperature along cannot achieve sufficient polymer coalescence. A quantitative relationship was established that could be used to quantify the extent of coalescence in EC curing to a reasonable accuracy. The NIR spectral data with the tool of chemometrics can enable accurate prediction of physicomechanical properties accurately. Dissolution models demonstrated the release mechanism of EC coated ER multiparticulate was predominately determined by the breaking down of the coating rather than diffusion of drugs through the EC coating layer. Fluoresence anisotropy was found to be useful in the solid system for the first time. By measuring fluorescence anisotropy in the fluorescence

labeled EC films can allow real time monitoring of the curing process. To justify biowaiver, it is essential to understand effects of API properties, formulation design, product characteristics, test method and its *in vivo* relevance. It is therefore concluded that the biowaiver criteria specified in the regulatory guidance should apply only to multiparticulate beaded dosage forms where strengths only differ in the number of beads containing the active moiety.

UNDERSTANDING CURING OF ETHYLCELLULOSE FILM COATING AND IN VITRO IN VIVO PERFORMANCE OF ORAL DOSAGE FORMS WITH SCIENTIFIC REGULATORY IMPLICATIONS ON BIOWAIVER

By
Zhongqiang Lin

Dissertation submitted to the Faculty of the Graduate School of the
University of Maryland, Baltimore in Partial Fulfillment
Of the Requirements for the Degree of
Doctor of Philosophy
2015

This Thesis is dedicated to my family, my parents who supported me through this and never let me doubt my ability to succeed, and to my important friends that provided encouragements over the years. Thank you for everything!

Acknowledgment

I would like to acknowledge all those who had an important contribution to my success throughout the process of obtaining a doctorate in Pharmaceutical Sciences.

This thesis would not have been possible without my advisor and mentor, Dr. Stephen. W. Hoag. It was you who believed in my ability to succeed in this new field for me before I had any pharmacy training from my undergraduate education by recruiting me into your lab and constantly guides me through the journey. I am also really appreciated for all your advice and suggestions in being a better person. Thank you.

I have a special thanks to Dr. Yihong Qiu from Abbvie Inc, who saw my potential in doing pharmaceutical industry related researches and entrusted me with summer internship opportunities to do research under your supervision. I have learnt immensely from you and I enjoyed every minute working in the company. Also, I must thank the colleagues in Abbvie that had helped me tremendously over my stay: Dr. Deliang Zhou and Dr. Donghua Zhu.

I would like to express my gratitude to my dissertation committee members, for their time and guidance over the years: Dr. James Polli; Dr. Jiabei Wang, Dr. Hazem Hassan and Dr. Raafat Fahmy; as well as Dr. Anjan Nan who was my committee member for my comprehensive exam in 2012.

I also need to express my gratitude towards Dr. Stephen Dordunoo for obtaining drug products from overseas for my research; without your help, the research can never be at this current level.

I would like to thank the main financial sponsor for my PhD work from FMC Biopolymers: Dr. Brian Carlin and Dr. Rina Choski. From you two, I had so many great discussions and especially Brian gave me many inspirations on how to evaluate ethylcellulose films.

I would also offer a thank you to Dr. Richard Thompson for the help with fluorescence anisotropy principles and provided guidance how to set up experiments and lent me one filter and one reagent for the experiments.

To all my lab colleagues over the last 5 years: Dr. Hanpin Lim, Dr. Harris Howland Jr, Dr. Bhavesh Kothari, Dr. Ravi Kona, Dr. Ting Wang, Dr. Seon Hepburn, Dr. Ahmed Ashour, Dr. Larisa Wu, Dr. Haibin Qu, Xuelian Zheng, Xiujuan Peng, Heather Boyce, Yuxiang Zhao, Xizhe Gao, Bowen Jiang and Tanvi Deshpande; it has been a great time, I learned many things from each of you, thanks for the help, and I look forward to continuing our careers together in the future.

Finally, with all my love and respect to my parents and important friends that have always been so supportive throughout my journey so that I can reach this stage, you make who I am and I am fully thankful.

Table of Contents

List of Tables

List of Figures

Chapter 4

Chapter 6

List of Abbreviations

AFM	Atomic Force Microscopy
API	Active Pharmaceutical Ingredient
DBS	Dibutyl Sebacate
DMA-DPH	1-(4-dimethylaminophenyl)-6-phenylhexatriene
DVS	Dynamic Vapor Sorption
EB	Erythrosin B
EC	Ethylcellulose
ER	Extended Release
FDA	Food and Drug Administration
HPLC	High Performances Liquid Chromatography
HPMC	HydroxyPropyl MethylCellulose
IVIVC	*In vitro In Vivo* Correlation
IVIVR	*In Vitro In Vivo* Relationship
LH	Low Humidity
MCC	Microcrysalline Cellulose
NIR	Near Infrared
NTI	Narrow Therapeutic Index
PAT	Process Analytical Technology
PCA	Principle Component Analysis
PLS	Partial Least Square
QbD	Quality by Design
RH	Relative Humidity
S/V	Surface to Volume Ratio
SEM	Scanning electron microscopy
SLS	Sodium Lauryl Sulfate
TEC	Triethyl Citrate
TS	Tensile Strength
WVP	Water Vapor Permeability
YM	Young's Modulus

Chapter 1 Introduction

1.1 Extended Release Solid Oral Formulations

Among all the pharmaceutical products, about 84% of the top selling drugs are delivered via oral route and majority of oral medications are solid dosage forms such as tablets capsules[1]. Solid oral dosage forms provide the most convenient user experiences and also allow easy and safe carrying the medications. The even more convenient medication is extended release (ER) solid oral formulations; which has been one of the crucial components of pharmaceutical products. ER falls into a broad realm of modified release where such products have fast onsite of effect and usually has therapeutic effects over a few hours. The main advantage of using such delivery systems is greatly improved patient compliance by reducing the frequency of taking medication but still maintaining the therapeutic effects at the same time[2]. Additional advantages of ER systems also include the reduction of peak-valley concentration fluctuations comparing with Immediate Release (IR) dosage forms and the reduction of toxicity due to overdose. Common extended release formulation systems include but not limit to: diffusion-reservoir systems (coated tablets/beads), matrix tablets; and osmotic pressure controlled systems.

For every ER products, polymers usually played extremely important role that often governs the release performances of drug products. They had various functions such as fillers, binders, filler-binders, controlling rate of release, disintegrant etc. For coating formulations, polymers are applied to the surface of the tablets/multiparticulated beads to achieve a prolonged release rate. However, with nowadays' aqueous coating being the

main stream of coating, it has become a challenge how to cure the film after the insoluble polymers were applied to the core. For matrix ER tablets, two common types of polymers are often come across: those with hydrophilic, soluble polymers such as different grades of hydroxypropyl methylcellulose (HPMC) and those with hydrophobic, insoluble polymers such as polyvinyl acetate (PVA). Based on Higuchi's estimates, the release of matrix hydrophilic active pharmaceutical ingredient (API) with hydrophobic polymer systems can be accurately modeled and predicted[3]. However, with the hydrophilic matrix tablet systems, the releases were hard to predict. This results in the problems that when generic manufacturers trying to produce a generic versions of the brand product, it is hard to justify biowaiver.

Extended release systems with aqueous pseudolatex coating systems and hydrophilic matrix tablets were selected to form the basis of the research investigation in this thesis aiming to gain more in-depth understanding to better understand the problem and propose changes to address corresponding issues.

1.2 Aqueous Pseudolatex Coating

1.2.1 Latex and Pseudolatex Systems in Coating

Film coating is an important process in both pharmaceutical and food operations. In pharmaceutical filed, such operations are usually engineered to give drug products desired properties such as change the aesthetic appearances, taste masking or achieve targeted drug release profiles, improve stability of coated drug product. The coating operations for solid oral dosage forms can be breaking down into generally 2 categories according to usage: functional and non- functional coatings. The non-functional coatings

mainly aim at tweaking the aesthetic appeal and masking the undesired properties such as taste, odor or colors. The non-functional coating also protects Active Pharmaceutical Ingredient (API) gently from the environments such as light, moisture, and oxygen.

Traditionally, pharmaceutical coating operations for extended release formulations were done using organic polymer solutions, where an organic solvent such as ethanol was used to dissolve polymers and then sprayed onto tablets or beads containing API[4, 5]. However, using polymer solutions with solvents such as Dichloromethane or ethanol can be environmentally unfriendly and by storing large amount of such organic solvent in warehouses increase potential damage and risk of unexpected explosions. Another significant disadvantages of using organic solvent were its low solid concentration. By dissolving polymers in organic solvent increases the solution's viscosity dramatically[6]; this would significantly increase the operation time to achieve a desired coating level.

In order to provide a better solution to address the issues, over the last 20 years, latex/pseudolatex systems have been used predominantly in pharmaceutical coating applications[7, 8]. A latex is an aqueous colloidal dispersion of solid polymer particles that is synthesized via emulsion polymerization[9]. The difference between latex and pseudolatex systems lies in the preparation method where pseudolatices are manufactured with polymer molecules whereras latex polymers are synthesized in the aqueous media. The films formed with such systems not only provide the alternative to the solvent coating processes, the use of safer and more environmentally friendly aqueous media also allows them to be easily implemented and prepared. Another practical advantage of

latex/pseudolatex dispersion is relative higher solid concentration but lower viscosity compared to organic polymer solutions.

1.2.2 Commonly Used Polymers in Coating

Coating in pharmaceutical operations often uses various polymers to achieve various goals. And by their applications, coating can therefore be categorized into 3 broad classes: the conventional film coating; modified release polymers and enteric coating polymers (Table 1.1)[10].

The conventional film coating is also termed as 'non-functional' coating, it is used mainly for improving products appearance, handling, preventing dust particles etc. This coating, when applied, do not affect the underlying release of the API. Hence the polymers used are often readily water soluble and easily broken down in the gastrointestinal tract, such as hydroxypropyl methylcellulose (HPMC) and methylcellulose.

The polymers used for modified releases are often insoluble across all physiological pH range. Methacrylate ester cololymers, famously known as Eudragit RS and RL can swell during dissolution and allow water and dissolved drug substance to leak out of the matrix to achieve the modified release function. The enteric coatings polymer can resist acidic environments in stomach and started to break down/solubilize when reaching the upper region of small intestine where the pH is above 5.5.

Table 1.1: The polymer commonly used for film coating

Application Classes	Category	Polymer Name
Polymers for Conventional Film Coating	Cellulose Ethers	Hydroxypropyl methylcellulose (HPMC)
		Methylcellulose (MC)
		Hydroxypropyl cellulose (HPC)
	Acrylic polymers	Poly(butylmethacrylate), (2-dimethylaminoethyl) methacrylate,methylmethacrylate
Polymer For Modified Release	Methacrylate Ester Copolymers	Poly(ethyl acrylate-co-methyl methacrylate-co-trimethylammonioethyl methacrylate chloride) 1:2:0.1
		Poly(ethyl acrylate-co-methyl methacrylate-co-trimethylammonioethyl methacrylate chloride) 1:2:0.2
	Cellulose Derrivatives	Ethylcellulose [11]
Polymers for Enteric Coating	Cellulose Derivatives	Cellulose acetate phthalate
		Cellulose acetate trimellitate (CAT)
		Hydroxypropyl methylcellulose phthalate (HPMCP)
		Hydroxypropyl methylcellulose acetate succinate (HPMCAS)
	Vinyl esters polyvinyl acetate	Polyvinyl acetate phthalate (PVAP)
	Methacrylic acid copolymers	Poly (methacrylic acid - ethylacrylate) MA:EA = 1:1
		Poly (methacrylic acid - methylmethylacrylate) MA:MMA = 1:1
		Poly (methacrylic acid - methylmethylacrylate) MA:MMA = 1:2

1.2.3 Latex/Pseudolatex Film Formations

Despite all the improvements of the latex systems, the nature of the latex system is more complex and difficult to comprehend. Differed from organic polymer solution, where polymer molecules all solvated; polymer existed in latex/pseudolatex dispersions as discrete particles having clear defined particle boundaries. Hence film formation requires higher energy to overcome the boundary potentials in such dispersions. The most widely accepted theoretical model for interpreting latex film formation was summarized as 3 primary stages[12]: 1) initial water evaporation provides the capillary driving force so that the polymer particles are pushed together, ie 'polymer reordering' (Fig 1.1). 2) At temperatures above the polymer's minimum formation temperature (MFT), the continued evaporation of water further squeezes the polymer molecules together into ordered arrays or in another words 'polymer particle deformation'; and polymer particles start to coalesce to form a transparent film from the usually opaque and cloudy suspension. 3) The further evaporation of water allows the coalescence of polymer molecules to interdiffuse through particle boundaries accompanied by glass transition temperature (Tg) increase (Fig 1.2). This results in the transparent film becoming stronger and more uniform. The last stage is usually regarded as the 'polymer curing' and takes place only when the temperature is above the polymer's Tg. Below the Tg, the polymers existed in 'glassy state' and are unable to coalescence or interdiffuse; above the Tg, polymer existed in a 'rubbery state' and possesses higher mobility to allow more sufficient polymer coalescence in the curing stage.

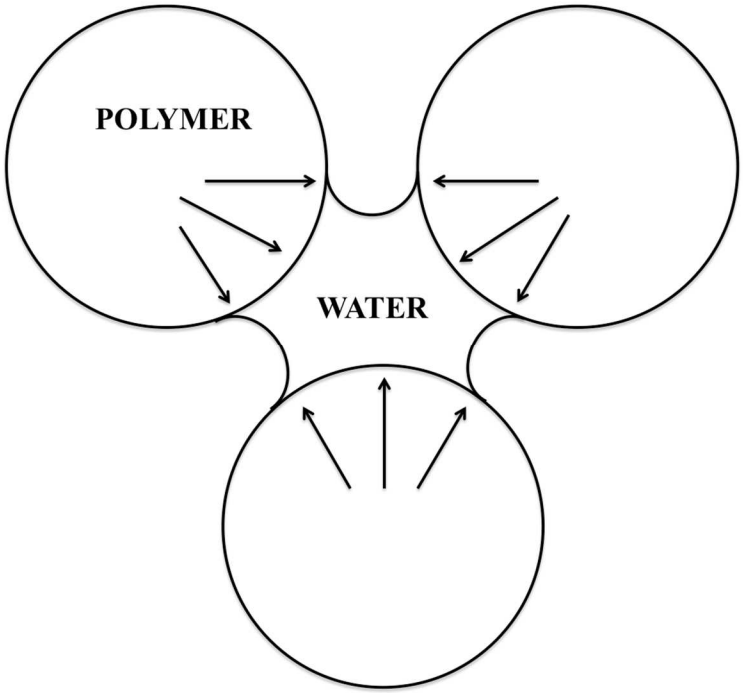

Fig 1.1. The evaporation of water creates driving force for particle deformation

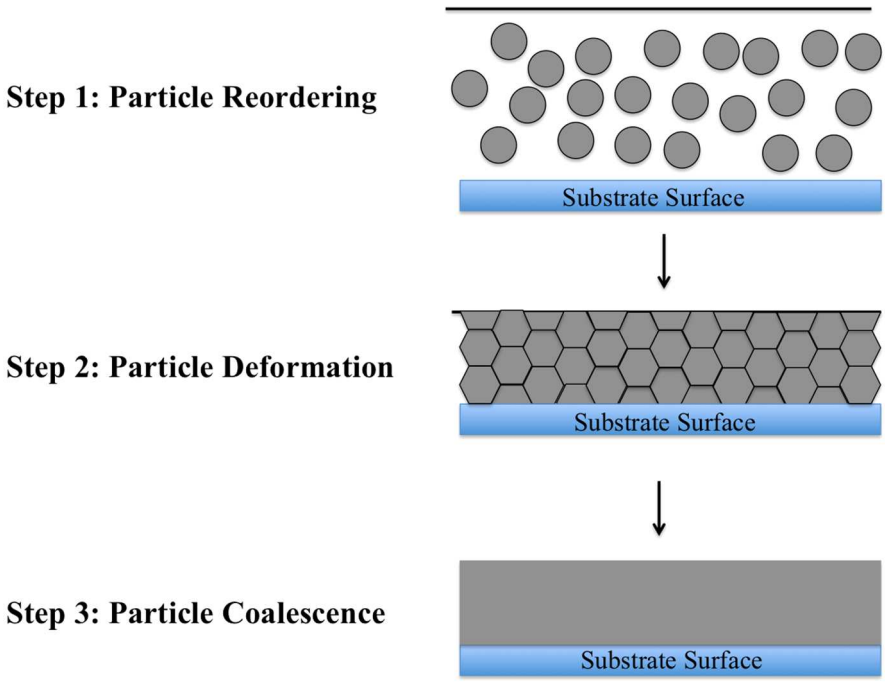

Fig 1.2. The schematic representation of the 3 stages of film formation of latex/pseudolatex systems

1.2.4 Pseudolatex film Curing Challenges

The curing of latex or pseudolatex system is the critical step of the final coating quality and drug release profiles. The fully cured polymer films provide optimal insulation and sealing of the core whereas incomplete curing will result in deviation from the target release profile for a specific drug. Curing on its own is a complex process and in recent years, efforts have been seen trying to understand how curing can affect the drug product. Investigations on film formation and curing had seen on many investigations with both free films and coated drug products. Guo et al used free films made from Aquacoat ethylcellulose dispersion and evaluated the effects of temperature and physical aging time; found that the vapor permeability increases when cured over 100°C; proposed a 'top-down' drying model indicating the film drying started form the top surface of the dispersion[13]. Also they demonstrated as plasticizer levels increases, the glass transition temperature (T_g) of the ethylcellulose system decreases. Bhattacharjua, et.al demonstrated using Eudragit® NE and RS as model systems showed the dissolution rate decreases upon curing at high temperature and the loss of plasticizer can lead to increase of drug release[14].

Temperature and time is not the only factors affecting the film formation for latex/pseudolatex dispersions, researches also demonstrated the moisture plays a crucial role in this process. Feng et al found the water affects the hydrophilic polymer latex film P(MAA-co-BMA) to increases the diffusion coefficient but has little effects on hydrophobic latex film with polymer PBMA other than changing the films' transparency[5]. Bodmeier et al used both ethylcellulose and Eudragit® systems and

compared the preparation of dry and wet processes in terms of mechanical properties[15]. They found the solution cast films (wet) had higher mechanical strength than pseudolatex dispersion films (dry). And proposed the release mechanisam of Aquacoat based ethylcellulose dispersion being osmotic pressure driven.

However, some of those studies had not been focused on the moisture effects, and few of the literature had been able to quantify such effects of moisture during curing stage. Water itself is able to provide plasticizing effects to relax polymers and facilitates the interdiffusion of polymer particles[10]. Further more, relatively more hydrophilic polymers having a higher water affinity may require less or even no water for curing but will still be able to undergo particle coalescence and interdiffusion [4, 10]. More hydrophobic polymers are expected to require large amount of water to achieve the same level of coalescence and molecular interdiffusion. With those uncertainties in mind, it is needed to investigate the effect of moisture on the curing step on a latex/pseudolatex system, with a focus on quantifying such effects by physical measurements. Furthermore, it has been no quantification model for the extent of film curing or particle coalescence, this will also be attempted in this work.

1.2.5 Ethylcellulose Pseudolatex Dispersion (Aquacoat) System

The polymer for this study is Aquacoat ECD, a commercial Ethylcellulose [11] pseudolatex nanodispersion[16] (solid content: 30% w/w). EC has been used extensively as a coating excipient in ER pharmaceutical formulations. Originally coating with EC was applied via organic polymer solution process and later more as latex/pseudolatex systems. The polymer possesses several interesting points that are worth investigating

into: pure EC has a high Tg around 145°C, therefore in the real application for film formation[17], plasticizers are usually required to lower Tg via the plasticizing effect allowing polymer molecules more mobility at lower temperature.[18] Besides, unlike polymers such as Ammonium methacrylate copolymers (under the trade name of Eudragit®) which possess ionic species that allowing the polymer more affinity towards water and easier for polymer coalescence in curing, EC is not readily soluble in water.

Because of the rigid backbone of the structure, it was found the glass transition temperature of difficult to measure. The other consequence of such property is the long time required for relaxation of the polymer chains. This is again reflected on the curing problem that often came across when EC was used as ER coating polymers. It has been puzzled both industry and academia many years to quantify the curing process, simply because it is the interplay of many components which are extremely hard to control in real process. In order to have a better understanding of the curing process, EC was used as a suitable model coating system for our investigation.

1.3 Quality by Design (QbD) Principle and NIR

Since the beginning of 21st century, the FDA continued to implement under the Pharmaceutical CGMP Initiative for the 21st Century – a Risk Based Approach[19], from which the purpose was to modernize FDA's regulation of pharmaceutical quality. An essential idea of this initiative was the implementation of the concept of Quality by Design (QbD) where it stated 'The focus of this concept is that quality should be built into a product with a thorough understanding of the product and process by which it is developed and manufactured along with a knowledge of the risks involved in manufacturing the product and how best to mitigate those risks.' As pharmaceutical

research is to serve for the ultimate production, it is therefore important to have this concept in mind.

International Conference on Harmonization (ICH) Q8 R2 specified the requirements and the procedures required for carrying out the pharmaceutical product development under the QbD approach, summarized in Figure 1.3. The most important properties of a finished drug product is described in the Quality Target Product Profile (QTPP), that described the properties and characteristic of the drug product to ensure the safety and efficacy; QTPP needs to specify the drug products' dosage form, route of administration, the patient usage (eg, adult, children), amount of drugs per dosage and stability. Then with this goal in mind, the critical quality attributes (CQA) need to be identified. CQAs usually related to physical, chemical, biological or microbiological properties or characteristics of the drug API, but often the excipients and intermediates during the manufacturing process can also be part of CQAs. The drug product CQA is key for drug products' safety and efficacy. In this investigation, the curing is one of the main parts of CQA for successful coating formulation development using EC as an extended release polymer.

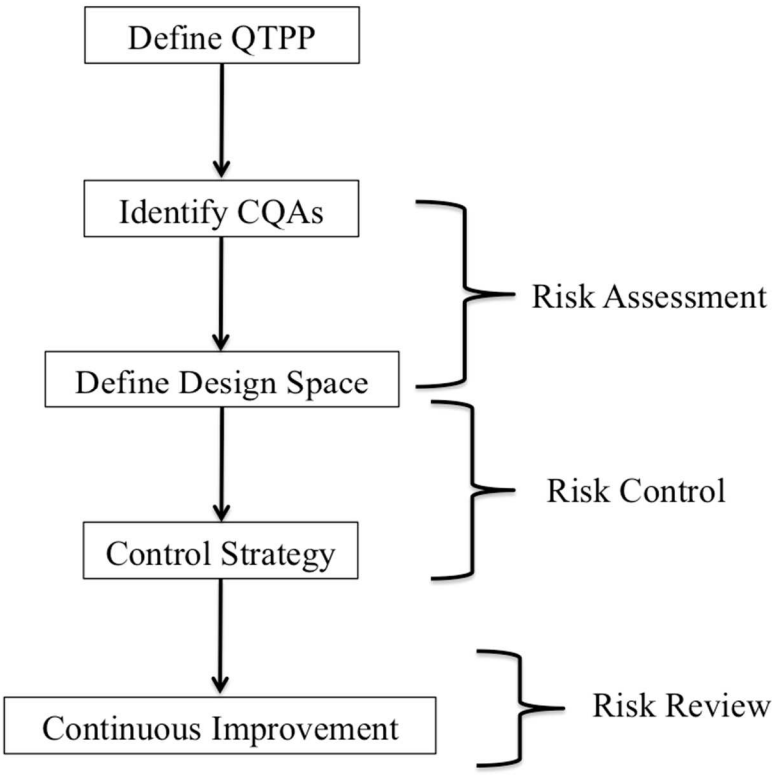

Fig 1.3: Road map of implementing QbD concept in pharmaceutical development

One of the essential purpose of QbD is trying to establish a 'Design Space' in a particular process, this is defined as 'The multidimensional combination and interaction of input variables that have been demonstrated to provide assurance of quality' [20]. In order to evaluate the factors such as temperature, time, moisture, plasticizers on the curing of EC polymer, systematic experiments were designed to understand the effects of these factors with the QbD concept bearing in mind.

1.3.1 Process Analytical Technology and Near Infrared Spectroscopy: Principles and Applications

In order to gain insight knowledge of a manufacturing process such as curing process, a process measurement technique is needed. Over the past decade, use of process analytical technology [21] has become a valuable tool in the development of knowledge of processing parameters and the control of manufacturing of pharmaceutical products[13]. Near Infrared Spectroscopy (NIRs) is a widely used technique for qualitatively and quantitatively analyzing pharmaceutical processes. Its electromagnetic spectrum spans wavelengths of 780-2526nm[14]. The absorption bands in the NIR region are related to overtones and combinations of fundamental vibrations of functional groups of -CH, -NH, -OH and -SH. The major advantages of NIR over traditional wet-lab analytical techniques include easy sample preparation, delocalization of measurement by fiber optic probes, and the accurate recording of chemical and physical information of samples. However, because the NIR's signal was from the overtones where $\Delta n>1$, these transitions are strictly forbidden with harmonic oscillators; the reason why these bands were still visible is because in reality, chemical bonds cannot be treated as harmonic oscillators, therefore, the selection rule $\Delta n=\pm 1$ can be violated. Despite this anharmonicity nature of the chemical bonds, the signal of NIR is still from forbidden transitions, therefore are weak, hence the NIR cannot be analyzed with individual peak areas such as Ultraviolet (UV), a different approach to this problem is needed.

1.3.2 Chemometrics Modeling (PCA and PLS)

Chemometrics is the choice for NIR data analysis. This is the method that utilized the statistical and mathematical modeling concept and computing power to analyze chemical

data. The advantage of such method is it can extract information from complicated data set where chemical trends are not quite visible. This is particularly useful when dealing with NIR spectra because each spectrum has at least a few hundred of variables (absorption values). It would be unwise to just look at a specific number of peaks. In the research with respect to the EC curing, two widely used techniques will be utilized, principle component analysis (PCA) and partial least square (PLS) regression.

Principle Component Analysis (PCA)

This important technique provides a clear visual representation of clustering for multivariate dataset, which usually comes in a form of rectangular box (tables, spreadsheet) with n rows and m columns and the number of rows equal to the number of objects or samples. The aim of PCA is to deconvolute a complex data set for pattern recognition. It is achieved by resolving a set of data into orthogonal components whose linear combinations approximate the original data with the desired degree of accuracy[22]. Each component accounts for the maximum possible amount of residual variance in the set of data and is smaller or equal to the number of variables.

In the case of spectroscopy data, the number of variables is the number of spectra. For a given matrix **X,** the PCA transformation is to resolve the matrix X in to the form of **X** = **T** □ **P** + E Where **T** is called the scores, and have as many rows as the original data matrix; **P** are the loadings, and have as many columns as the original data matrix. In simple terms, the original data matrix X, in our case, the spectra data will be categorized into different PCs and each PC will have a score and loading. Then by looking at scores plot with respect of different PCs will see directly how different spectra differ with each

other. Loading is representing the important contributions from the spectra. By looking at the loadings, we will be able to identify the most useful frequency regions

Partial Least Square (PLS) Regression

PCA allowed the visual representation of the spectral data, however, it did not correlate the spectra to the physical quantities we may be interested in. Therefore partial least square regression is the method used when trying to correlating physical quantities. Instead of finding hyperplanes of minimum variance between the response and independent variables, it finds a linear regression model by projecting the predicted variables and the observable variables to a new space[23].

PLS is used to find the fundamental relations between two matrices (**X** and **Y**), it is particularly suited when the matrix of predictors has more variables than observations (X set). This is particularly useful when NIR come to play.

When it comes for the prediction, two models will be generated for X and Y

$\mathbf{X} = \mathbf{T} \square \mathbf{P} + E$

$\mathbf{Y} = \mathbf{T} \square \mathbf{q} + f$

Where the **q** is analogous to the loading matrix. The product of T and P approximates to the spectral data and the product of T and q to the physical quantities of interest; the common link is **T**. An important feature of PLS is that it is possible to obtain a scores matrix that is common to both the physical quantity of interest (y) (in this case, our mechanical property) and measurements (x) (In this case, NIR spectrum).

1.3.3 NIR in Pharmaceutical Usages

NIR provided a much easier way sampling, however, because of it lacks the ability to identify samples by merely inspecting spectra and the analysis often requires sophisticated mathematical treatment, the NIR applications in pharmaceutical industry has only started in the past 20 years, even though this techniques had been known since the 1960s[24].

One of the most important usages for NIR spectroscopy is used for raw material identification. Because pharmaceutical manufacturing needs to rely on raw materials that have the highest quality and ensure the consistency throughout the cycles of productions, multi-sensing NIR can have a great impact in quality control of pharmaceutical API and excipients and it can greatly accelerate the analysis throughput. The QC can often be done by library approach, where spectral library was used to cross refernece the test sample's spectra and then evaluate the identity of the tested material [11, 25, 26].

The NIR also found extended usages in the analysis of intact dosage forms where the physical, chemical and biopharmaceutical characteristics can be revealed. This type of analysis brings significant improvement for on-line or at-line qualification of dosage forms; it can effectively prevent rework or disposal of the entire batch before release. The first example of such analysis was seen in 1966 by Sinsheimer and Keuhneilian where they invested gated pharmacologically active amine salts, although no calibration were carried out, they demonstrated the potential for quantification of drugs in solid state[27]. In the landmark paper in 1987, Lodder et al tested adulterated capsules using

NIR, not only could they analyze the foreign compound inside the capsules down to a small limit, they were also able to detect where the positions of adulterants were inside tested capsules[28]. In addition to chemical properties, physical properties of intact dosage forms can also be detected: Morisseau et al showed the NIR could be used to accurately predict hardness of tablets with the same level of accuracy with the conventional techniques[29].

Noninvasive detection of manufacturing process and fast measuring time make the NIR an ideal tool for process monitoring and has become a key contributor to the development of PAT. Blending/mixing is the most commonly seen usages of NIR in pharmaceutical operations because it dramatically improved the accuracy of end point detections and shortens the analysis effort dramatically[30]. Recently, it was also pointed out that using multiple censors inside a V-blender during blending could improve the end point detection more accurately[31]. The strong absorption of O-H band allows on-line NIR monitoring of moisture possible and suitable for various drying processes to allow the drying to be more efficient and energy saving. In one of the early works, White demonstrated using NIR to measure moisture level in the process of microwave drying[32]. Coating operations have been explored extensively and it is also one of the main research interests in our laboratory. In 1994, Kisch et al demonstrated using EC (Aquacoat ECD) and HPMC as coating polymer on tablet with an at-line NIR detector can be used to monitor the weight gain of the coating[33]. Tabasi et al demonstrated the at-line NIR measurements could accurately predict coating thickness with Eudragit RL/RS coating on orbifloxacin tablets; besides, with the same PLS approach, the

dissolution release of the coated tablets could also be accurately predicted[7, 8]. Kona et al demonstrated with innovative on-line NIR probe and humidity data logger to create a multivariate statistical process control charts (MSPC). This not only could monitor the end point of a drying process in the granulation, but it could also detect potential failure of a running batch[34].

1.4 Analysis of Cast Free Films: Formulation and Test Methods

1.4.1 Formulation

The investigation of the film curing should begin with a simplest format and that is the free cast film. By using free cast films, the complex processing parameters of coating can be avoided and the casting process can be easily controlled. The pseudolatex dispersion for both free film casting and subsequent coating operation was maintained at 15% solid content with triethyl citrate [11] as a plasticizer (25% w/w of EC solid). This formulation was chosen based on the common practical knowledge. Throughout the investigation on EC curing, this formulation is kept the same except a swap in the hydrophilic TEC with a hydrophobic dibutyl sebacate (DBS) as a comparison. The prepared dispersion will be cast into a petri dishes and aluminum circular disks. Preliminary works showed the dispersion casting on other materials surfaces such as glass and Teflon plates were difficult to peel off for subsequent analysis.

1.4.2 Mechanical Tests

Finished strips samples need to be analyzed with a reliable method in order to reflect on their properties. To analyze the mechanical samples, a method was adapted from the

ASTM V-638 method. The test station is an Instron® 8521 System with a Tension/Compression 100N Load Cell (Fig. 1.4). And the test samples were cut into shapes specified with ASTM D-638-V 'dogbone' punch (Fig 1.4). The reason to use such shape was the results obtained from preliminary experiments where we found that the rectangular strips tend to break at the grips and not able to generate reproducible, consistent results. The tensile tests were performed using Instron® 8521 System with a Tension/Compression 100N Load Cell. For each test, one sample strip was first measured its thickness and then held vertically between G227 Lightweight Screw Vise Grip and J227 Jaws as outlined by ASTM D882.

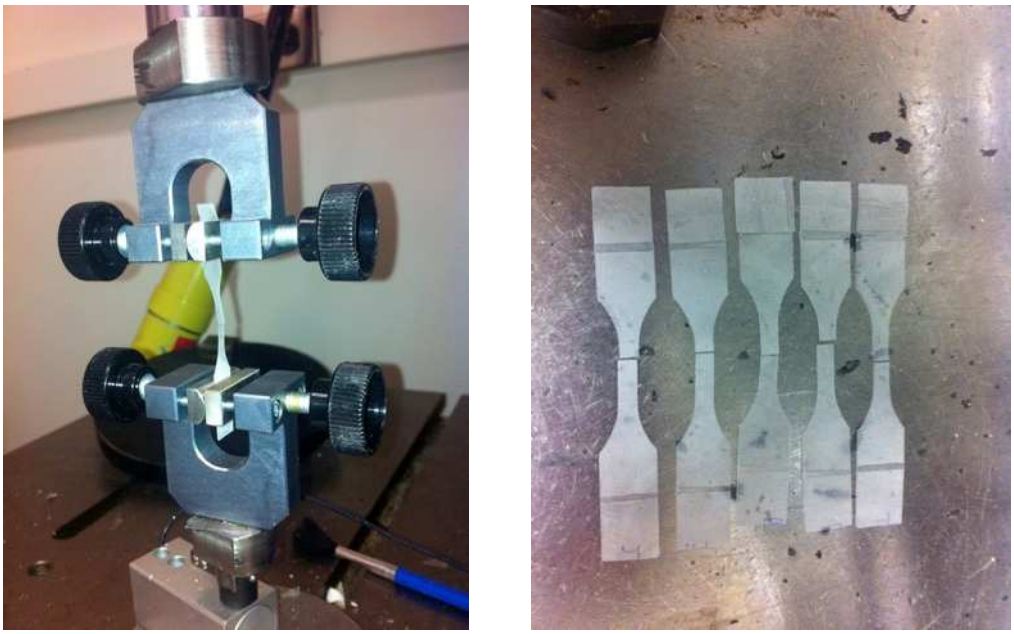

Fig 1.4(a) (L) The Mechanical testing set up with a Instron tester Fig 1.4b (R): The strips after the test showing the breaking point in the center of the strip to ensure the reproducibility and consistency for the mechanical test.

The force and the elongation were recorded by a computer. Analysis was carried out according to the 4 equations given below to obtain the value of: tensile strength (TS),

percent elongation at break (PEB) and Young's modulus [16]. The result of a single sample film was shown in Fig 1.5 with demonstrations of some of the key areas reflecting in Eq 1-3 for the important mechanical properties to be evaluated.

TS= Load at failure / Initial film thickness × Initial film width Eq.1

PEB= ×100 Increase in length of film / Initial gage length (Narrow region) Eq.2

Young's Modulus= Slope of stress vs strain in elastic deformation region Eq.3

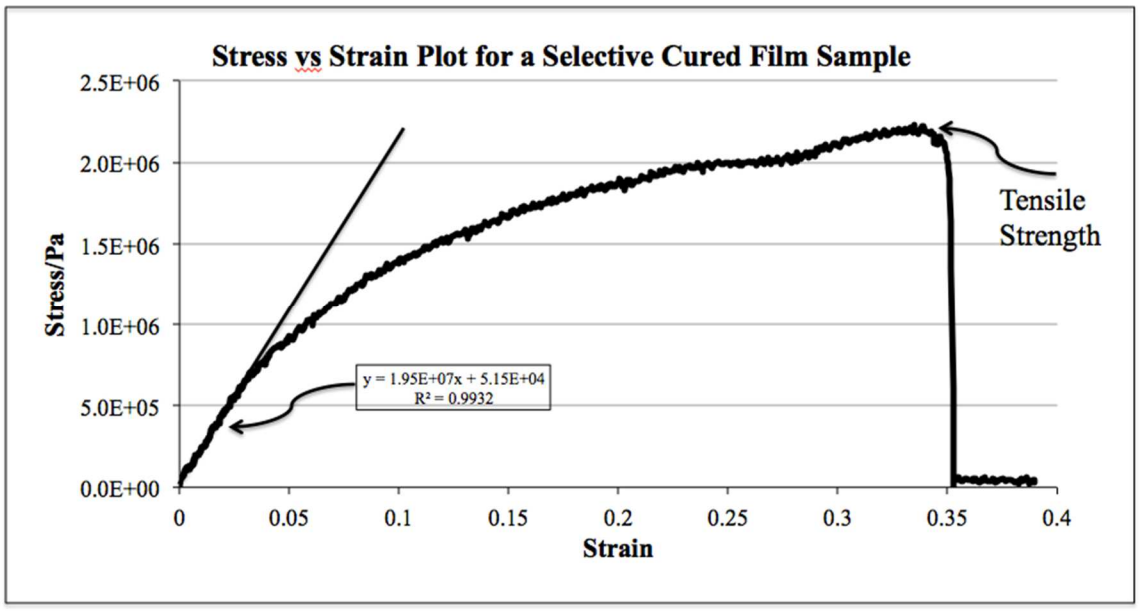

Fig 1.5. Sample Curve of the Stress vs Strain Plot for a sample pesudolatex film that had been cured under 60°C 75% for 3 hours. The Young's Modulus was estimated from the initial slope of the curve to be 1.95E+07 Pa.

1.4.3 Water Vapor Permeability

The other critical property of the film samples besides mechanical property is the films' permeability. For a pharmaceutical coating film, permeability is crucial determining the permeation of the drug molecules into dissolution medium. Despite the permeability's importance on dissolution, very few systematic studies has been carried out for the effect on curing on latex/pseudolatex films. Permeability was calculated based on the equation

below (Eq.4). Where P is the water vapor permeability; dM/dt is the rate of moisture passing the film; h is the thickness of film; A is the area of the film; Δp is the difference in vapor pressure gradient across the film. The ASTM permeability methods were carefully considered and then rejected because of several difficulties in: 1. The measurements require possession of a balance at full time; 2. It require large film samples (d=10 cm); 3. Permeability was highly sensitive to the environmental conditions; no constant reading will be achieved without controlling the environmental humidity and temperature[35]. Hence it was both not efficient for repeating and not practically possible for making large film samples.

Preliminary experiments demonstrated the dried EC films were very brittle and great cares are required during peeling of such films. Therefore, a modified method slightly deviating the ASTM method but with same principle was developed. Dessicant containing glass vials are therefore used to test the water permeability through the free films. The dry films were cut into small round pieces and then glued to the opening of each glass vile that ensuring no moisture leakage. The films were then placed in relative humidity controlled desiccator with saturated salt solution. (Set up shown below Fig 1.6a and b). The desiccator was then placed into a temperature controlled oven at 28°C to allow a constant moisture transfer. By doing so, it was able to tightly control 3 highly sensitive parameters: the surface area A, the difference in vapor pressure Δp and temperature. The measurements were carried out by monitoring the weight gain of the vial over one day to determine directly the mass transport of moisture: dM/dt and then the

vapor permeability were calculated using Eq.4 with a known thickness h, which was measured before. Each film measurements were repeated with at least n= 6.

Fig 1.6a (L): Colored indicator and glass vial, the blue means the desiccants were dry and red indicated it was moisture obsorbed so no longer good for usage; Fig 1.6b (R): 75%RH humidity controlled desiccator containing vials with films glued on top. Each experiment was repeated with n=6.

Permeability: $$P = -\frac{dM}{dt}\left(\frac{h}{A \cdot \Delta p}\right)$$ Eq.4

1.4.4 Surface Evaluation of Cast Films

Scanning Electron Microscopy

The microscopic techniques are very useful for surface examinations. Scanning Electron Microscopy [36] had been seen a lot of usages in recent research. In SEM measurements, a beam of electrons is fired at the samples' surfaces then fast electron scans were performed to gain the information on the topology of the sample surface. In conventional measurements, a layer of ultrathin conductive metal is needed to coat on the surface of measuring samples to enhance signal/noise ratio and also to ensure the conductivity of surfaces. The common metal used are gold, palladium, platinum and osmium etc[37].

With technological advancement, the environmental scanning electron microscopy (ESEM) was developed that do not require the coating on sample preparation. This method uses a low vacuum (compared to high vacuum in the SEM) and a closer optical distance, will also produce the surface morphology for samples. This technique brings tremendous advantage to samples that are fragile and valuable that may not be retrieved after SEM measurements[38].

Atomic Force Microscopy

Unlike the SEM, the atomic force microscopy (AFM) technique actually produced images by "touching" the specimen. It is one of the most advanced microscopy techniques invented in the 1980s[39, 40]. It was able to produce images in the resolution of nanometers, greatly improved from the optical microscopy. The schematic representation of the AFM principle was showed in Fig 1.7. The detector detects the light signal from a focused laser light reflected off the back of the cantilever. The cantilever, usually made of piezoelectric materials, moves along the surface of a specimen, maintained an interaction with the surface. The surface roughness causes the cantilever to displace vertically, and such displacements are tracked by the reflected light by the photodiode detector. The piezoelectric signal from the cantilever is translated into the surface topography of the measured specimen.

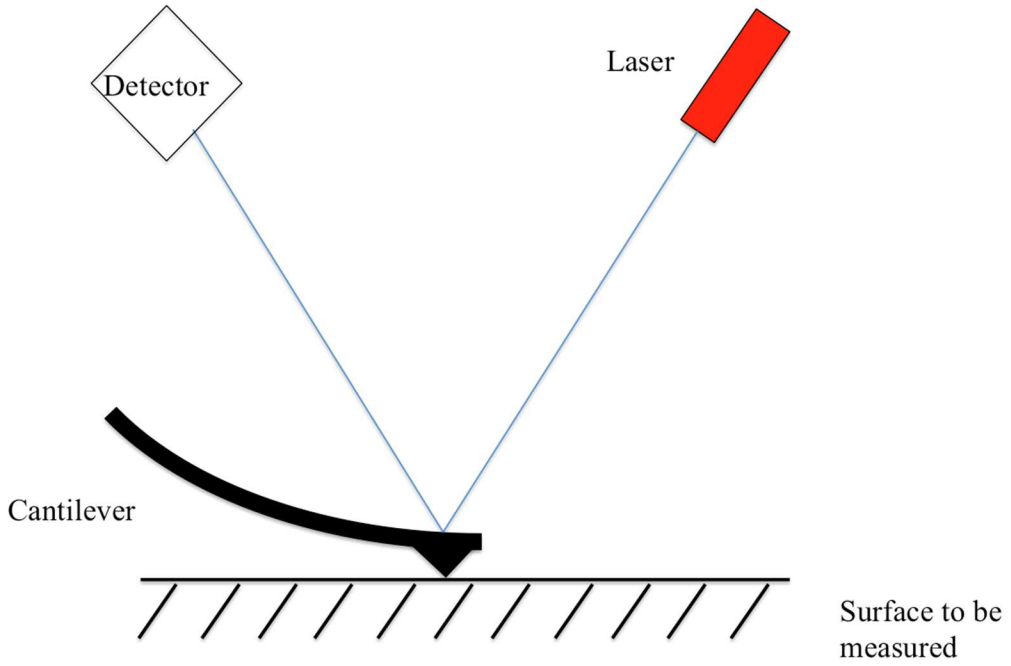

Fig 1.7: Schematic diagram showing the working principles of an AFM.

1.4.5 Thermal Analysis: DSC

The thermal analysis techniques are commonly seen for pharmaceutical API and excipients. Among them differential scanning calorimetry (DSC) is one of the key techniques; it allows the analysis of the samples melting point, glass transition temperatures (Tg) and is also able to detect different polymorphs of crystals. DSC works by measuring the difference between the test sample and a reference sample, usually an empty container pan. By applying a constant heat flow to both sample and the reference, the different response of the two is recorded. From the different shape of the response curve, one is easily to distinguish the peaks of primary transition such as melting, freezing or recrystallizing; it can also detect secondary transitions such as the glass transition in polymers. One of the most important properties for polymeric system is to detect the Tg of a polymeric systems and DSC is able to provide this accurately.

1.5 Fluid Bed Film Coating and Dissolution Release

1.5.1 Bosch Mycrolab Coater: Unique Coating Solution

Despite the usefulness of analyzing the curing with respect to the free films, it is not sufficient to evaluate the effect of curing only with free films. The effect of temperature, relative humidity time should also be evaluated by realistic coating application. This not only allows us to observe the effect in action, it also served as proof of concept or reassuring for the findings on the free films. The coating performed in the investigation utilized a cutting-edge equipment: Bosch Mycrolab fluid bed coating system, which possesses some unique aspects, and technical innovations that allowed operators to achieve better outcome (Fig 1.8) The first innovation comes from the patented process gas distributor blade Diskjet, the diskjet was one the bottom of the coating bowl where pellets settle upon; during coating, the process air blows through the diskjet and fluidize the pellets. Unlike the traditional Wurster process, the circuar Diskjet plate had have slits opening tilted to 45° angle so that the air going through automatic forms a vortex pattern. This will allow the pellets fluidizing in the chamber to have a more predictable moving pattern.

Fig 1.8. The set up of the Bosch Mycrolab fluid bed coating equipment. The Pump and balances was also needed for the coating process

The second unique feature of the Bosch Mycrolab system is its 'Microclimate' feature (Fig 1.9). This is to use the air blowing around the liquid spraying nozzle so that the spraying cone are not directly exposed to pellets near the nozzle tip. The result of this design prevents the nozzle clogging. These two unique aspects allowed this technology being more superior to Wurster process in a number of ways: first, bottom-spraying Wurster process can only fluidize pellets/beads inside the column; for the spaces inbetween the center column and the outer cone, the beads were relatively stationary, which may lead to potential agglomeration.

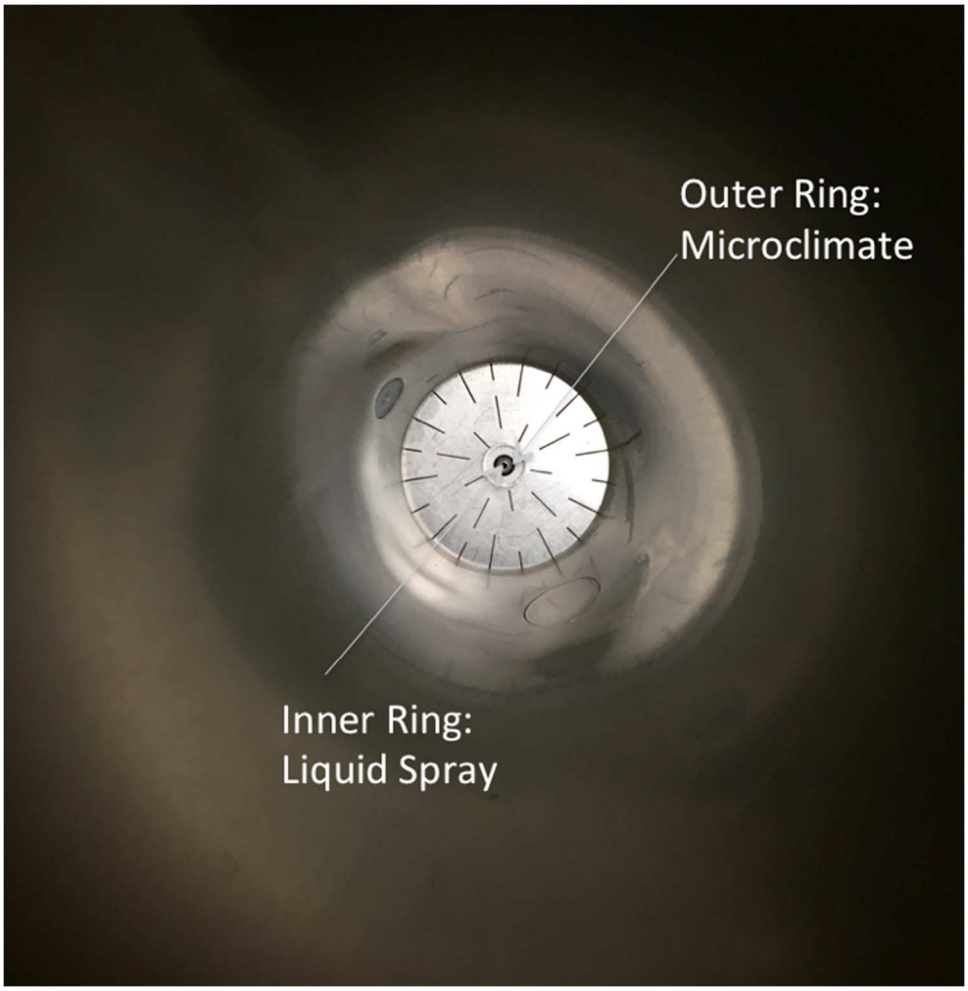

Fig 1.9 Inside fluidizing chamber: the illustration of the Microclimate. The inner hole/ring is where the spraying liquid coming out and the outer ring is where the pressurized air blowed through which can protect the spraying liquid so to avoid nozzle clogging

1.5.2 Mechanisms of Release of Coated Pharmaceutical Products

Ozturk et al have summarized the four mechanism of release from pellets coated with ethylcellulose[41]. They can be put into: solution/diffusion through the continuous polymer phase and/or plasticizer channels; diffusion through aqueous pores and osmotically driven release through aqueous pores. The authors also examined the effect on different plasticizers. However, so far no literature was seen discussing the effect of coalescence/ curing on mechanisms in terms of the curing. Ethylcellulose is a polymer

not soluble in water, therefore the effect of directly diffusion from the polymeric phase may not going to be significant. To really assess the effects on the curing on EC, it would be to leave out the pore formers such as HPMC.

1.5.3 Dissolution Tests and HPLC

Dissolution tests are utilized extensively to assess the performances of pharmaceutical products. It has been used routinely for stability and quality control for oral and non-oral products. This is also the most widely used technique for assessing in vitro performances of drug products and although not always, it can often provide insights into possible in vivo performances. Dissolution allowed the assessment and categorizing for different drug release profiles such as immediate release, sustained/controlled release, delayed release and pulsatile releases etc. Based on dissolution profiles obtained based on different formulations, formulators will be able to pick up potential problem easily such as dose dumping or unwanted interactions with selected medias. Not only dissolution is a neat tool for new pharmaceutical product development, it is also extremely important for generic pharmaceuticals for establishment of Bioequivalence (BE)[42] and hence influence the decision- making process. It can be used to waive the in vivo test for immediately release drug product for BCS Class I drugs when the API release is over 85% release in 15 min; for multi-strength ER product, the dissolution can be used to waive BE study requirements for one or more additional strengths based on dissolution tests if the drug product with the same dosage form, but in a different strength and proportionally similar in its active and inactive ingredients to the strength that BE was already established; for non-oral dosage forms such as ophthalmic suspensions, generic liposome

formulations, rectal and vaginal suppositories, FDA also recommends and encourages the dissolution method to be developed/to be followed to characterize the in vitro release.

Because of the crucial role of the dissolution tests, USP (United State Pharmacopeia) has set forth a series guidance on the methods of dissolution tests. The method was summarized in the document '<711> Dissolution'. There are four sets of apparatus, the Apparatus I and II are most common, the Apparatus I is the Rotating Basket method where it is mainly used for light beads/pellets and also capsules and tablets where the dissolved API are able to leak out from the mesh of the basket. However, the drawback of this method is that sometimes soluble rate controlling polymers can adhere to the mesh of the basket and block release of the API. The Apparatus II is most often used for single unit matrix tablets, sometimes, a sinker is needed to prevent the tablet/capsule from floating. Apparatus III the Reciprocating Cylinders and IV Flow-Through are less commonly used due to the limited application field and complex set up.

Once the dissolution samples are collected, these samples are analyzed by high-performance liquid chromatography (HPLC), this is a most widely used technique by analytics for pharmaceutical industry because it provided both qualitative and quantitative assessments. This technique uses a packed column to separate the components in a mixture under high pressure. The pressurized solvent pass a pressurized liquid solvent containing the sample mixture through a column filled with a solid adsorbent material. Because the polarity difference in a mixture, each component interacts slightly differently with the adsorbent material inside the column, causing

different flow rates for the different components and leading to the separation of the components as they flow out the column. For most pharmaceutical products, it is required for proper development and validation of HPLC methods before approval and the HPLC methods need to be accurate, robust and reliable.

1.6 Fluorescence Anisotropy

1.6.1 Definition and Applications

Fluorescence spectroscopy is a type of electromagnetic spectroscopy which analyzes fluorescence from a sample. This fluoresence transition spectrum is occured from the excitation of π electrons (usually in the aromatic molecules) into higher electronic and vibrational state, then the exited electrons undergo a series of possible decay process including internal conversion (IC) or inter system crossing (ISC). During these processes, fluorescence light is emitted[43].

Fluorescence anisotropy is also of great importance besides the conventional fluorescence spectroscopy. It is the phenomenon where the light emitted by a fluorophore has unequal intensities along different axes of polarization and this intensity greatly affected by the motion of the probe[44, 45]. For further investigate the coalescence stage in real time, fluorescence probes will be added into the dispersion and will then participate into the polymer matrix upon drying. With such incorporation, it is able to detect the microenviromental changes inside polymer film during curing by monitoring the changes to the fluorescence anisotropy. Because of the measurements require complete films be held in the cuvette, only dry films will be used. During curing, internal free volume immediately surrounding the probe decreases as particle coalescence takes

place. This decrease of the free volume will likely to decrease the rotational diffusion coefficient D. Rotational correlation time θ is inversely proportional to D, and by Perrin equation (Eq.4), where r is anisotropy, r_0 is fundamental anisotropy, τ is fluorescence life time. Hence, as the curing progresses, the anisotropy r increases as θ increases due to decreases of the rotational diffusion coefficient D. By monitoring and controlling the films' temperature and humidity inside the fluorescence cuvette, we can monitor curing in real time.

$$r = \frac{r_0}{1+\frac{\tau}{\theta}} \qquad \text{Eq.4}$$

1.7 Investigations on Extended Release Tablets With the Implications on Biowaiver

1.7.1 Background on Generic Drugs: Advantages and Shortcomings

The modern US generic drug industry began with the signing of The Drug Price Competition and Patent Term Restoration Act of 1984 (US Public Law 98-417), also commonly known as the Hatch-Waxman Act. This act was signed into law on September 24th 1984. TheHatch-Waxman Act amended the Federal Food, Drug and Cosmetic Act (FDCA) and the Patent Act, established an abbreviated new drug application [46] process[47].

Before the Hatch-Waxman Act, the development of generic drug products were lengthy and costly and there were very few number of generic versions on the market. Ever since the onset of the act, the generic market has seen an impressive growth, according to

McKinsey&Company, over the past decade, the annual revenue increase for the industry is often at double-digit, the average for net revenue growth from 2009-2012 is an impressive 8%[48]. In 2012, generics reached 84% of dispensed prescriptions, and spending in this segment grew by $8billion[49]. In 2013, global generic market is worth $150 billion, with US market being the biggest of 45% and developing countries India and China having huge production volume. In the next five years, the emerging market are expected to have a 15-20% growth and the matured market at 6-10%[50].

The reason why the generic industry has ben enjoying the dramatic growth was the patents expiration of a number of blockbusters drugs. It is estimated between 2010 and 2017 there are $150 billion worth of drug products to lose patent protections. The driving force is the patients' urgent needs for affordable, but reliable, high quality generic replacement of the brand pharmaceuticals. The Hatch-Waxman Act grants a competition advantages for generic manufacture with 180 days of exclusivity if they successfully filed the Paragraph IV ANDA[51]. The Paragraph IV filing is a patent challenge filing, it is when a generic manufacturer challenge a patent that has not yet expired and successful receive an approval. Because of the exclusivity could possibly bring enormous financial advantages for generic manufacturers along with an early capture of the generic market, this remained one of the main motivation for many generic manufacturers trying to bring their generic version first to the market. However, in the beginning years when the Hatch-Waxman Act was just in effect, from 1984-1989, the so called Generic Drug Scandal almost killed this nascent industry: evidence of FDA reviewers were found to be guilty of bribery with Bolar Pharmaceuticals. Luckily, the FDA took swift action against this

criminality and eventually was able to restore the confidence of the public on generic drugs.

1.7.2 FDA's Regulation on ANDA and Biowaiver

For oral administering solid dosage forms, in order to ensure the generic drugs have the 'switchability' to the brand drugs (that is often indicated by the AB rating in the FDA's Orange Book), the generic drugs need to be bioequivalence to the reference listed drugs (RLD) which are usually branded drugs that had been through the phase I- III trials. Two pharmaceutical products are said to be bioequivalence if they are pharmaceutically equivalent and their bioavailabilities (rate and extent of availability) after administration in the same molar dose and their effects, with respect to both efficacy and safety, can be expected to be essentially the same. Pharmaceutical equivalence implies the same amount of the same active substance(s), in the same dosage form, for the same route of administration and meeting the same or comparable standards[52].

In order for the generic drugs to be bioequivalent to the RLD, the FDA requires the generic be bioequivalent if the test drug meet the confidence interval (C.I) requirements: for both the C_{max} and AUC (area under the curve) determined by single dose blood level studies, the 90% C.I. are within the range of 80%–125% of the. C_{max} is the highest concentration in blood it is a measure of rate of absorption over what time period the drug is absorbed. The AUC measures the extent and exposure of drug absorption. Because the blood tests in patients are costly, the FDA allows the ANDA applicants to have biowaiver to certain cases where the generic manufacturers can use the in vitro test method (often dissolution) to justify such waiver can be granted based on the methods' high prediction

power on the in vivo performances. As mentioned previously, for BCS class I drugs whose API is both highly soluble and highly permeable, is able waive the *in vivo* test provided the drug dissolved fast enough.

1.7.3 Switching Issues of Pharmaceutical Bioequivalence

The biowaiver can also be granted for ER formulation drugs, however ER formulations are often more challenge to copy for generic manufactures. For extended release single unit oral solid dosage forms, according to FDA's guidance[53, 54], it is required to demonstrate the bioequivalence only in the highest strength generic products; and for the lower strength products, biowaiver can be assured if the lower strength products can have the similar in vitro behavior based on the f_2 similarity tests[55]. The f_2 tests is known for its simplicity to compute and provide a number for straight forward comparison, however, it possess disadvantages such as the lack of information on subtle difference in release mechanism and sensitivity to the number of points used[56].

Because of the natural intention of reducing development cost for generics. Based on these guidance documents, FDA has approved lower strengths (and sometimes higher strength) single unit extended-release products without requiring bioequivalence studies. However, medications that is perception sensitive and having high complexity of formulation, such as ER formulations are more prone to switchability issues; especially for cases where the release of the product was determined by dosage designs and when the inactive components in the dosage forms govern the drug performances. Recently, Teva and Watson's generic Wellbutrin XL 300mg were pulled from the market due to bioinequivalence after FDA's investigations[57]. It was revealed that both generic forms

of Wellbutrin XL were approved based on the basis of bioequivalence data extrapolated form the approved 150 mg but not from the direct bioequivalence study on 300 mg tablets. Another famous case is Cardizem CD – a 24hr sustained release treatment for high blood pressure and chronic stable angina (chest pain). Its RLD has a ratio of fast and slow releasing component of the API of 40:60 to provide a double-peak blood level concentration profile whereas generic companies attempted with only one type of the release but still able to meet the C_{max} and AUC requirement set forth by the FDA[58].

As a result, different strengths of many ER tablets on the market today may unlikely to be bioequivalent and would likely expose the patients onto greater risk than the RLD. The carelessness on *in vitro* and *in vivo* relationship which depending on drug properties, formulation design and in vitro test methods, leading to compromised product quality and performance. The effect of this bioinequivalence may not be always noticeable but poses a potential threat. This is of particular concern for products with narrow therapeutic index drugs. In recent years, there has been an increasing trend of negative patients impacts when switching from the brand to generic products[59].

1.8 References for Chapter 1

1. Walker, R.B., Modified-Release Drug Delivery Technology. 2nd Edition ed. Vol. 1. 2008: Informa Healthcare.

2. P.Ratnaparkhi, M. and P.G. Jyoti, Sustained Release Oral Drug Delivery System - An Overview. International Journal of Pharma Research & Review, 2013. 2(3).

3. Higuchi, T., Mechanism of sustained-action medication. Theoretical analysis of rate of release of solid drugs dispersed in solid matrices. Journal of Pharmaceutical Sciences, 1963. 52(12): p. 1145-1149.

4. Felton, L.A. and J.W. McGinity, Aqueous Polymeric Coatings for Pharmaceutical Dosage Forms. 3rd ed. DRUGS AND PHARMACEUTICAL SCIENCES, ed. J.W.M. Linda A. Felton. 2008: Dekker.

5. Feng, J. and M.A. Winnik, Effect of Water on Polymer Diffusion in Latex Films. Macromolecules, 1997. 30(15): p. 4324-4331.

6. Rubinstein, M. and R.H. Colby, Polymer Physics 2003.

7. Tabasi, S.H., et al., Quality by design, part III: study of curing process of sustained release coated products using NIR spectroscopy. Journal of pharmaceutical sciences, 2008. 97(9): p. 4067-86.

8. Tabasi, S.H., et al., Quality by design, part II: application of NIR spectroscopy to monitor the coating process for a pharmaceutical sustained release product. Journal of pharmaceutical sciences, 2008. 97(9): p. 4052-66.

9. Keddie, J.L., Film Formation of Latex. Materials Science and Engineering, R Reports, 1997. 21: p. 101-170.

10. John.E.Hogan, Pharmaceutical Coating Technology Ch 2: Film-coating materials and their properties, ed. G. Cole. 2002.

11. Corti, P., et al., Application of NIRS to the control of pharmaceuticals identification and assay of several primary materials. Pharm. Acta Helv., 1992. 67: p. 57-61.

12. Joseph Keddie and A.F. Routh, Fundamentals of Latex Film Formation: Processes and Properties. First Edition ed. 2010: Springer Laboratory.

13. Guo, J.-H., R.E. Robertson, and G.L. Amidon, An Investigation into the Mechanical and Transport Properties of Aqueous Latex Films: A New Hypothesis for the Film-Forming Mechanism of Aqueous Dispersion System. Pharmaceutical Research, 1993. 10(3): p. 405-410.

14. Bhattacharjya S Fau - Bhattacharjya, S. and D.E. Wurster De Fau - Wurster, Investigation of the Drug Release and Surface Morphological Properties of Film-Coated Pellets, and Physical, Thermal and Mechanical Properties of Free Films as a Function of Various Curing Conditions. AAPS PharmSciTech, 2008. 9(2).

15. Bodmeier, R. and O. Paeratakul, Mechanical Properties of Dry and Wet Cellulosic and Acrylic Films Prepared from Aqueous Colloidal Polymer Dispersions Used in the Coating of Solid Dosage Forms. Pharmaceutical Research, 1994. 11(6): p. 882-888.

16. Biopolymer, F., Aqueous Coating Acuacoat ECD Sustained Release Moisture Barrier Taste Masking.

17. Aqueous Polymeric Coatings for Pharmaceutical Dosage Forms. DRUGS AND PHARMACEUTICAL SCIENCES, ed. J.W. McGinity. 1997: Dekker.

18. M.R., H., G.-S. I, and N. R.U., A Water-Based Coating Process for Sustained Release. Pharmaceutical Technology, 1986.

19. FDA, PHARMACEUTICAL CGMPS FOR THE 21ST CENTURY —A RISK-BASED APPROACH. 2004.

20. HARMONISATION, I.C.O., PHARMACEUTICAL DEVELOPMENT Q8(R2) 2009.

21. Duan, J., K. Riviere, and P. Marroum, In Vivo Bioequivalence and In Vitro Similarity Factor (f2) for Dissolution Profile Comparisons of Extended Release Formulations: How and When Do They Match? Pharmaceutical Research, 2011. 28(5): p. 1144-1156.

22. ASTM, Standard Definitions of Terms and Symbols Relating to Molecular Spectroscopy, in Vol.14.01, Standard E131-90.

23. Brereton, R.G., Chemometrics: Data Analysis for the Laboratory and Chemical Plant. 2003: John Wiley & Sons, Ltd.

24. Reich, G., Near-infrared spectroscopy and imaging: Basic principles and pharmaceutical applications. Advanced Drug Delivery Reviews, 2005. 57(8): p. 1109-1143.

25. Ulmschneider, M., et al., Transferable basic library for the identification of active substances using near-infrared spectroscopy. Pharm. Ind., 2000. 62: p. 301-304.

26. Kramer, K. and S. Ebel, Application of NIR reflectance spectroscopy for the identification of pharmaceutical excipients. Anal. Chim. Acta, 2000. 420: p. 155-161.

27. Sinsheimer, J.E. and A.M. Keuhnelian, Near-infrared spectroscopy of amine salts. Journal of Pharmaceutical Sciences, 1966. 55(11): p. 1240-1244.

28. Lodder, R.A., M. Selby, and G.M. Hieftje, Detection of capsule tampering by near-infrared reflectance analysis. Analytical Chemistry, 1987. 59(15): p. 1921-1930.

29. Morisseau, K. and C. Rhodes, Near-Infrared Spectroscopy as a Nondestructive Alternative to Conventional Tablet Hardness Testing. Pharmaceutical Research, 1997. 14(1): p. 108-111.

30. Ciurczak, E.W., Pharmaceutical mixing studies using nearinfrared spectroscopy. Pharm. Technol., 1991. 15: p. 140-145.

31. El-Hagrasy, et al., Near-infrared spectroscopy and imaging for the monitoring of powder blend homogeneity. J. Pharm. Sci., 2001. 90: p. 1298-1307.

32. White, J., On-Line Moisture Detection for a Microwave Vacuum Dryer. Pharmaceutical Research, 1994. 11(5): p. 728-732.

33. Kirsch, J. and J. Drennen, Near-Infrared Spectroscopic Monitoring of the Film Coating Process. Pharmaceutical Research, 1996. 13(2): p. 234-237.

34. Kona, R., et al., Application of in-line near infrared spectroscopy and multivariate batch modeling for process monitoring in fluid bed granulation. International Journal of Pharmaceutics, 2013. 452(1–2): p. 63-72.

35. Kablitz, C.D. and N.A. Urbanetz, Characterization of the film formation of the dry coating process. European journal of pharmaceutics and biopharmaceutics : official journal of Arbeitsgemeinschaft fur Pharmazeutische Verfahrenstechnik e.V, 2007. 67(2): p. 449-57.

36. Notario, G.F., et al., Extended Release Formulations of Erythromycin Derivatives. 2003, Abbott Laboratories: USA.

37. Suzuki, E., High-resolution scanning electron microscopy of immunogold-labelled cells by the use of thin plasma coating of osmium. Journal of Microscopy, 2002. 208(3): p. 153-157.

38. HortolÀ, P., SEM examination of human erythrocytes in uncoated bloodstains on stone: use of conventional as environmental-like SEM in a soft biological tissue (and hard inorganic material). Journal of Microscopy, 2005. 218(2): p. 94-103.

39. Cappella, B. and G. Dietler, Force-distance curves by atomic force microscopy. Surface Science Reports, 1999. 34(1–3): p. 1-104.

40. Lang, K.M., et al., Conducting atomic force microscopy for nanoscale tunnel barrier characterization. Review of Scientific Instruments 2004. 75(8): p. 2726–2731.

41. Ozturk, A.G., et al., Mechanism of release from pellets coated with an ethylcellulose-based film. Journal of Controlled Release, 1990. 14(3): p. 203-213.

42. Anand, O., et al., Dissolution testing for generic drugs: an FDA perspective. The AAPS Journal, 2011. 13(328-335).

43. MEHTA, A. Animation for the Principle of Fluorescence and UV-Visible Absorbance. 2013; Available from: http://pharmaxchange.info/press/2013/03/animation-for-the-principle-of-fluorescence-and-uv-visible-absorbance/.

44. Lakowicz, J.R., Principles of Fluorescence Spectroscopy. 3rd ed. 2006: Springer.

45. Weber, G., Rotational Brownian motion and polarization of the fluorescence of solutions. Adv. Protein Chem, 1953. 8: p. 415-459.

46. Felton, L.A. and M.L. Baca, Influence of Curing on the Adhesive and Thermomechanical Properties of an Applied Acrylic Polymer. Pharmaceutical Development and Technology, 2001. 6(1): p. 53-59.

47. Boehm, G., et al., Development of the generic drug industry in the US after the Hatch-Waxman Act of 1984. Acta Pharmaceutica Sinica B, 2013. 3(5): p. 297-311.

48. McKinsey&Company, A Review of the Use of Medicines in the United States: Generating value in generics: Finding the next five years of growth. 2013.

49. IMS, Declining medicine use and costs: for better or worse? A review of the use of medicines in the United States in 2012. 2013.

50. Chidambaram, A. Global Generic Pharmaceutical Market - Qualitative and Quantitative Analysis. 2014.

51. Yu, Y. and S. Gupta, Pioneering advantage in generic drug competition. International Journal of Pharmaceutical and Healthcare Marketing, 2014. 8(2).

52. Birkett, D.J., Generics – equal or not? Australian Prescriber 2003. 26(4): p. 85-87.

53. (CDER), F.C.f.D.E.a.R., Guidance for Industry Bioavailability and Bioequivalence Studies for Orally Administered Drug Products — General Considerations Rev 1,. Mar 2003.

54. (CDER), F.C.f.D.E.a.R., Guidance for Industry Bioavailability and Bioequivalence Studies Submitted in NDAs or INDs —General Considerations DRAFT GUIDANCE. 2014.

55. (CDER), F.C.f.D.E.a.R., FDA, Guidance for Industry Waiver of In Vivo Bioavailability and Bioequivalence Studies for Immediate-Release Solid Oral Dosage Forms Based on a Biopharmaceutics Classification System. 2000.

56. J. Duan, K. Riviere, and P. Marroum, In Vivo Bioequivalence and In Vitro Similarity Factor (f2) for Dissolution Profile Comparisons of Extended Release Formulations: How and When Do They Match? . Pharmaceutical Research, 2011. 28(5): p. 1144-1156.

57. Update: Bupropion Hydrochloride Extended-Release 300 mg Bioequivalence Studies. 2013; Available from: http://www.fda.gov/drugs/drugsafety/postmarketdrugsafetyinformationforpatientsandproviders/ucm322161.htm.

58. Lodin, S. Reply to citizen petition: Cardizem CD. Docket no.98P-0145/PRC 1. 2000; Available from: http://www.fda.gov/ohrms/dockets/dailys/00/mar00/032300/pdn0002.pdf.

59. M.A. Katzman, Did a switch to a generic antidepressant cause relapse? Journal of Family Practice, 2008. 57(2): p. 109-114.

Chapter 2 Hypothesis and Specific Aims

2.1 Hypothesis 1

If water can act as a plasticizer for EC curing, and then by measuring films' physicomechanical properties such as tensile and permeability at various relative humidity levels can affect the rate and extent of curing of EC films. This differnet rate and extent of curing can reflect on changes on the extent of coalescence. The extent of coalescence can therefore be quantified by analyzing the physicomechanical properties. This would allow the extent of coalescence to be quantified for the first time in literature if successful.

2.2 Hypothesis 2

If spectral methods of NIR and fluorescence anisotropy can reflect physical and chemical information of the free films then new physicomechanical properties can be accurately predicted from the spectra data and such relationship can be used to further assess the extent of coalescence in curing of ethylcellulose dispersion films and to monitor the changes during curing that no previous methods has been capable of.

2.3 Hypothesis 3

For monolithic single unit extended release tablets, proportionally similar lower strength tablets to the higher strength tablets are not guaranteed to be bioequivalent even if the two possess similar *in vitro* dissolution profiles, and conversely proportionally similar lower strength tablets to the higher strength tablets can still be bioequivalent if the *in vitro* dissolution profiles of the two are different.

2.4 Specific Aim 1: Measure Physical-mechanical Quantities During Curing Process

Use ethanol cast ethylcellulose [11] film as 100% coalesced reference for quantifying the extent of coalescence. Use tensile properties of pseudolatex EC free films to reveal the effect of moisture (both the enviromental humidity and the residual water on the film) on film curing. Measure the water vapor permeability across the free EC films to further investigate and evaluate the curing of EC.

2.5 Specific Aim 2: Spectroscopic Modeling of Properties of Free Films

Collect NIR spectra data of pseudolatex EC free films and the spectral data with the help of chemometric tools to model physicomechanical properties of the free casted EC films so that allowing the films' physicomechanical properties be accurately predicted. Investigate the possibilities of using fluorescence anisotropy to monitor curing process with EC films incorporated with fluorescence rotating probes

2.6 Specific Aim 3: Fluid Bed Coating on Model Drug Beads

To apply ethylcellulose pseudolatex dispersion as a coating agent on MCC beads with colored dye as a model drug to investigate the effect curing on the release performances and as an evaluation of the results obtained with the free films. Then from the release data to obtain a more general description on curing effects on the drug release (possible mathematical equation).

2.7 Specific Aim 4: In Vitro Test on the Oral Extended Release (ER) Products

Prepare of lower and higher strengths tablets by following current manufacturing procedures. Match drug release profile of commercial products. Then compare *in vitro* drug release using f_2 statistic using approved method with 3 pH media (1.2, 4.5, 6.8) per guidance for high and low strength tablets. Finally evaluate *in vivo* performances of the higher and lower strength tablets using available data and compare with the outcome of the *in vitro* evaluation.

Chapter 3 Study of Aqueous Ethylcellulose Films Curing: Part I: Mechanism and Theory

3.1 Abstract

Latex and pseudolatex coating systems have been extensively used in the pharmaceutical industry to replace solvent based coatings that use harmful organic solvents. On issue with latex or pseudolatex coatings is that film formation depends upon latex particle coalescence, and the mechanism of coalescence is not fully understood especially how moisture affects film formation. This study used Aquacoat® ECD, a commercial ethylcellulose (EC) pseudolatex nanodispersion. The goal was to investigate the film curing mechanism with a focus on how moisture affects the free films' physicomechanical properties and to establish a quantification method that is able to assess the extent of coalescence during curing. Ethanol cast films were prepared as the reference to simulate the fully coalesced state. A quantification method using mechanical data was established and can be utilized to assess the extent of coalescence. The water vapor permeability was found to increase with the increase of coalescence of EC films.

Keywords: Ethylcellulose, Film Curing, Mechanical properties, permeability, AFM

3.2 Introduction

In the past, pharmaceutical coating operations were done using polymer solutions, where organic solvents were used to dissolve the polymers and then sprayed onto tablets or beads containing active pharmaceutical ingredients (API)[1, 2]. However, using a

polymer solutions with solvents can be environmentally unfriendly, put facilities and workers at risk for solvent explosions and worker exposure and increase regulatory requirements to ensure the absence of residual solvents[3]. Therefore, in recent years, latex/pseudolatex systems have been extensively used in pharmaceutical coating applications[4, 5]. The films formed with such systems not only provide an alternative to the solvent coating processes, the use of safer and more environmentally friendly aqueous media also allows them to be easily implemented and prepared. Another practical advantage of latex/pseudolatex dispersion is relative higher solid concentration but lower viscosity compared to organic polymer solutions[6].

Despite all the improvements in latex systems, the nature of the latex film formation is not well understood. Differed from organic polymer solution, where polymer molecules all solvated and such films formed upon drying were strong and all polymer chains were entangled throughout. However, with latex dispersions the polymer exists as discrete particles having clear defined particle boundaries. Hence latex film formation requires energy to overcome the surface energy barriers during the spraying and drying phases of coating[5, 7]. During drying, evaporation of water first allows the particles to move close to each other, so particle deforms and form the initial film under the capillary force of water evaporation. Then upon further water evaporation and increase of temperature, this allowed polymer chains to coalesce and to interdiffuse through particle boundaries. This coalescence stage of film formation often called ‘polymer curing’ is where the latex particles coalesce into a uniform film without boundaries between the original latex particles. This process only takes place when the curing temperature is above the

polymer's glass transition temperature Tg. Below the Tg, the polymers existed in 'glassy state' and are unable to coalesce or interdiffuse; above the Tg, polymer existed in a "rubbery state" and the polymer chains possess higher mobility, which allows coalescence out occur[8].

A fully cured polymer film provides optimal protection and stability against the environment whereas incomplete curing can result in polymer aging, which can lead to deviations from the target release profile. Curing is a complex process, over the past years, research has examined how temperature and plasticizers affected curing and hence affect the drug release of coated products[4, 9-13]. However, water is known to plasticize polymers such as methacrylic acid copolymers and ethylcellulose; water affects the polymers relaxation and facilitates the coalescence of polymer particles[11]; many of those studies had not focused on the moisture effects. Our laboratory has been interested in studying the curing phenomena for a long time; in the past Howland et al demonstrated the use of Young's Modulus (YM) to describe the curing for Eugragit polymers (Methacrylic acid copolymers)[14]. However, there were several aspects we can improve upon: 1) there was no references used to assess the 100% fully coalesced state in order to have an estimation on the level of completeness on curing; 2) there was no extensive study on the effect of moisture on the curing.

Based on the previous knowledge, we hypothesize because water is a plasticizer for ethylcellulose (EC), that by measuring a pseudolatex film's physical-mechanical properties cured at various moisture contents, the role of water and extent of coalescence can be quantified. Therefore, the aim of the present investigation is to establish a system

that can be utilized to quantify the extent of coalescence for EC curing using mechanical properties. Ethylcellulose aqueous dispersion was selected as a model system with ethanol cast films as reference for 100% coalesced standard based on the research of Korber et al, where they demonstrated ethanol solution ethylcellulose film would not undergo further coalescence[15]. In preliminary experiments, we noticed that EC pesudolatex film samples with higher coalescence films can have greater water vapor permeability through the films. This contradicted the original expectation that coalescence should increase the moisture resistance. Hence, pseudolatex film permeability to water vapor were also analyzed to further assess this phenomenon. Additionally, atomic force microscopy (AFM) was utilized to study the surface properties under the effect of curing.

3.3 Materials and Methods

3.3.1 Materials

Ethylcellulose (EC) pseudolatex dispersion (30% solid content) Aquacoat ECD 30D was donated by the FMC Biopolymer, Ewing, NJ. lot: JN11823341). Triethyl citrate [16] was donated by Vertellus Inc. (Indianapolis, IN, lot: 116266). Dibutyl sebacate (DBS) wsa purchased from Sigma-Aldrich Inc (Lot: BCBD7540V), sterile square petri dishes (SARSTEDT Australia Lot: 120722) and 70 mm round aluminum pans were purchased from VWR, (Cat.No. 25433-085). Drierite® Calcium Sulphate color indicating desiccants (Sigma Aldrich, Lot: MKBR1419V). Circular punch set were obtained from Neico, (Model: 02614A). Cyanoacrylate Super Glue (LOCTITE, Westlake, OH Lot: 1750270); Nylon membrane with 0.2 μm pore sizes (Waters, Lot T92949). Pure

ethylcellulose powder NF grade was obtained from Dow Chemicals (Midland, MI, Lot: QJ25013T01); Double-sided tape (Scotch, 3M).

3.3.2 Design of Experiments

The process flow diagram for making EC pseudolatex films is outlined in Fig 3.1. The films were analyzed via mechanical and water vapor permeability measurements, as well as atomic force microscopy (AFM). The test methods for the mechanical, and permeability studies are described in sections 3.3 and 3.4, respectively.

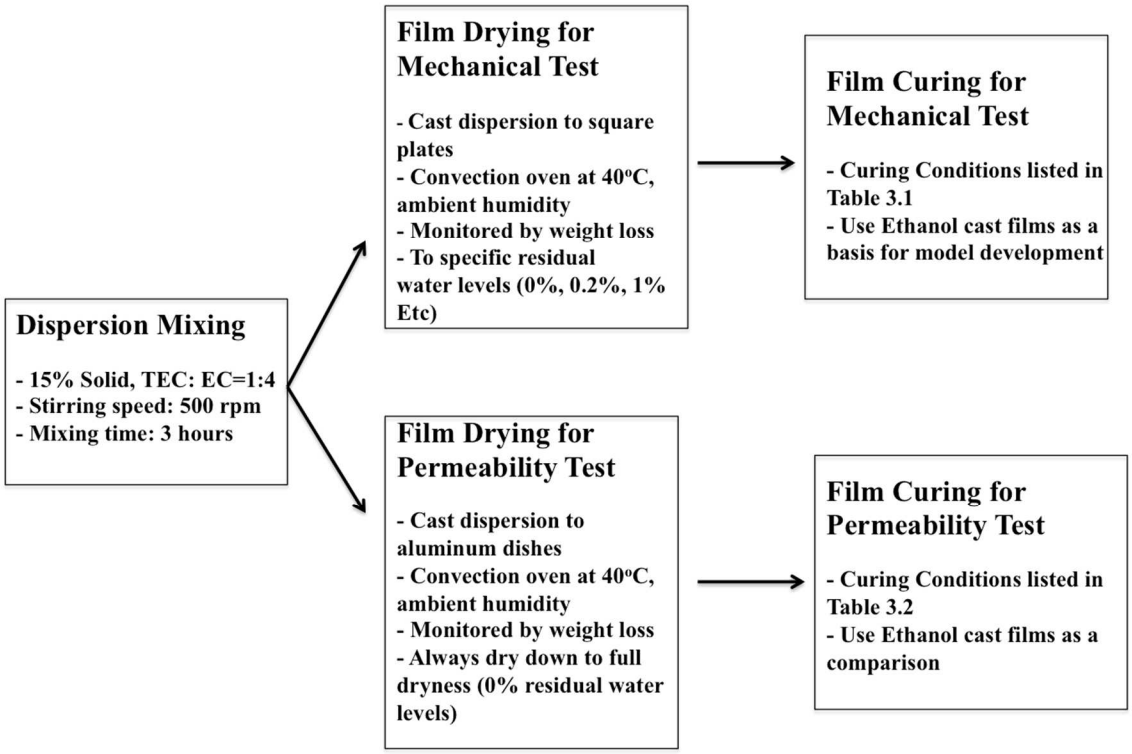

Fig 3.1: Process for EC pseudolatex film investigation.

3.3.3 Mechanical Testing

Film Casting: the EC dispersion (15% w/w total solid content) was prepared by mixing Aquacoat dispersion, TEC and water; the dispersion was mixed for 3 hours using a magnetic stirrer. The amount of TEC added was 25% w/w of the Aquacoat solids content on a dry weight basis. Then the dispersion was cast onto square petri dishes. **Film Drying:** 10 g EC dispersion was cast onto square petri dishes (10 cm ×10cm); the amount was chosen to give the final film thickness to be in the range of 200-300 μm. The dishes containing dispersion were then placed on a horizontal leveling table and dried in 40°C in a convection oven. After drying the stored in a freezer (-20ºC), until used for study. The drying endpoint was determined gravimetrically based upon the theoretical solids content, and this endpoint was confirmed by independent loss of drying (LOD) measurements; i.e. the samples were dried to a target moisture content based upon the theoretical solids content. For these studies the ambient moisture contents (AMC) was the lowest moisture content we could achieve; this was achieved by drying the samples until no further weight loss of cast dispersions can be measured. The LOD measurements were done by using 0.5 g of the dried samples and heated to 105°C over 5 minutes and maintained until no further wright loss was seen. The targeted dry films (0% residual moisture) were evaluated to have LOD of 0.54%. Also, some samples were dried down to a specific residual moisture levels; since the LOD was not able to be done on the samples after drying with residual water levels greater than 0% (because the sample was too wet), therefore the residual water level was used in this investigation, bearing in mind that the LOD and residual water levels do not mean the same thing. The residual water level is defined as the amount of water left over after drying, it is calculated as the percentage of

the total water in the dispersion. For our 10g of dispersion containing 15% solid, therefore there was 1.5g of solid (EC+TEC) and 8.5 water, the 1% of the residual water level therefore means the 1% of the 8.5g of water, which is 0.085g was left over in the system before drying was deliberately stopped.

Ethanol cast EC films were used as the 100% coalesced (fully-cured) reference standard, these films were prepared by mixing powdered pure NF grade ethylcellulose and TEC (4:1) in ethanol to form a solution and then dried under ambient condition. The samples were dried in ambient conditions because drying in a convection oven was too fast and the films had a rippled texture on the surface, and there are safety issues with drying flammable solvents in a convection oven. The thicknesses of the ethanol cast films were controlled between 150-360 μm to assess the thickness effect over a wide range of the films.

Film Curing: The curing conditions for pseudolatex EC films carried out for mechanical tests after drying are summarized in Table 3.1. These parameters were chosen based on preliminary studies; the relative humidity of the curing conditions was controlled using saturated salt solutions. For each film, curing was carried out in humidity controlled desiccators. This experimental plan aimed to investigate the effect of curing time, temperature, humidity and residual water content on film curing. For example, the Gp 2-5 and Gp 10-15 compare specifically the effect of curing time at 60°C with different curing humidities; Gp 16 and 17 investigated the specific effect of residual water levels.

Table 3.1. List of mechanical investigation experiments, compounded groups (eg Gp 2-5) differed only in the curing time

Test Group	Curing Conditions	Residual Water Content	Curing Time/h
Gp 1	No Curing	0	0
Gp 2-5	60°C 30% RH	0	8, 12, 24, 36
Gp 6	60°C 30% RH	0	72
Gp 7	60°C 30% RH	0.22%	72
Gp 8	60°C 30% RH	1.0%	72
Gp 9	45°C 75% RH	0	72
Gp 10-15	60°C 75% RH	0	3, 12, 24, 72, 144, 240
Gp 16	60°C 75% RH	0.5%	24
Gp 17	60°C 75% RH	1.0%	24

Film Testing: Before testing, the pseudolatex EC films were removed from the freezer and allowed to warm up to room temperature for at least 30 min but not more than 90 min. Then films were removed carefully from the Petri dishes with a sharp knife. The whole film from each Petri dish was then cut into rectangular strips with dimension of 1 × 7 cm; each of these strips were then stamped out using the ASTM D-638-V 'dogbone' punch into the final shape, see Fig 3.2A. The "dogbone" shape was used because the rectangular strips tend to break at the grips and not generate reproducible consistent results. The tensile tests were performed using Instron® 8521 System with a Tension/Compression 100 N Load Cell. For each test, the sample strip thickness was measured and then

clamped vertically between G227 Lightweight Screw Vise Grip and J227 Jaws as outlined by ASTM D882; see Fig 3.2A and 3.2B.

The grip separation (speed) in each test was a constant 0.5 mm/min; this rate was obtained through preliminary testing of the films for all the curing conditions. For each specific group, at least 5 samples were tested. The Instron system measures the forces and the film extension (elongations). The tensile strength (**TS**), percent elongation at break (**PEB**) and Young's Modulus (**YM**) were calculated using equations Equation 1, 2 and 3, respectively.. The TS is the ultimate stress (σ) calculated by dividing the load at break (F_b) by the initial cross-sectional area whose thickness and width is denoted by h_0 and w_0. The strain $\boldsymbol{\varepsilon}$ is calculated by the ratio of the change in length divided by the original length of the specimen ($\Delta L/L_0$). L_0 is the original gage length, measured in mm; ΔL_b is the extension of the sample at the point of break. For the ASTM D638 "dogbone" design, L measures 7.62 mm.. Young's modulus is calculated from the initial linear portion of the stress (σ) strain (ε) curve. The ethanol cast films were also cut in the same way to produce 'Dogbone' shape specimens and were analyzed in the same way. The regression analysis for linear model was used SAS® statistics software v9.3.

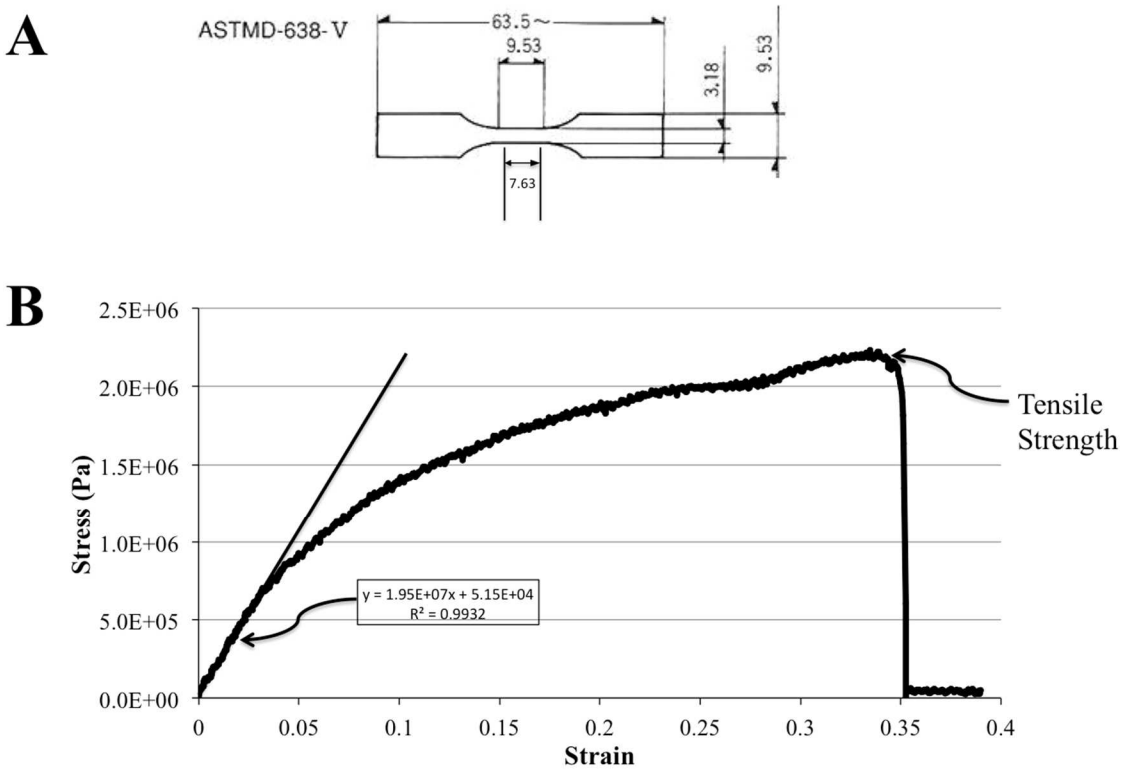

Fig 3.2A: the "Dogbone" design of the ASTM D638-V, unit in mm, and B: a representative stress vs strain profile of Gp10 (curing at 60°C 75% for 3 hr) for analysis of a cured film cut into the "dogbone" shape with Young's Modulus being 1.95E+07 Pa

Tensile Strength: $\sigma_b = \frac{F_b}{h_0 \times w_0}$ Eq.1

PEB $= 100 \times \frac{\Delta L_b}{L_0}$ Eq.2

Young's Modulus $= \frac{d\sigma}{d\varepsilon}$ Eq.3

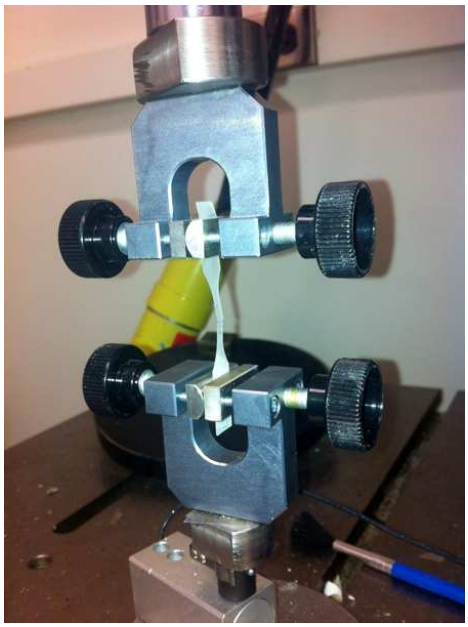
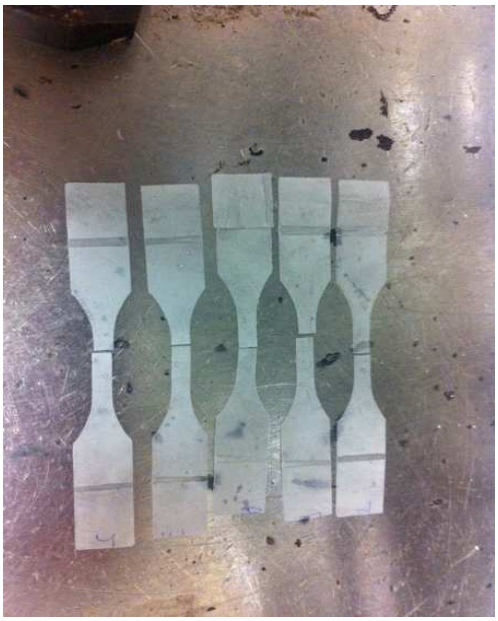

Fig 3.3A (left) and 3.3B (right): the configuration of the Instron® and the strip breaking points, which all strips broke relatively at the center position, this provided consistency and reliability for mechanical measurements.

3.3.4 Permeability Testings

Film Casting: the EC dispersion (15% w/w) was prepared as described previously in the mechanical test section, and the compositions were the same, see Table 1. After stirring, 6 g of the EC suspension was cast into an aluminum pan. **Film Drying:** the pans containing dispersions were then placed on a horizontal leveling table and dried in 40°C in a convection oven to maximum dryness (as described above, i.e., until no further weight loss was observed) to produce the films with thickness in the range of 200-300 μm. Ethanol cast EC films were also prepared by casting the EC dispersions into aluminum pans and the target film thickness was around 250 μm. **Film Curing**: conditions used for curing dried pseudolatex EC films for permeability tests were listed in Table 3.2. The study investigats the effect of curing temperature (50 vs 60°C), plasticizer type (TEC vs DBS) and curing humidity (30 and 75% RH) on curing. Note the "LH" label in the curing condition means the curing was carried out in ambient humidity

with no control; for the curing temperatures used the relative humidity was very low, measured to be 3-5%, hence "LH" was used to describe the was a low humidity in the environment. The experimental groups in Table 3.2 were combined based on the same curing conditions but differed in the curing time. One special curing group (Gp 40) was created to analyze the effect of surface exposure to the moisture. Nylon membranes were placed directly on top of films to be measured, as shown in Fig 3.4. The reason to cover films with nylon membrane was to investigate how direct exposure to water above the film is able to affect the outcome of vapor permeability. By using such membranes, it did not change the equilibrium between the film and its curing environments; however, it provided a barrier for the water directly interact with the films surface..

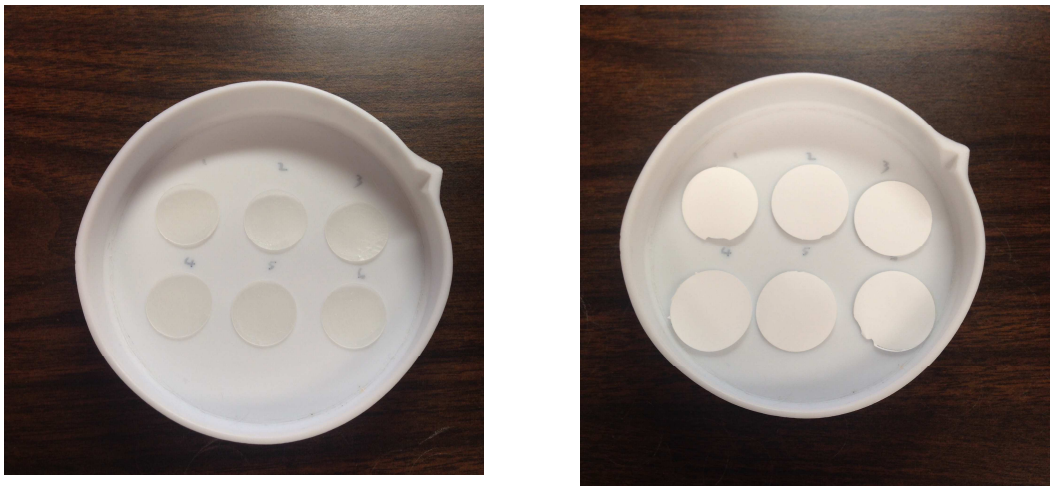

Fig 3.4A: The normal film curing setup with 6 pseudolatex EC dry films for permeability test; Fig 3.4B: the set up for same dried EC films but with covered nylon membranes above the film specimen for permeability measurements.

Film Testing: Permeability was calculated based on the equation below (Eq.4):

Permeability: $$P = -\frac{dM}{dt}\left(\frac{h}{A \cdot \Delta p}\right)$$ Eq.4

Where P is the water vapor permeability; dM/dt is the rate of moisture crossing the film in terms of weight; h is the thickness of film; A is the surface area of the film; Δp is the

difference in vapor pressure across the film. The testing method was based upon ASTM E-96 weight gain method [17]. The original ASTM vapor transmission were carefully considered and then modified because of several difficulties in: 1) ASTM measurement requires using an analytical balance throughout the course of one measurement, which is time consuming and cannot be reproduced easily; 2) It requires large film samples (d≈11 cm); 3) Permeability was highly sensitive to the environmental conditions; no constant reading will be achieved without controlling the environmental humidity and temperature.

Table 3.2. The curing conditions used for Permeability Experiments

Test Group	Curing Conditions	Plasticizer	Curing Time (h)
Gp 18	Dry (No Curing)	TEC	0
Gp 19	Dry (No Curing)	DBS	0
Gp 20-22	50°C LH	TEC	0.5, 2, 4
Gp 23-26	60°C LH	TEC	0.5, 2, 4
Gp 27-29	50°C 30% RH	TEC	0.5, 2, 4
Gp 30-32	60°C 30% RH	TEC	0.5, 2, 4
Gp 33-35	50°C 75% RH	TEC	0.5, 2, 4
Gp 36-38	60°C 75% RH	TEC	0.5, 2, 4
Gp 39	60°C 75% RH	DBS	4
Gp 40	60°C 75% RH with Nylon Membrane	TEC	4

All permeability studies were conducted using glass scintillation vials (20 mL, 1.55 cm diameter of the opening of the vials)to test the water vapor permeability through free films. Each vial contained 15 g Calcium Sulphate with color indicated desiccants. The dred films were cut into small round pieces by a round hollow punch (diameter 0.78 inch). The films were then glued to the opening of each glass vile with cyanoacrylate glue to provide a completely tight air seal. To measure the permeability, all the films were placed in 75% relative humidity controlled desiccator (Set up shown in Fig 3.5A and 3.5B, the 75% RH was provided with saturated sodium chloride solution). The desiccator was then

placed into a temperature controlled oven at 28°C to allow a constant moisture transfer. The 28°C was selected to be used because it is higher than room temperature around 25°C so that water transmission can be speed up, on the other hand, it is below the galss transition of the film which is around 35°C so the polymers cannot be going to the rubbery state, This method allowed for tight control of the surface area A, the difference in vapor pressure Δp and temperature. The measurements were carried out by monitoring the weight gain of the vial over at least one day period to determine directly the mass transport of moisture: dM/dt. The first weight measurements were taken at least 2 hours after the set up in order for the vapor transfer to reach steady state; preliminary results showed this was the time it took to reach steady state. Each film measurements were repeated with at least six time, n= 6 and the experiment run time was for at least 24 hours so that several weight measurements can be collected to provide a better estimation of the permeability. The water vapor permeability for ethanol cast EC films were determined using the same experiment set up

Fig 3.5A(Right): Colored indicator and glass vial used for permeability test; Fig 3.4B(Left): the 75% humidity controlled desiccator containing vials with films glued on top which created a constant humidity difference and provided a constant driving force for vapor transmission.

3.3.5 Surface Experiments

The film surface roughness was measured by Atomic Force Microscopy (AFM Asylum Research, Model: MFP-3D-BIO), and the AFM probe used was silicon probe, Al reflex coated, purchased from Olympus (Cat. No. AC240TS-10, tip size: 9 nm). The measurements were performed with tapping mode. The samples for AFM measurements were carried out on selected dry film samples and film cured at 60°C 75% RH for 3 days (Gp13) and dry film (Gp 1). Sample specimen was peeled from the square plate and then adhered to glass plate using double sided plate so it would not move during measurements. For each tested group, AFM measurements were made on height retrace and amplitude retrace. The scanned area was fixed to 20μm ×20μm. The average surface roughness measurements were carried out on 6 sample films, and each film had 2 repeat measurements.

3.4 Results

In this section, the analysis begins with the mechanical evaluation of ethanol cast EC films, which will serve as a basis for calculating the extent of coalescence for pseudolatex EC films. Then the mathematical model is used for the evaluation on pseudolatex EC films, analyzing important factors during curing. Then water vapor permeability of pseudolatex films is given, as a further evaluation of the mechanical results. Finally the surface properties were assessed using AFM.

3.4.1 Analysis of Mechanical Properties

Quantification of the Extent of Polymer Coalescence Using Ethanol Cast Films

A completely cured EC pseudolatex films should have the highest Tensile Strength (TS) because of a higher degree of polymer chain entangled, and should have the lowest Young's Modulus because the more coalesced polymer chains reduces stiffness of films so that films are more flexible. The complete cured films should also have the highest Percent Elongation of Break (PEB) because of the improved flexibility due to coalescence. This was demonstrated for our EC pseudolatex dispersion films in our studies, for a dry, uncured film, the TS was found to be 1.85±0.16 MPa, YM of 31.5±1.8 MPa and PEB of 9.6±1.4%; whereas for films cured at 60°C, 75% RH, the values of the three becomes: TS of 2.06±0.15 MPa, YM of 19.3±2.0 MPa and PEB for 42±3.7%, consistent with the statement previously. When working with a latex film, knowing what the fully cured state is, can be hard to determine, because it depends upon many parameters such curing time, temperature, moisture content and plasticizer content. However, working with ethanol cast films could provide a consistent reference frame for which to evaluate the extent of coalescence, because the polymer chains are completely dissolved in the ethanol and dried, there is no coalescence and the degree of polymer entanglement would be consistent, i.e., solvent casting would produce films with a consistent degree of entanglement, which would be easier to reproduce experimentally. Thus, we started our mechanical investigations with ethanol cast films because ideally, those films should provide the highest TS, lowest YM and highest PEB. These quantities can be used either collectively or individually as 100% coalesced reference standard for pseudolatex dispersion films. Also it is necessary to take thickness into account: unless

thickness is accounted for, it is useless to compare TS, YM or PEB between ethanol cast films and pesudolatex films. Therefore, a range of ethanol cast films were first generated (150-360 μm) to study how the thickness affect the mechanical properties and how these mechanical properties can be used further to quantify the extent of coalescence in curing.

The PEB data of ethanol solution cast EC films were insensitive to thickness variations, with all the films having the extension around 40%. Therefore, PEB cannot be used as a potential predictor for extent of coalescence due to this insensitiveness. A different result was observed after analyzing the values of TS and YM. As stated before, TS is higher when the extent of coalescence is greater; and on the contrary, YM is lower when extent of coalescence is greater. Hence the ratio of the two, $\frac{\mathrm{TS}}{\mathrm{YM}}$, should be highest for completed coalesced ethanol cast films. In other words, for a given thickness of one pseudolatex dispersion film, the value of $\frac{\mathrm{TS}}{\mathrm{YM}}$ is always going to be lower than that of ethanol cast films at the same thickness. The value of $\frac{\mathrm{TS}}{\mathrm{YM}}$ is greatest for the ethanol cast films and no pseudolatex dispersion films could have values exceed this ideal value. Harris et al also used this quantity $\frac{\mathrm{TS}}{\mathrm{YM}}$ as an indicator for crack resistance for pseudolatex dispersion films made with Eudragit, but no further analysis was carried out for this ratio. After regression analysis, it was found this ratio had a good linear correlation with the film thickness, see Fig 3.6.

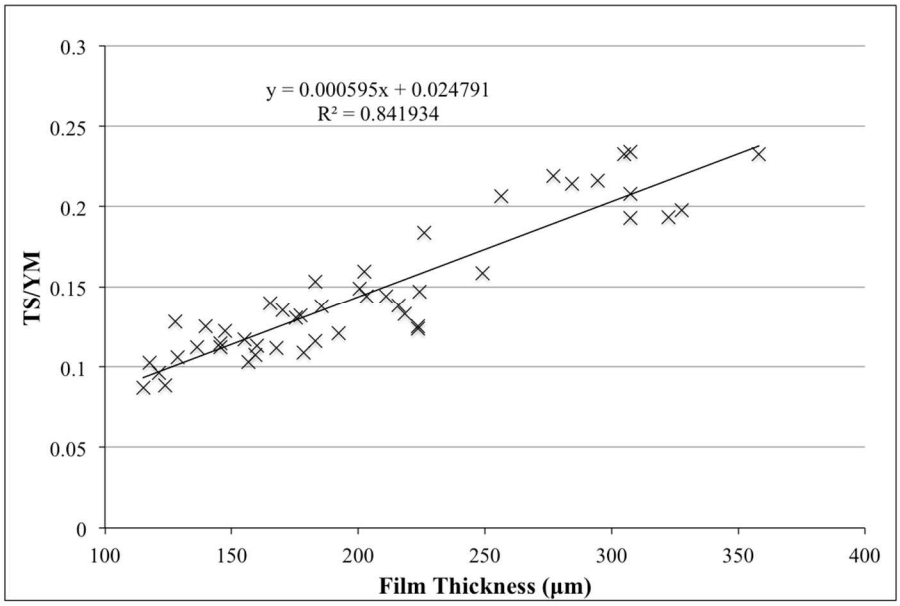

Fig 3.6: Plot of the ratio of TS/YM of the ethanol cast films versus the film thickness. The linear relationship can be used to estimate the TS/YM for pseudolatex films at a given thickness with the range of this linear relationship.

To assess the regression model, we tested the null hypothesis that the slope equals 0; the F statistic equaled to 239.7, and the t-statistic was 15.5. In both cases, the p-value is less than 0.001. Indicating the statistically significance correlation between the $\frac{\mathrm{TS}}{\mathrm{YM}}$ ratio and the film thickness. Although the R^2 value was slightly low (below 0.9), this can be attributed to the noisy data generated by manual operation during film drying, cutting and carry out the mechanical tests.

This mechanical linear relationship generated from ethanol cast films was used as the 100% theoretical coalesced reference state for estimating extend of coalescence in the pseudolatex EC films. For a given pseudolatex film "dogbone" specimen with thickness h, the theoretical 100% coalesced value of TS/YM was determined using Eq.5:

$$\frac{\mathrm{TS}}{\mathrm{YM}} = 0.000595\mathrm{h} + 0.024 \qquad \text{(Eq.5)}$$

And the measured TS/YM value of the pseudolatex dispersion films was divided by theoretical 100% coalesced value to obtain an estimated extent of coalescence, expressed as percentages.

As mentioned previously, the other important property commonly used to estimate the extent of coalescence was percent elongation at break (PEB), which was also expressed as percentages and this quantity was also measured as a check value for extent of coalescence estimated from TS/YM.

Effect of Time and Relative Humidity on Curing Pseudolatex Dispersion EC Films

Using the relationship obtained earlier (Eq.5), the estimated extent of coalescence, as well as the PEB values for pseudolatex EC films Gp1, 2-5 and 10-15 are shown in Fig 3.7 and 3.8. Both values are expressed as percentages. Samples for Fig 3.7 were measured at 30% RH and Fig 3.8 at 75% RH. Both figures also assessed the effect of curing time. For each figure, the control was the Gp 1, which was the dry film without undergoing any further curing treatment.

The dry pseudolatex EC films had estimated coalescence of 38% and PEB of 10%, red from the first column in Fig 3.7. When the relative humidity is low, at 30%RH, it is expected the extent of coalescence to be lower, and indeed this was what the data shown. For Gp2-5, there is little difference on the estimated extent of coalescence comparing to the control group (Gp1). The PEB data agreed with the estimated coalescence extent. However, for pseudolatex films cured at 60ºC/75% RH (Fig 3.8), estimated coalescence increased dramatically from 38% and quickly reached a steady state within after 3 h at

around 62%; the difference is significance between the 2 groups (Gp1 and Gp10). Then after 3 hours, both quantities remained relatively unchanged up to 10 days. In this higher environmental humidity, films would undergo a greater extent of coalescence. These findings suggested RH is the crucial factor affecting the extent of coalescence. Temperature along without sufficient environmental moisture cannot reach the same extent of coalescence.

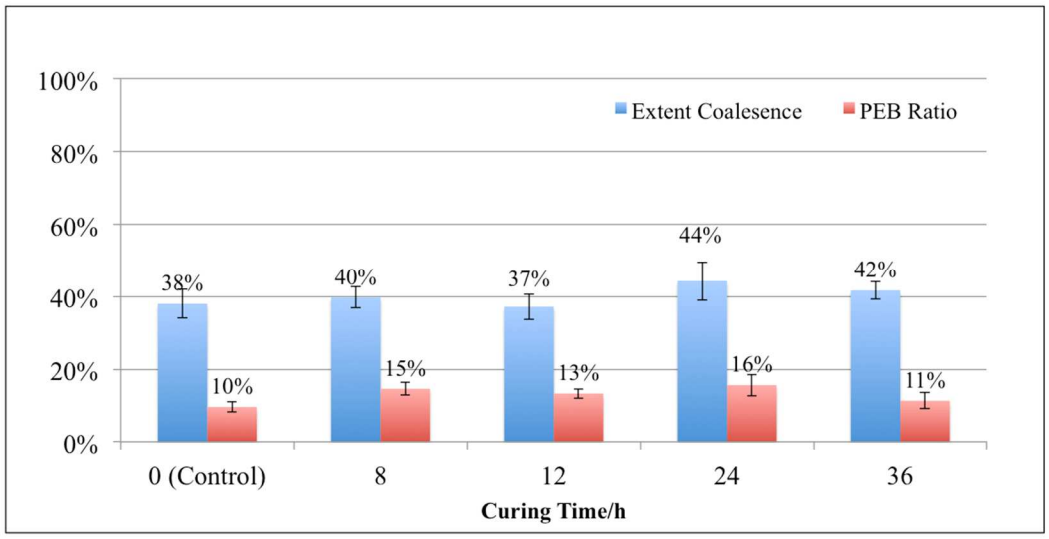

Fig 3.7: Analysis of Gp 1-5: Plot of curing extent and elongation at 60ºC 30% RH. The Control is Gp1, n is in the range of 4-6. Statistical analysis on both extent of coalescence and PEB did not reveal significant difference for the 6 data sets compared to the 0 (Control) group.

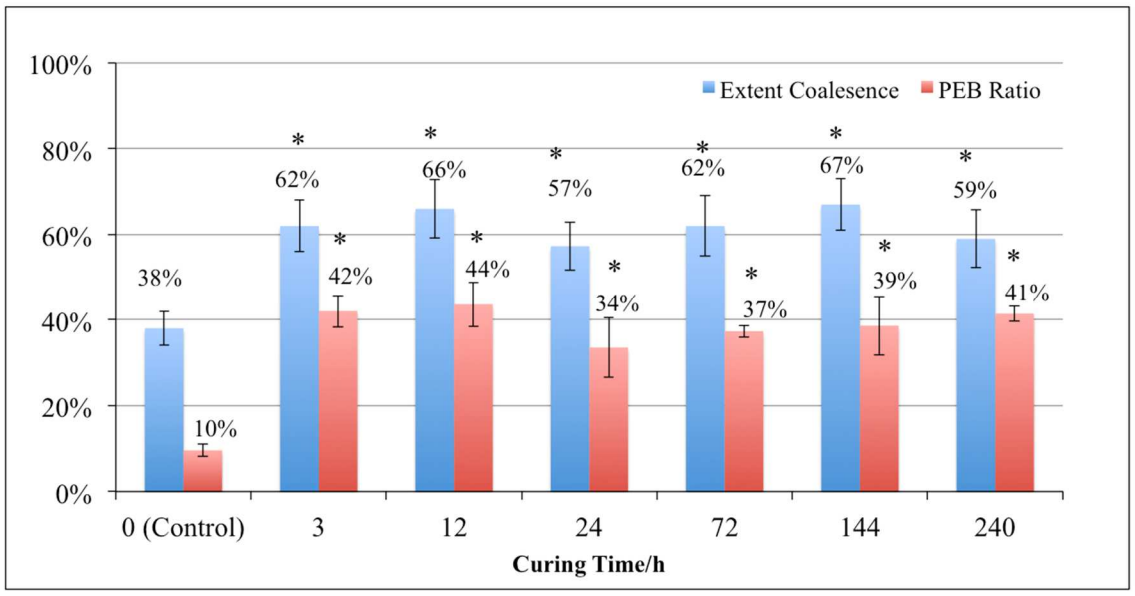

Fig 3.8: Analysis of Gp 1, 10-15: Plot of curing extent and elongation for pseudolatex films over extended period for 60ºC/ 75% RH for up to 10 days (240 hours). The values shown were mean ±SD with n in the range of 5-7 for test groups. The * indicates the statistical significance ($p<0.05$) compared to the 0 (Control) group. The statistical analysis was carried out by One-way ANOVA test with post Dunnett's multiple comparison test with the 0 (Control) group with GraphPad Prism 6.0.

Effect of Residual Water

The effect of residual water levels (explained earlier in method section 3.3.3, represented with %R) was shown in Fig 3.9 and 3.10 with the estimated coalescence, and PEB for Gp 7-9 and Gp 13, 16, 17, respectively. In Fig 3.9 (Gp7-9), by our estimation method (Eq.5), it can be seen clearly the importance of the environmental humidity: when the relative humidity is low at 30% RH, the residual water played a significant role in the extent of coalescence. The increase from 0.22% to 1% can increase the estimated extent of coalescence from 35% to 55%. When films were cured at a higher humidity (75% RH, Gp9), even lower temperature (45ºC) can achieve adequate level of coalescence (53%). In Fig 3.10 (Gp 13, 16, 17), with curing at 60ºC 75%, we do not see significant difference in the estimated extent of coalescence across these three groups despite the

residual water levels. In these two figures, the estimate on coalescence and PEB values were also in good agreement.

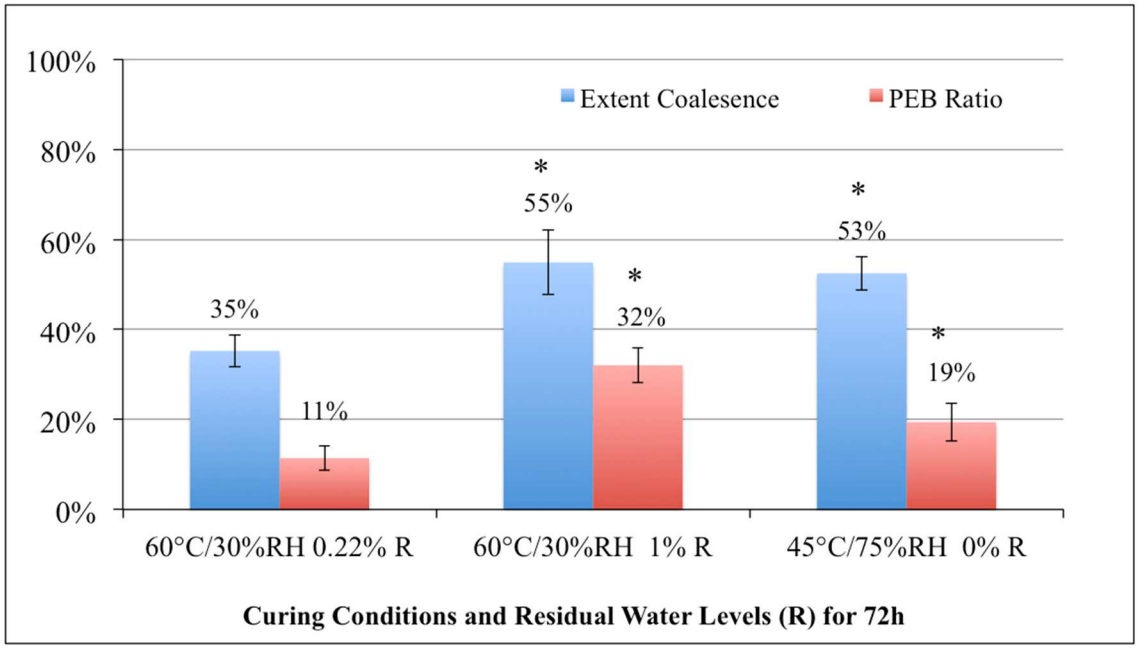

Fig 3.9: Analysis of Gp 7-9: Plot of 72h curing with different residual water levels (%R) and. The values shown were mean ±SD with n in the range of 5-7 for test groups. The * indicates the statistical significance ($p<0.05$) compared to the Gp7 (the films cured at 60°C 30% RH with 0.22% residual water. The statistical analysis was carried out by One-way ANOVA test with post Dunnett's multiple comparison test with the Gp7 (GraphPad Prism 6.0).

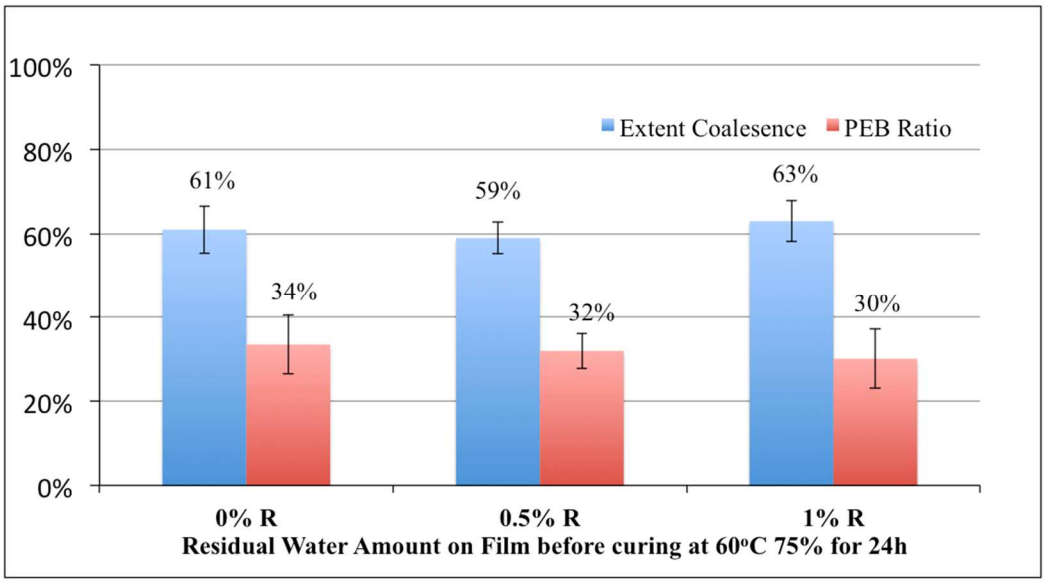

Fig 3.10: Plot of Gp 13, 16, 17: Plot of 24h curing with curing conditions of 60°C and 75% RH for 24 hours at different residual water levels (%R). The values shown were mean±SD with n=5 for all three groups. Statistical analysis of the extent of coalescence and PEB for the 3 data sets did not reveal significant differences (GraphPad Prism 6.0).

3.4.2 Permeability Measurements

Vapor Permeability of Ethanol Films and Pseudloatex Films with DBS and TEC as Plasticizers

As stated before, preliminary results showed the water vapor permeability had an increasing trend with the increase of extent of coalescence. In order to systematically study this, the ethanol solution cast films were prepared once again as the 100% coalesced reference to evaluate the phenomenon. The Comparison between the Ethanol film and the dry pseudolatex dispersion film (Gp18) was shown in Fig 3.11A.

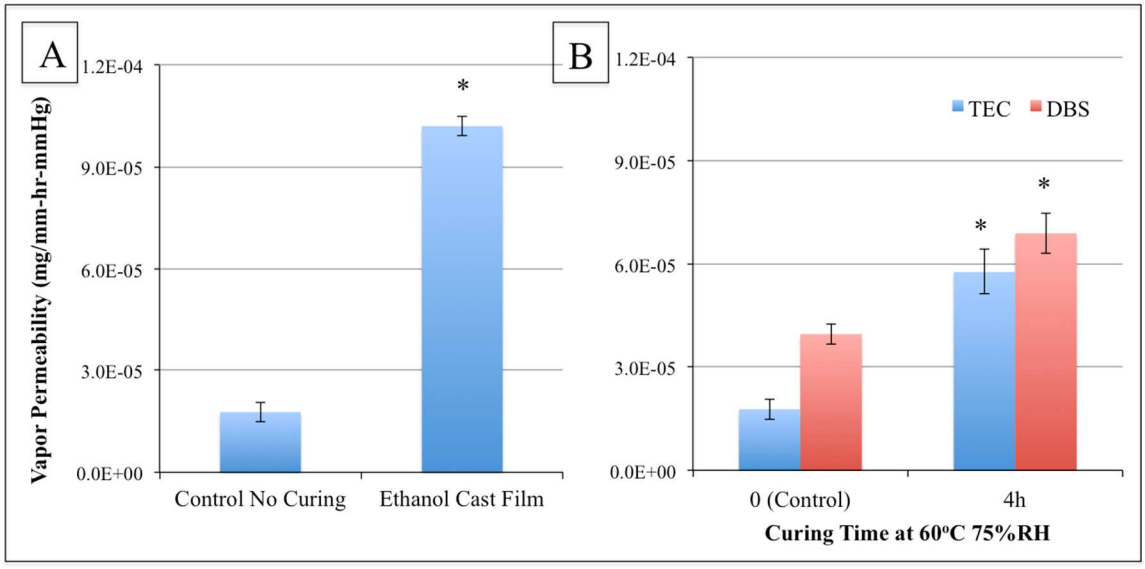

Fig 3.11A: Permeability of dry pseudolatex films (Gp 18) compared with ethanol cast films with TEC as plasticizers (n=6); 3.11B: Comparison of pseudolatex films made with TEC and DBS as plasticizers (n=6), with the lowest (dry films Gp18, 19) and highest coalescence (Films cured at 60°C 75% RH for 4 hours Gp38, 39).The values shown were mean±SD.The statistical analysis of paied t-test showed the difference was significance ($p<0.05$) for ethanol cast film and high coalesced films copared to control groups respectively (MS Excel).

The control group for permeability measurements is the TEC pseudolatex EC films. It is obvious that EC ethanol cast films had much higher water vapor permeability than the dry pseudolatex EC films with TEC as a plasticizer (p-value of t-test is 4.97×10^{-8}). Fig 3.11B compared the difference of films cured under 60°C 75% with the dry films for both TEC and DBS pseudolatex films (Gp18, 19 and Gp38, 39). For both plasticizers, the increase in vapor permeability after 4h of curing was significant: p-value for t-test of TEC films was 5.87×10^{-4} and 2.90×10^{-6} for DBS films.

Factors Affecting Water Vapor Permeability

Similar to previous mechanical tests, relative humidity, temperature and curing time were then evaluated to better understand the performance of the curing process with permeability as the indicator of the extent of coalescence for pseudolatex EC films. The

previous mechanical tests indicated the curing for peudolatex films with TEC as plasticizer can reach a steady state in the first 3 hours of curing under 60°C 75%RH, the estimated coalescence went from 38% to 62% (Fig 3.8). Based on this observation, the curing time was kept shorter for up to 4 hours for permeability investigations. It is important for pharmaceutical industry to shorten the curing time for pharmaceutical coating in order to save unnecessary energy spending. By keeping the curing time under 4h allowed us to focus how fast coalescence can reach steady state. In addition to the curing temperature of 60°C used in previous mechanical tests; 50°C alongside with 60°C to assess if this reduction in temperature can still produce the same outcome.

The results for permeability study with varying curing conditions were listed in Fig 3.12-3.14, TEC pseudolatex films cured at 2 different temperatures and 3 different humidity environments for the duration of 4 hours were plotted. Note the value for 0h permeability is the same as the control group in Fig 3.11, which is the dry film without further curing (Gp18). It can be noticed from the figures that, same as the mechanical properties, at low humidity environment (relative humidity below 30%), the permeability had hardly any changes for either group cured at 50 or 60°C (Fig 3.12, 3.13). Despite the films cured at 30% (Fig 3.13) had more fluctuation than the group cured at LH (ambient humidity, Fig 3.12), statistical calculations with t-test did not show significant difference in vapor permeability after 4 hours of curing.

The difference in permeability were observed in groups cured at 75% RH (Fig 3.14), both groups had significant changes in permeability over 4h; the p-value for t-test for 0h

and 4h for curing at 50°C 75% RH is 0.000107 and as stated before, the p-value for 4h curing at 60°C 75% is 5.87×10^{-4}. Interestingly, despite the permeability for films cured at 50°C 75% (Gp33-35) increased less quickly than films cured at 60°C 75%, the statistical analysis showed there is no significant difference (p-value= 0.3) in permeability between the films cured for 4h with 60 and 50°C (Gp35 and Gp38).

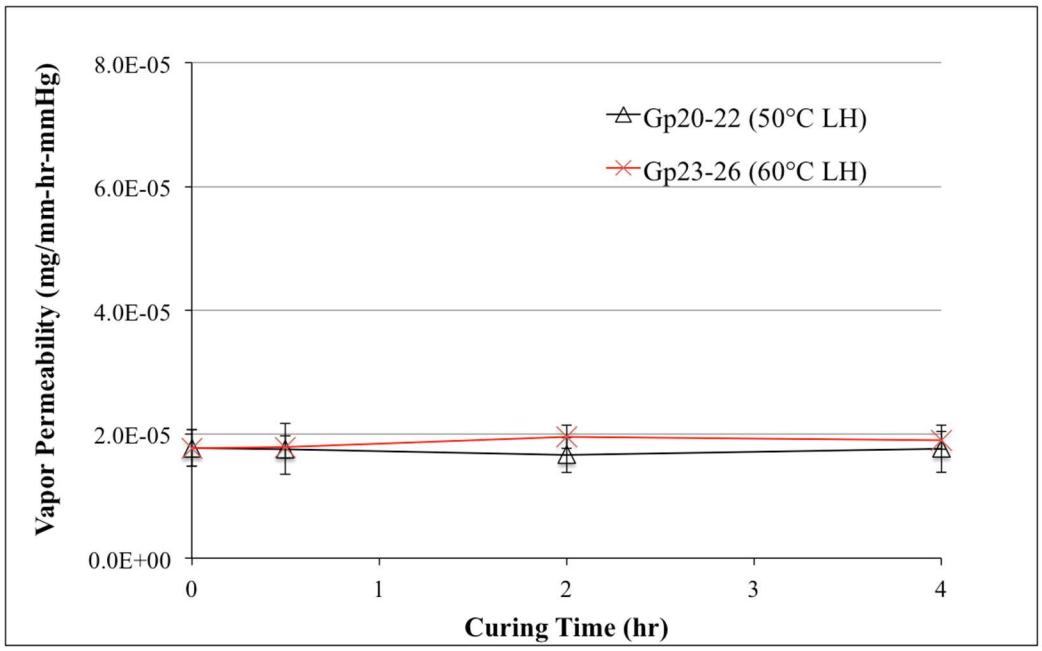

Fig 3.12: The permeability of pseudolatex films cured at ambient humidity (LH) at 50 and 60°C (Gp20-26, with Gp18 as control at 0 hr) for up to 4 hours. The values shown were mean±SD with n=6. There is no change of vapor permeability when cured at this condition.

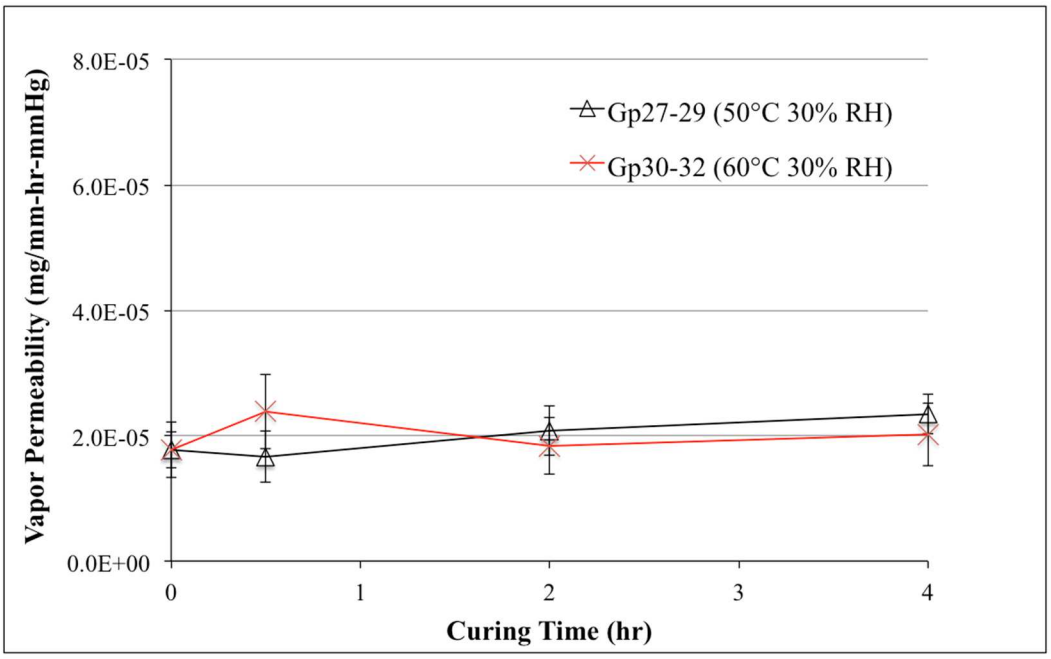

Fig 3.13: The permeability of pseudolatex films cured 30% RH at 50 and 60°C (Gp27-32, with Gp18 as control at 0 hr) were monitored up to 4 hours. The values shown were mean±SD with n=6. There is no change of vapor permeability when cured at this condition.

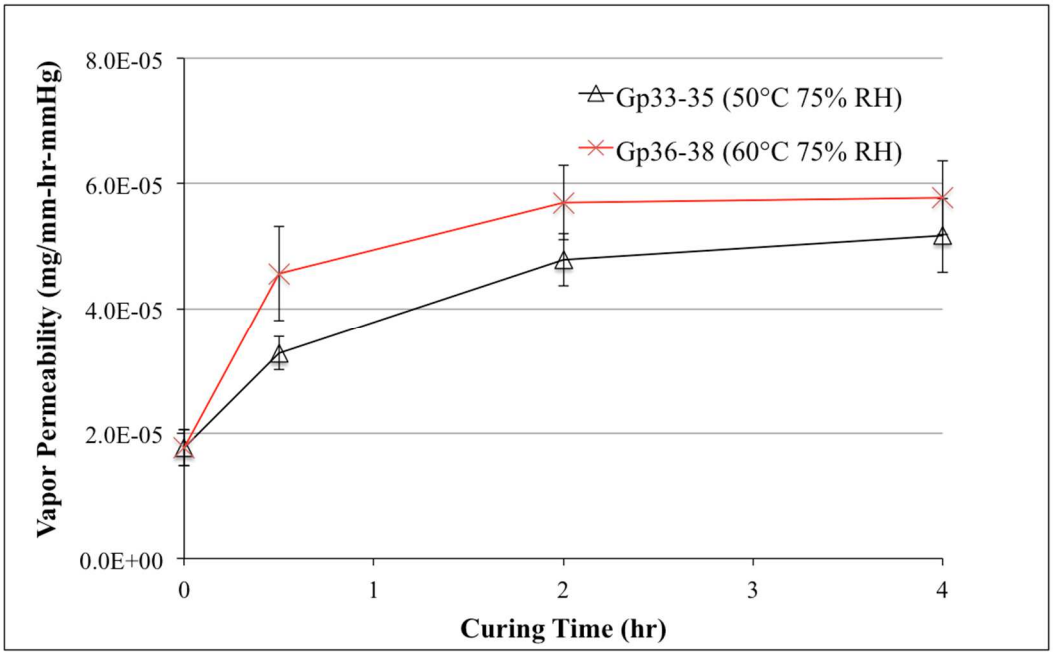

Fig.3.14: The permeability of films with 75% RH at 50 and 60°C (Gp33-38, with Gp18 as control at 0 hr) were monitored up to 4 hours. The values shown were mean±SD with n=6. The films cured at 60°C were shown to have increased faster initially and reached the permeability plateau faster than 50°C.

Surface perturbation using Nylon membranes were then evaluated (Gp40) and the results shown in Fig 3.15. The reason of this set of tests was to alter the rate of water molecules interact the films' surface but at the same time, still maintained the environmental humidity. Since nylon membranes did not completely seal the surface of the pseudolatex film samples underneath it, we can assume that the presence of such nylon film did not alter the humidity we previously set at (75% RH). In Fig 3.15, the first 3 columns represent samples cured with no nylon membrane at 60ºC 75%; the results were similar to Gp36-38 in Fig 3.13. For the final column, the experiment was done in such a way that the film was first cured without nylon membrane for 30 min, then for the next 3.5 h films covered with nylon films. If there were no nylon film covering film, we would expect the final column being exactly equal to the column 3 under 4 hour curing. In reality, the final column presents a significant difference to column 3.

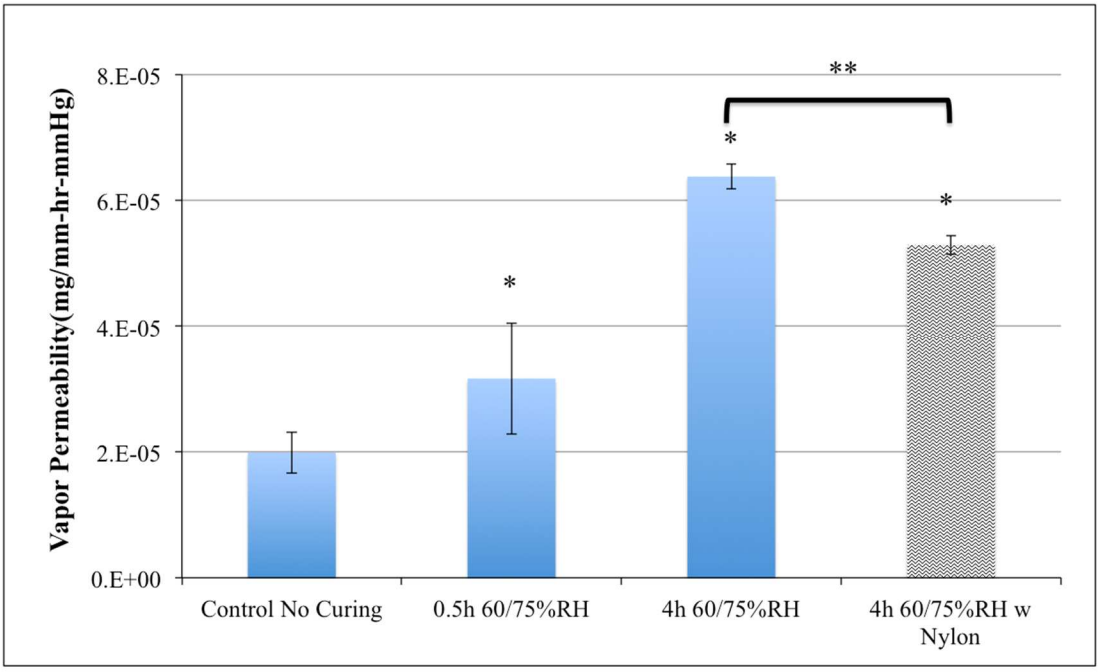

Fig 3.15: Gp40 analysis: Permeability of pseudolatex films with cured at 60°C 75% RH for up to 4 hours. One group covered with nylon membrane for 3.5 hours after first 0.5 hour for up to 4 hours with treatment involving nylon membranes. The values shown

were mean±SD with n=6 for all three groups. * Indicates the significant difference to the Control No Curing group ($p<0.05$) and the** indicates the significance between the nylon covered group and non-covered group, both cured for 4 hours ($p<0.05$). The statistical analysis was carried out by One-way ANOVA test with post Tukey's multiple comparison test (GraphPad Prism 6.0).

3.4.3 Surface Roughness Measurements By AFM

The surface properties measurements were aimed to elucidate further details of the curing process and would served as a tool for further in-depth understanding of the curing process. The images of the dry TEC film and 3 day coalescence under 60ºC/75% RH (Gp1, 13) are shown in Fig 3.16, the average Root Mean Square (RMS) peak-to-valley distance along z axis of the film surface showed a significant difference of films before and after curing treatment (p-value of t-test is 0.00047). The surface of the film was relatively smooth at the beginning and became rougher once it was undergo substantial curing treatment under 60ºC 75% RH.

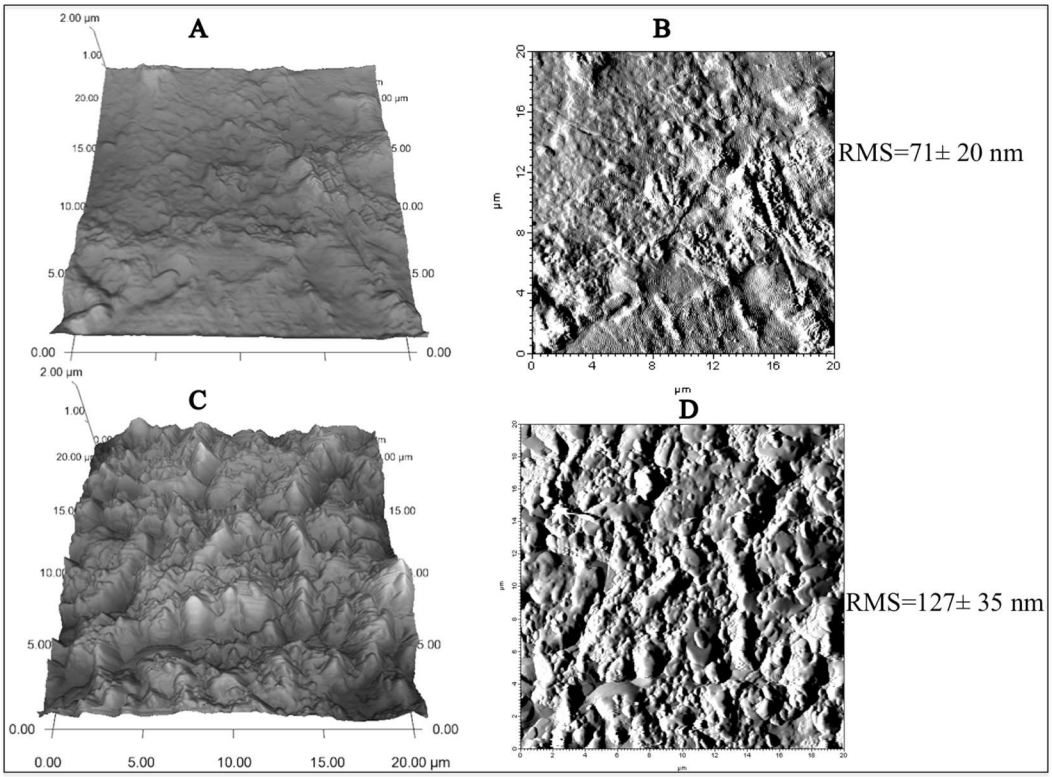

Fig 3.16: AFM Photos of Gp1 and 13: Height retrace and amplitude retrace of the surface of dry film before curing (Gp1: **A and B**); height retrace and amplitude retrace of the surface of 3 day curing at 60ºC/75% RH (Gp13: **C and D**). The root mean square (RMS) distance were shown by mean±SD with n=6. The graph showed the higher coalesced films had a rougher surfaces than the films that was not cured at low extent of coalescence.

3.5 Discussions

3.5.1 Quantifying Extent of Coalescence using Mechanical Properties

Tensile Strength (TS), Young's Modulus (YM) and Percent Elongation at Break (PEB) are important indicators for assessing the extent of coalescence for perudolatex EC films curing. TS and YM represent the two aspects of films that would undergo substantial changes during curing: the strength and the flexibility. The ratio of TS and YM should provide the highest value for ethanol solution cast films because no further coalescence is possible. The PEB was also an important indicator for the extent of coalescence, but

because it is not sensitive to thickness, it cannot be used to predict coalescence for pseudolatex films. The regression analysis (Fig 3.6) and the establishment of Eq.5 provided an opportunities that extent of coalescence can be estimated from the physical-mechanical properties from the free films. Previous studies, often uses the drug performances to evaluate the extent of curing, but lacks the study on fundamental physical properties on the film itself[4, 18]. This relationship (Eq.5) was then used for estimating extent of coalescence for pseudolatex films and PEB values were also recorded as a check for this method of estimation.

At low relative humidity 30% or below (Fig 3.7), the estimated coalescence provided by the ratio $\frac{\mathrm{TS}}{\mathrm{YM}}$ were relatively unchanged (estimated to be around 40%) for 36 hours and PEB values were also fluctuated between the ranges of 10-16%. When the temperature is the same (60°C) and the relative humidity increased to 75% (Fig 3.8), we observed a significant increase in both the estimated coalescence (from 38% to 62%) and PEB also increased dramatically from 10% to 42% in the first 3 hours. Again, the results of estimated coalescence and PEB values were in good agreement hence it is can be said with confidence that by using the linear relationship (Eq.5) developed using $\frac{\mathrm{TS}}{\mathrm{YM}}$, it is able to estimated coalescence with a reasonable accuracy.

3.5.2 Effect of Moisture

Once the quantification method for estimating extent of coalescence was established, it can be used for the analysis for the effect of moisture. Water is known for its hydroplasticization effect and can act as plasticizers for polymer coalescence. In the

pharmaceutical operations, moisture played important roles in operation and storage and it is one of the most significant factors governing the stability of drugs. The moisture in coating can come from two sources: either from the environment humidity or from the residual water that was leftover from the process. The effect of environmental humidity (Fig 3.7 and Fig 3.8) was demonstrated to be extremely important: for both dry films cured at 60°C, the relative humidity (30% vs 75%) can change film strength and flexibility dramatically. The films can reach a steady state in 3 hours under 75% RH and remained unchanged for more than 10 days. The importance of the environmental humidity can be shown in another piece of data: in Fig 3.9, when the dry films cured at 45°C 75%RH, it can reach a coalescence extent of 53%, a significant increase from the original around 38% (Fig 3.8). This information is particularly important for film coated EC products that have incomplete curing: once the drug is subject to high relative humidity, it is likely the film property will undergo further change and then lead to the change of the release profile.

On the other hand, the effect of residual moisture water level cannot to be ignored too. This is an area that has not yet been studied yet. As shown in Fig 3.9, the increase of residual water from 0.22% to 1% led to the change of extent of coalescence from 35 to 55% at 30% relative humidity. Compared with the previous experiments (Fig 3.6), it is obvious that with plenty of residual water is able to improve the strength and flexibility greatly. The residual water and environmental relative humidity can work separately but achieving the same coalescence results under different curing conditions: for the values of Gp8 and 9 in Fig 3.8, with two different relative humidity (30% and 75%), 2 different

temperatures (60 and 45°C) and different residual water levels at 1% and 0%, the two curing conditions achieved almost equal coalescence extent 53% and 55%.

However, for hydrophobic ethylcellulose polymer chains, sample with 1% of residual water was observed to be very wet during sample preparation; and in practice it is impossible to leave tablet or beads with so much liquid on the surface because it is more likely to cause aggregation problem. Therefore despite the usefulness of reaching substantial coalescence, the way of using residual water to achieve complete curing may not be feasible, to achieve substantial coalescence for ethylcellulose, it is best to provide enough supply of environmental high humidity, through either coating process or after coating in a humidity controlled chamber.

From all the figures of mechanical test data, the estimate of coalescence produced results that were in good agreement with the PEB value. By using the ethanol cast films as references, this estimate can provide a direct expression on a process that was previously not able to quantify. However, the limitation of such quantification method is also present: ethanol cast films were inherently different system to the pseudolatex system, in the pseudolatex aqueous dispersion systems, there are other components in the system such as cetyl alcohol, sodium lauryl sulphate, although we assumed the small amount of these other components would not affect our estimation significantly, their effects may still present so that the true 100% reference state may be different than the standard using the ethanol cast films.

Our study on film curing has the goal of ultimately serve as the tool for pharmaceutical coating applications. With the estimated of coalescence being a useful indicator, it is useful to summarize the output of the films (extent of coalescence) with respect to the important factors such as curing temperature, relative humidity and residual water levels after drying. Two 3D plots were generated with the data shown above. Fig 3.17 shows the effect of temperature and relative humidity, the graph clearly demonstrated the high extent of coalescence (60-70%) occurs with high humidity and high temperature. Fig 3.18 shows the variation of extent of coalescence on relative humidity and residual water level when the curing temperature is held constant at 60°C; by examining the plot, it was demonstrated clearly the residual water level after drying had more influence when relative humidity is low, but once the relative humidity increases, the effect of residual water level is not as influential.

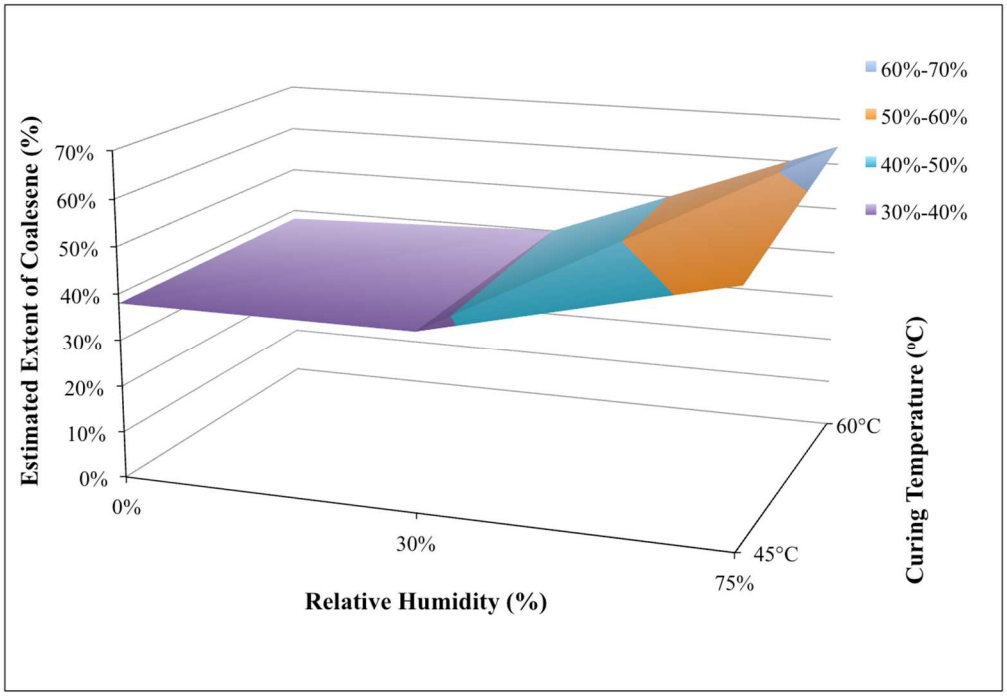

Fig 3.17 3-D surface plot of estimated extent of coalescence with respect to relative humidity and curing temperature when residual water level is 0% after drying.

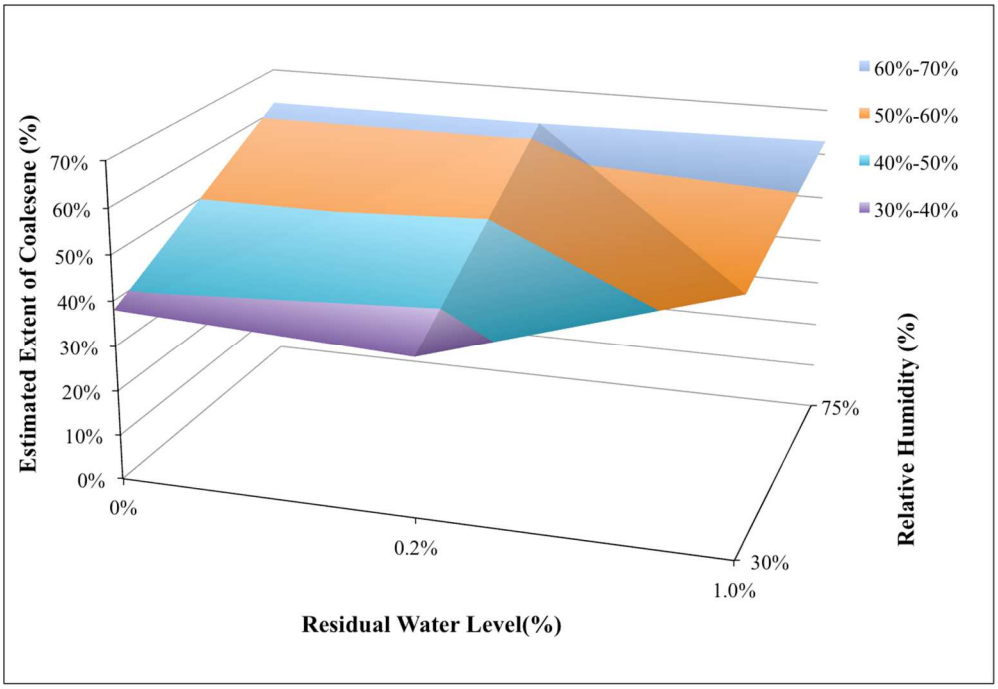

Fig 3.18 3-D surface plot of estimated extent of coalescence with respect to residual water level and relative humidity when the curing temperature is 60°C.

3.5.3 Permeability Data Analysis

The use of mechanical data and ethanol cast films provided a good way of estimating the extent of coalescence and agreed well with another indicator for coalescence, the elongation. The extent of coalescence can also be reflected by permeability, as the polymer molecules inter-diffuse through particle boundaries, this motion is expected to introduce changes to the free volume in the cured films. By using same ethanol cast film with pseudolatex cured films, systematic evaluation of water vapor permeability were carried out.

Permeability of Ethanol Films and DBS, TEC films

The ethanol cast solution films are expected to be 100% coalesced and it was used first as a comparison to the dry pseudolatex films with respect to water vapor permeability. A somewhat surprising result was observed (Fig 3.11A): ethanol cast films had much higher

permeability than the dry pseudolatex films with TEC. The same results were also observed for pseudolatex dispersions films with DBS and TEC as plasticizers (in Fig 3.11B): the permeability was higher for pseudolatex films with higher extent of coalescence (Gp38 and 39) than the uncured films (Gp18, 19). Based on these observations, it is certain that the permeability is affected by the extent of coalescence and the higher the extent of coalescence comes with higer water permeability.

Despite the films with higher extent of coalescence were observed to have a higher permeability for both TEC and DBS films (Fig 3.11B, Gp18 and Gp19), the permeability of the DBS films was higher than TEC films. Based on the fact the higher permeability equals to higher extent of coalescence, this higher extent of coalescence for DBS films can be explained by the nature of the two plasticizers: TEC is a hydrophilic polymer, it would tend to dissolve in the aqueous phase; whereas DBS is a hydrophobic polymer, which had a greater affinity towards the polymer, hence will participate in a greater extent during the stirring and the casting. Because of this greater participation, the polymers started at a higher degree of coalescence and this was reflected by the increased in permeability comparing to the TEC films.

Factors Affecting Water Vapor Permeability

From Fig 3.12 and 3.13, the results showed no difference on the permeability values at either temperature 50 or 60°C with relative humidities (LH or 30% RH). Based on the observation from Fig 3.11A and B, the higher permeability is a representation of higher extent of coalescence. These two figures agreed with the mechanical results (Fig 3.7): at low relative humidity below 30% RH, there is minimal coalescence movement going on

inside the pseudolatex EC films. It can be confirmed again the coalescence cannot take place without sufficient environmental moisture.

The significant changes in permeability started at higher relative humidity were showed in Fig 3.14. When pseudolatex film samples were cured at high RH (75%) at both 50 and 60°C, permeability increased dramatically in 4 hours. The results were as expected, it was also in agreement with previous mechanical analysis that the extent of coalescence increased from 38% to 62% in 3h (Fig 3.8, Gp1 and 10). By examination of the curves, it can be noticed the films cured at 60°C reached the steady state more quickly than 50°C, since there is no significance between the permeability value at 4h for either curing temperature, same extent of coalescence can be achieved for both 50 or 60°C, the only difference was the time to reach this coalesced state. Therefore, generally for coating using Aquacoat EC, the time required to reach stable coalesced states at sufficient relative humidity (for example 75% or above) can be achieved within 4 hours, with temperature of curing at 50°C or above.

The results of surface perturbation with nylon membranes (Fig 3.15) can further confirm the importance of the relative humidity: if without the presence of nylon membrane, 4h curing should give a slightly higher value of permeability; the presence of the nylon film reduces the interaction of environment moisture with the surface of the films, because of the movement of water molecules being perturbed by the presence of the nylon film, the polymer cannot relax/coalesce to the same extent.

3.5.4 Understanding Surface Properties of EC Films in Curing

The technique of the AFM provides precise assessment to samples' surfaces without sophisticated pretreatment[19]. The measurement of AFM was carried out when an oscillating tip of a sensitive cantilever is brought extremely close to the surface and the tip makes intermittent contact with the surface. A laser light beam that was focused on the back of the cantilever tracks the movement of the cantilever deflection and hence provides the surface information of a sample. From the AFM picture (Fig 3.16), the films with higher extent of coalescence showed the increase in the peak-to-trough differences. It was different from the reported literature observations: Goudy et al showed the peak-to-trough distances for polystyrene latex films decreased when dried polystyrene latex films were annealed above its Tg; during this process, polystyrene particles can undergo coalescence and the peak-to-trough distance significantly reduced during this process[20]. To understand the difference our EC films and polystyrene in the literature, one must look at the compositions on the film: in our peudolatex dispersion Aquacoat films, apart from the main component EC, there were also other components: cetyl alcohol and sodium dodecyl sulfate (SLS) with solid content of 8.7% and 4.2% out of the total solid in Aquacoat; whereas in the work done by Goudy et al there was no surfactant involved. The two surface-active compounds are used to stabilize the original aqueous dispersion. Generally, during latex film formation when coalescence was initiated, surfactants can be pushed out of the polymer phase and enrich in air or substrate interphase. Some surfactants can also aggregate in blocks or partially miscible with polymer phase[7]. It has been noticed by Belarouri et al, with the use of Raman spectroscopy the authors demonstrated SLS can aggregate on the air-film interface after the film formation of

acrylic polymers[21]. The potential interaction of surfactants and pseudolatex polymers during film formation and curing is a complex process and likely to vary on a case-by-case basis. Our best explanation for the phenomenon of increasing surface roughness and increase of permeability at higher extent of coalescence of EC therefore is: at high environmental moisture level (75% RH) and higher temperature above the Tg; EC polymer chains were mobile and therefore can undergo significant movement to overcome particle-particle boundaries to form a strong flexible film; in the same time, the movement of the polymer chains pushed the surfactant molecules out of the polymer phase. Surface-active compounds being pushed out of the polymer phase have high affinity towards the moisture in the air so they tend to migrate and aggregate into the surface of the film. The outcome of such movements created more void spaces in the film hence the water vapor permeability was higher than the original dry films (Gp18) and the aggregation of SLS on the film-air surfaces can also cause the increase in the peak-to-trough distances as observed in the AFM measurements.

3.6 Conclusion

A systematic curing study has been carried out in EC pseudolatex films. A quantification method has been proposed using new innovative approach based on mechanical tests. Permeability was also evaluated and was also found to be useful in describing the extent of coalescence in curing, Permeability of the films with higher extent of coalescence were found to be surprisingly higher. The surface roughness was analysis by AFM and surface perturbation using nylon membranes were also tested to

reveal it was the complicated interaction of polymer, surfactants and moisture that together resulted in the change in surface morphology and permeability.

3.7 References for Chapter 3

1. Feng, J. and M.A. Winnik, *Effect of Water on Polymer Diffusion in Latex Films.* Macromolecules, 1997. **30**(15): p. 4324-4331.
2. Felton, L.A. and J.W. McGinity, *Aqueous Polymeric Coatings for Pharmaceutical Dosage Forms*. 3rd ed. DRUGS AND PHARMACEUTICAL SCIENCES, ed. J.W.M. Linda A. Felton. 2008: Dekker.
3. Yihong Qiu, Y.C., Geoff G. Z. Zhang, *Developing Solid Oral Dosage Forms Pharmaceutical Theory and practice*. 2009: ELSEVIER.
4. Tabasi, S.H., et al., *Quality by design, part III: study of curing process of sustained release coated products using NIR spectroscopy.* Journal of pharmaceutical sciences, 2008. **97**(9): p. 4067-86.
5. Keddie, J.L., *Film Formation of Latex.* Materials Science and Engineering, R Reports, 1997. **21**: p. 101-170.
6. *Aqueous Polymeric Coatings for Pharmaceutical Dosage Forms*. DRUGS AND PHARMACEUTICAL SCIENCES, ed. J.W. McGinity. 1997: Dekker.
7. Joseph Keddie and A.F. Routh, ***Fundamentals of Latex Film Formation: Processes and Properties***. First Edition ed. 2010: Springer Laboratory.
8. Felton, L.A. and M.L. Baca, *Influence of Curing on the Adhesive and Thermomechanical Properties of an Applied Acrylic Polymer.* Pharmaceutical Development and Technology, 2001. **6**(1): p. 53-59.

9. Bhattacharjya, S. and D.E. Wurster, *Investigation of the drug release and surface morphological properties of film-coated pellets, and physical, thermal and mechanical properties of free films as a function of various curing conditions.* AAPS PharmSciTech, 2008. **9**(2): p. 449-57.

10. Guo, J.-H., R.E. Robertson, and G.L. Amidon, *An Investigation into the Mechanical and Transport Properties of Aqueous Latex Films: A New Hypothesis for the Film-Forming Mechanism of Aqueous Dispersion System.* Pharmaceutical Research, 1993. **10**(3): p. 405-410.

11. Hutchings, D., S. Clarson, and A. Sakr, *Studies of the mechanical properties of free films prepared using an ethylcellulose pseudolatex coating system.* International journal of pharmaceutics, 1994. **104**(3): p. 203-213.

12. Wurster, D.E., S. Bhattacharjya, and D.R. Flanagan, *Effect of Curing on Water Diffusivities in Acrylate Free Films as Measured via a Sorption Technique.* AAPS PharmSciTech, 2007. **8**(3).

13. Kablitz, C.D. and N.A. Urbanetz, *Characterization of the film formation of the dry coating process.* European journal of pharmaceutics and biopharmaceutics : official journal of Arbeitsgemeinschaft fur Pharmazeutische Verfahrenstechnik e.V, 2007. **67**(2): p. 449-57.

14. Howland, H., *Application of NIR Spectroscopy and Fluorescence Spectroscopy for Monitoring of Curing of Sustained Release Coatings*, in *School of Pharmacy*. 2011, University of Maryland.

15. Korber, M., et al., *Effect of unconventional curing conditions and storage on pellets coated with Aquacoat ECD.* Drug development and industrial pharmacy, 2010. **36**(2): p. 190-199.

16. Corti, P., et al., *Application of NIRS to the control of pharmaceuticals identification and assay of several primary materials.* Pharm. Acta Helv., 1992. **67**: p. 57-61.

17. ASTM, *Standard Test Methods for Water Vapor Transmission of Materials*. 2000.

18. Tabasi, S.H., et al., *Quality by design, part II: application of NIR spectroscopy to monitor the coating process for a pharmaceutical sustained release product.* Journal of pharmaceutical sciences, 2008. **97**(9): p. 4052-66.

19. Binnig, G. and C.F.Quate, *Atomic force microscopy.* Phys Rev Lett, 1986. **56**: p. 930-933.

20. Goudy, A., et al., *Atomic Force Microscopy Study of Polystyrene Latex Film Morphology: Effects of Aging and Annealing.* Langmuir, 1995. **11**(11): p. 4454-4459.

21. Belaroui, F., et al., *Distribution of water-soluble and surface-active low-molecular-weight species in acrylic latex films.* Journal of Colloid and Interface Science, 2003. **261**(2): p. 336-348.

Chapter 4 Study of Aqueous Ethylcellulose Films Curing Part II: Spectroscopic Modeling and Release Research

4.1 Abstract

Background: In previous works (Chpater 3), it was discovered that the ratio between two tensile properties: Tensile Strength (TS) and Young's Modulus (YM), $\frac{\mathrm{TS}}{\mathrm{YM}}$ can be used to provide a quantification method for coalescence of curing in ethylcellulose (EC) pseudolatex films. The water vapor permeability (WVP) was also found to be related to the coalescence of EC. **Methods:** in this study, the pseudolatex EC dispersion cast free films were analyzed with NIR spectroscopy with $\frac{\mathrm{TS}}{\mathrm{YM}}$ and WVP. Aqueous EC dispersion was also applied to MCC beads with a model drug to assess the curing effect on drug release after coating. Other techniques such as dynamic vapor sorption study was carried out on the dry beads to further evaluate the water permeabtion properties of EC films; scanning electrion microscopy (SEM) pictures were taken for selected beads before and after dissolution to assess the effects of various conditions of beads curing. **Results:** The PLS regression showed the NIR can be used to predict these quantities accurately and hence would be a great tool for estimating extent of coalescence of EC curing. The DVS study on the coated beads showed the same trend of as the previous vapor permeability. The dissolution release study on the beads further confirmed the release was mainly dominated by the strength of EC coating film rather than permeability of the films. A mathematical model was proposed and was the model was evaluated. SEM was also used as a supporting tool for our model for drug release. **Conclusions:** the NIR models can be

used for potential quality control of the curing of EC free films, the release mechanism confirmed the film strength played dominant role in the drug release for EC coated beads.

Keywords: Near Infrared, Tensile Strength, Young's Modulus, Dissolution, Ethylcellulose, SEM

4.2 Introduction

Different to the solvent coating, today's pharmaceutical coating processes usually uses an aqueous dispersion prepared from insoluble polymers so that it is more environmental friendly and easier to handle. Because of the insolubility of the polymers used in the coating, curing is an important part of the coating operation when using latex or pseudolatexes systems such as ethylcellulose (EC). After coating is applied to the substrate on the surface, the films can be formed upon temperature above the minimum film formation temperature. Once a film is formed, a curing step is required for the coated products at a specific amount of temperature and humidity so that the polymer chains in particles can overcome particle-particle boundaries and eventually become a strong and flexible film[1]. Curing plays an important role in the stability and release performance of the final coated pharmaceutical products[2]. Uncured or not fully coalesced drug products can undergo further gradual coalescence that slowing down the release rate upon long term storage leads to sub-optimal performances[3].

In our previous work (Chapter 3), a common used aqueous pseudolatex systemAquacoat ECD30, an ethylcellulose (EC) pseudolatex dispersion, was studied to analyze its physical-mechanical properties under different curing conditions, the properties examined included Tensile Strength (TS), Young's Modulus (YM) and water vapor

permeability (WVP). It was discovered that the ratio of TS and YM:$\frac{TS}{YM}$, was proportional to the thickness of the ethanol cast EC solution films. Because ethanol cast films had the fully coalesced EC polymer chains, and hence the highest value of $\frac{TS}{YM}$, the linear relationship was then utilized for estimating the extent of coalescence for pseudolatex EC films and was found to be accurate. The WVP of pseudolatex films was found to increase with increase of the extent of coalescence. In this current work, we want to assess the predictability of the $\frac{TS}{YM}$ with the spectroscopy technique of NIR; also we would like to assess via dissolution, how do the increase of WVP affect the drug release when EC pesudolatex dispersion was used as a coating agent.

4.2.1 Quality by Design and Process Analytical Technology

In pharmaceutical manufacturing, Quality by Design (QbD) principle is widely adapted, it is required for pharmaceutical developers to fully understand the process and with established control strategy to ensure the products to have the desired quality safety and efficacy[4]. In order to achieve this, process analytical tools such as spectroscopy methods were often used. In this study, we will try to establish a quantification model that can predict the extent of coalescence without the destructive tests such as the mechanical tests. To do this, Near Infrared Spectroscopy (NIRs), which has been widely used for qualitatively and quantitatively analyzing pharmaceutical systems will be tried[5]. The major advantages of NIR over traditional wet-lab analytical techniques include easy sample preparation, delocalization of measurement by fiber optic probes, and the accurate recording of chemical and physical information of samples. Since NIR can reflect the physical and chemical properties imbedded in the sample, assuming the

NIR spectra of the EC films is correlated to film coat's properties so the properties can be expressed in mathematic models.

The NIR has been used in many occasions for pharmaceutical operations, such as raw material identification[6, 7]; analyzing intact dosage forms[8, 9] and as a monitoring tool for process analytical technologies [10] [11, 12]. Our laboratory has a long interest in the phenomena of film curing and we have used NIR as a monitoring tool to predict the thickness and dissolution of tablets[2, 13]; as well as physical-mechanical properties such as Young's Modulus[14]. However, these NIR studies had not analyzed film samples that cured in different moisture environments. As seen in the previous chapter (Chapter 3), the moisture had significant effect on the outcome of physical-mechanical properties of EC films. The adequate coalescence of films cannot be achieved without sufficient supply of either environmental moisture or residual water levels. In this chapter, the NIR analysis was carried out on free films that were cured in different moisture environments. Two properties discussed earlier, which possessed characteristics of estimating extent of particle coalescence: $\frac{\mathrm{TS}}{\mathrm{YM}}$ and water vapor permeability were used to establish models that can be potentially used for future drug development.

4.2.2 Water Vapor Permeability and Release Mechanism

From Chapter 3, physical-mechanical properties of the Aquacoat EC free films were examined. The results of the mechanical properties, such as Tensile Strength and Percent Elongation at Break showed expected trend that, under high temperature, high humidity environment the films became more flexible and strong. However, it was surprising to find the water vapor permeability of such free cast films had a counter-intuitive trend:

upon higher coalescing conditions, i.e. high temperature, high relative humidities, the permeability increased significantly compared to dried, uncured films; rather than the usually expected trend of reduction of the permeability[15, 16]. In addition, mechanisms of drug release from ethylcellulose films had been proposed in the past and osmotic pressure was considered to be the main reason with Fickian diffusion also contributing partially[17]. But these mechanisms ignored the effects of the curing during their discussions. A series of dissolution studies using the Aquacoat ECD 30 as coating agent to study curing effects on plasticizer, humidity, temperature and time had also been demonstrated, but lacks of the discussions on release mechanism[18]. Hence, there is a need to carry out dissolution study on EC coated beads in order to assess 1) if the beads still possess the same trend of permeability as observed in the previous WVP study; 2) how do coating levels (thickness) and different curing conditions (temperature; relative humidity, time) affect the release of a model drug.

Based upon our aims, we evaluated the moisture absorption by those beads so as to compare to the vapor permeability in the free films. Then analyzed drug release under different conditions of coating levels (thickness), curing temperature and humidity. The aim of this dissolution study is not only to further evaluate physical-mechanical properties such as permeability or moisture absorption, but also to be able to summarize the curing effects on drug release with a mathematical description so that a better understanding of the relationships between the permeability, film strength and drug release can be obtained. Scanning electron microscopy (SEM) was also used as a supportive tool for our evaluations.

The coating of Aquacoat EC dispersion was carried out on microcrystalline cellulose (MCC) beads using new coating equipment: the Mycrolab fluidized coater (Bosch, Schopfheim Germany). This bottom spray coating equipment features an innovative disk-jet design wheret it allows the fluidizing air come out from the bottom to move in a centrifugal fashion. Such movement was created with a perforated stainless steel pan that had slots opening with 45° angle. This bottom pan therefore distributes air to flow in a vortex and then leads to the flow pattern of beads inside the fluidizing chamber. With this technique, the dead spots in coating can be effectively minimized to prevent aggregation. The liquid spraying zone of spray nozzle is protected by an unique technique called Microclimate where pressurized air was generated to embrace the spraying cone so that it effectively prevent the nozzle clogging. The dye-layered beads were utilized as a model drug product as the core of subsequent coating investigations.

4.3 Materials and Methods

4.3.1 Materials

Ethylcellulose (EC) dispersion Aquqcoat ECD 30® (FMC Biopolymer, Ewing, NJ, lot: JN11823341), triethyl citrate [19] (Vertellus, Indianapolis, IN, lot: 116266). CELPHERE CP-708 Microcrystalline Cellulose (MCC) beads (Asahi Kasei Corporation, Japan, lot: 77J4, average size: 838 μm). Hydroxylmethylcellulose (METHOCEL HPMC) E15LV (Dow Chemical, Newark, DE, Lot: 12063/63449-41-2); water soluble FD&C yellow #6 (Warner-Jenkinson Co.,lot: 451AF).

4.3.2 NIR Measurements on Free Films

The NIR measurements were done using the same samples that was prepared using method described in Chapter 3, as listed in Table 3.1 and 3.2 (attached). **Film Casting**: EC dispersion (15% w/w) was prepared by mixing Aquacoat dispersion TEC and water; the dispersion was mixed for 3 hours using a magnetic stirrer. The amount of TEC added was 25% w/w of the Aquacoat solids content. Then the dispersion was cast onto square petri dishes. **Film Drying**: for samples in Table 3.1, 10 g EC dispersion was cast onto square petri dishes 10 cm×10 cm; the amount was chosen to give the final film thickness to be in the range of 200-300 μm. The dishes containing dispersion were then dried in 40°C in a convection oven then stored in a refrigerator (-20 ºC), until used for study. The end point of completely dry was determined by weighing, until no further weight loss of cast dispersions can be measured. Some samples were dried down to a specific amount of residual water levels, which is the water required to remove in order to reach complete dryness, it was also determined by weighing the petri dishes during drying (for example, 0% being completely dry, meaning there would be no further weight loss if drying were continued; 1% of residual water level means there is still 1% of water needed to be evaporated in order to achieve dryness). For samples prepared in Table 3.2, 6 g of the EC suspension prepared was poured into round aluminum crinkle dishes; then the dishes were dried in 40°C in a convection oven to completely dryness (as described above, until no further weight loss was observed) to give the films with thickness in the range of 200-300μm..For NIR measurements, two shapes of film strips were evaluated: rectangular film strips (1 cm x 7 cm) for tensile tests (samples from Table 3.1) and circular (diameter= 19.8 mm) film strips for permeability tests (samples from Table 3.2). The

thickness of all films was controlled between 200-300 μm. All films were scanned by NIR spectrometer (XDS system, Metrholm, Switzerland) at full range from 400-2500 nm. Since the films tested were semi-transparent, a 99% reflecting ceramic reference standard (Methholm, Switzerland) was placed above the film specimens in NIR measurements, if no such standard were in place, the signal of NIR absorption of films would be too low to carry out further analysis. Triethyl citrate was also scanned using NIR, a few drops of the liquid plasticizer was placed on top of a glass plate, then a covering glass was placed on top of the liquid droplet, ensure there was no air bubbles underneath the cover glass. Then the same 99% reflecting standard was used during the NIR measurement. Statistical chemometric softwares Unscrambler® 8.0 (Camo, Woodbridge, NJ) and PLS Toolbox® (MathWorks, Natick, MA) were used to analyze the NIR spectroscopic data on EC pseudolatex cast films.

Table 3.1. List of Mechanical Investigation Experiments, compounded groups (eg Gp 2-5) differed only in the curing time. he same samples were used in the NIR calibration of PLS models

Test Group	Curing Conditions	Residual Water	Curing Time/h
Gp 1	No Curing	0	0
Gp 2-5	60°C 30% RH	0	8, 12, 24, 36
Gp 6	60°C 30% RH	0	72
Gp 7	60°C 30% RH	0.22%	72
Gp 8	60°C 30% RH	1.0%	72
Gp 9	45°C 75% RH	0	72
Gp 10-15	60°C 75% RH	0	3, 12, 24, 72, 144, 240
Gp 16	60°C 75% RH	0.5%	24
Gp 17	60°C 75% RH	1.0%	24

Table 3.2. Permeability Experiments Lists, the same samples were used in the NIR calibration of PLS models

Test Group	**Curing Conditions**	**Plasticizer**	Curing Time/h
Gp 18	Dry (No Curing)	TEC	0
Gp 19	Dry (No Curing)	DBS	0
Gp 20-22	50°C LH	TEC	0.5, 2, 4
Gp 23-26	60°C LH	TEC	0.5, 2, 4
Gp 27-29	50°C 30% RH	TEC	0.5, 2, 4
Gp 30-32	60°C 30% RH	TEC	0.5, 2, 4
Gp 33-35	50°C 75% RH	TEC	0.5, 2, 4
Gp 36-38	60°C 75% RH	TEC	0.5, 2, 4
Gp 39	60°C 75% RH	DBS	4
Gp 40	60°C 75% RH with Nylon Membrane	TEC	4

4.3.3 Beads Coating

The coating on beads had two steps for two layers: 1) the coating of the colored dye and 2) the coating of ethylcellulose. For the first layer, HPMC 4.5 g and 1 g of FD&C Yellow 6 were dissolved in 150 g of water to prepare coating solution. Then MCC beads was coated using this coating solution to prepare the dye-layered beads using bottom spraying fluid-bed coater and the peristaltic pump. The coating product temperature was maintained at 32-33°C and the spray rate at 0.7-1.2 g/min (3-5 rpm on the pump). The spray atomization pressure was set at between 0.7-0.8 Psi, the microclimate was set at 0.2-0.3 Psi, and air volume used for fluidizing the beads was 10-12 m^3/min. After the solution was sprayed, the beads were dried in the fluid bed for another 30 min at 40°C. The dye-layered beads were utilized as a model drug product as the core of subsequent coating investigations.

For the coating of the second layer, the colored beads were then spray coated with the same EC dispersion used for making free films: Aquacoat EC dispersion 15% solid, with plasticizer TEC (25% of Aquacoat solid), stirred for 3 hours prior to coating. The coating product temperature was maintained at 32-33°C and the spray rate at 0.7-1.2 g/min (3-5 rpm on the pump). The spray atomization pressure was set at between 0.7-0.8 Psi, the microclimate was set at 0.2-0.3 Psi, and air volume used for fluidizing the beads was 10-12 m^3/min The coateing levels were controlled to be 3%, 8%, 15% an 20% of the beads weight before the second coating step, aiming for low to high coating thickness range (Table 4.1).

After the MCC beads were spray coated by the second EC layers to the desired coating level, the samples were then collected and then put into a tray for stationary curing using an oven at 60°C ambient humidity (Low RH%) and 60°C 75% RH (obtained with saturated NaCl solutions) for 4 hours. The LOW RH% (LH) label for curing at 60°C ambient humidity was used to represent an almost no humidity environment. The beads after curing were then preserved in desiccators containing desiccants to ensure the beads would be dry before the start of dissolution tests. For dissolution tests, 1.5g equivalent colored beads were evaluated in dissolution for all EC layered beads (3%, 8%, 15%, 20%), the release of the beads was measured using an 1700 PharmaSpec UV-Visible Spectrophotometer (Shimadzu Columbia, MD) at 484 nm. The dissolution tests for beads were evaluated with SR8 PLUS Dissolution Test Station (Hanson Research, Chatsworth, CA) using USP II paddle method at 37°C in 900 mL of deionized water. The paddle

rotational speed for dissolution testing for Gp41-46 (3% and 8% w/w coating level) were 50 rpm and for Gp47-52 (15% and 20% w/w coating level) the speed were 100 rpm.

Table 4.1 The Beads prepared by fluid bed coating and different curing conditions.

Group No.	Coating Level	Drying Condition	Curing Temperature	Curing Humidity	Curing Time
41	3%	40°C Ambient	No Curing	No Curing	No Curing
42	3%	40°C Ambient	60°C	LH	4h
43	3%	40°C Ambient	60°C	75% RH	4h
44	8%	40°C Ambient	No Curing	No Curing	No Curing
45	8%	40°C Ambient	60°C	LH	4h
46	8%	40°C Ambient	60°C	75% RH	4h
47	15%	40°C Ambient	No Curing	No Curing	No Curing
48	15%	40°C Ambient	60°C	LH	4h
49	15%	40°C Ambient	60°C	75% RH	4h
50	20%	40°C Ambient	No Curing	No Curing	No Curing
51	20%	40°C Ambient	60°C	LH	4h
52	20%	40°C Ambient	60°C	75% RH	4h

4.3.4 Beads Evaluation

The dynamic vapor sorption (DVS) measurements were carried out for assessing the water vapor uptake of the coated beads. This is to assess the vapor permeability on the beads. The study was evaluated on the 15% w/w coated beads. The curing conditions were uncured (dry), 60°C 75% 4h and 60°C LH 4h (Group 47-49 Table 4.1). The beads

specimens were first dried at 60°C for 1 hour and then evaluated at 25ºC, 50% RH with an eight hour dwell time and weight stabilization was set at +/- 0.01%/5 minutes in Q5000 Dynamic Vapor Soption (DVS) tester (TA Instruments, New Castle, DE).

The thickness of the beads before and after coating with EC was done by laser diffraction using Mastersizer 2000 particle size analyzer (Malvern, Columbia, MD). The d(50) for the beads after coating were then subtracted by the the original d(50) of the beads to obtain the coating thickness. The volume of the coated beads were estimated by the volume of a sphere $V=\frac{4}{3}\pi r^3$ where r is the radius of the measured samples. Then the volume of the EC coated on each bead was calculated by subtracting the volume of the beads with 0% EC coating from the EC coated beads.

The samples for SEM were carried out with Quanta 200 Electron Microscope (FEI, Hillsboro, OR). Selected from the beads coated with 20% w/w level. 5 sets of samples were evaluated, consisted of the beads before and after dissolution: uncured (dry), 60°C 75% 4 h and 60°C LH 4h (Gp50-52, Table 4.1) were analyzed before dissolution. The other 2 sets of samples were beads of Gp50 and Gp51 after 4 hours of dissolution. The beads after dissolution were dried O/N in convection oven at 40ºC before taking SEM measurements.

4.4 Results and Discussions

In the previous study, the tensile stress, Young's Modulus and permeability to water vapor were measured to assess the effect environmental and residual water on free film curing. In this study, the focus is two folds: the first is the continuation from the investigation on the free pseudolatex EC films, to developo NIR models that can be used

to further predict the physical-mechanical properties investigated earlier; the second was to apply the EC pseudolatex dispersion on to MCC beads and investigate the curing effect on the drug release. The reason we also need to investigate the beads performances was because EC pseuodlatex dispersion was primarily used for controlled release coating formulation and curing has a great impact on the release profile of this coating process. The release performances of the beads were analyzed to make connection and to draw further conclusions from the previous free film results.

4.4.1 NIR Analysis

The spectra of the free films, both the raw spectra and with second derivative preprocessing with the comparison of TEC were given (Fig 4.1). The second derivative treatment is useful in modeling with NIR spectra because it corrects the baseline shifts between different samples. Such as in Fig 4.1b, for purely as a comparison purpose, the TEC curve had a much lower base line absorption because it is totally transparent liquid, whereas the film samples showed in Fig 4.1a were cloudy, therefore had a higher baseline than the TEC curves. Despite the difference in the baseline, the second derivative treatment was able to correct the baseline difference and bring all the curves into the same level (Fig 4.1b). Since the film specimens were prepared with difference appearances, it is impossible for all film specimens to have the same baseline, the second derivative treatment was therefore always used before further data analysis. From Fig 5.5a, for pseudolatex dispersion EC films, there was an absorption peak at around 1930 nm, as the films become more coalesced from dry film to cured film for 0.5 hour in 60°C 75% RH, the three samples had an increasing trend in coalescence, and we also observed

a same increasing trend in the NIR absorption band. In Fig 4.1b, the second derivative curves still had the same trend for the three EC pseudolatex film samples.

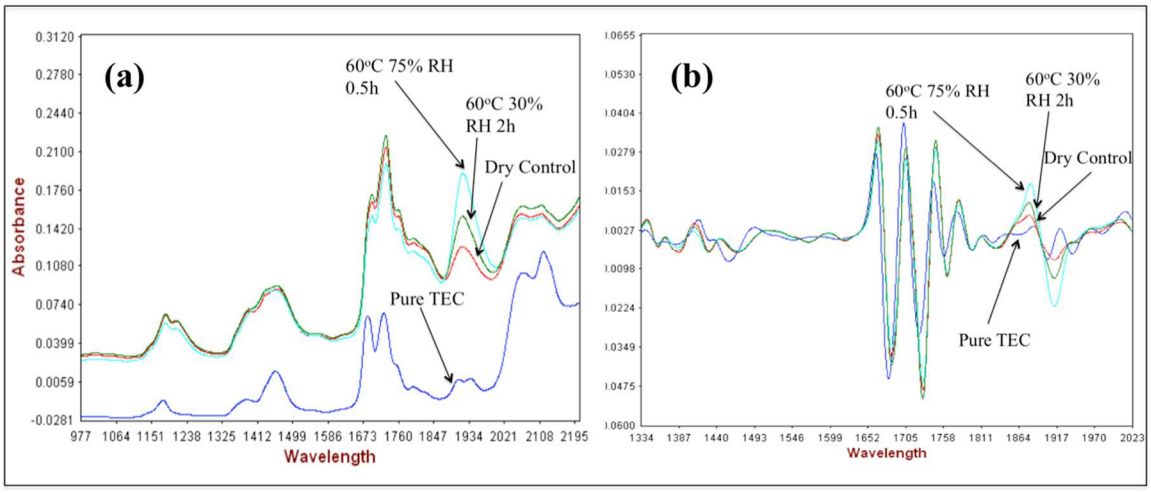

Fig 4.1(a) Raw NIR spectra of free pseudolatex cast films and pure TEC (b) The same spectra after treatment via second derivative were seen to remove the baseline difference but still be retain the information of the difference on the peaks.

Effect of Film Thickness

The film thickness is an important property of the free films samples that can affect many physical-mechanical properties such as spectral absorption values. By Beer Lambert law, absorbance is proportional to the path length. In the case of NIR measurements, the path length will be the thickness of the free films. The Principle Component Analysis (PCA) plot of NIR spectra of the free films samples were shown in Fig 4.2, the samples were categorized according to the thickness. The plot showed the thickness were scattered across the Principle Component 1 and the order of the thickness groups matched the order of the PC1 scores from left to right (the x-axis). The PC1 accounts for about 83% of the variance. The PCA plot showed the thickness is probably the most influential parameter in the NIR spectral data. If this spectral data were used in a partial least square regression against the thickness data, then the nearly perfect linear

lines showed a strong relationship between the two (Fig 4.3). The partial least square (PLS) regression is commonly used for spectral data analysis to predict physical values because its power of reducing complicated data set into simple matrix formats[20]. The Fig 4.3 was generated using the raw spectra and the physical quantity to predict was the film thickness. As can be seen, the PLS showed the raw spectral data can be used to predict thickness in an accurate fashion with R^2=0.929, root mean square error of calibration (RMSEC) is 3.13×10^{-3}. The validation method used was venetian blinds with 9 data splits. The root mean square error of cross validation (RMSECV) is 3.23×10^{-3}, which is in the same magnitude with the RMSEC.

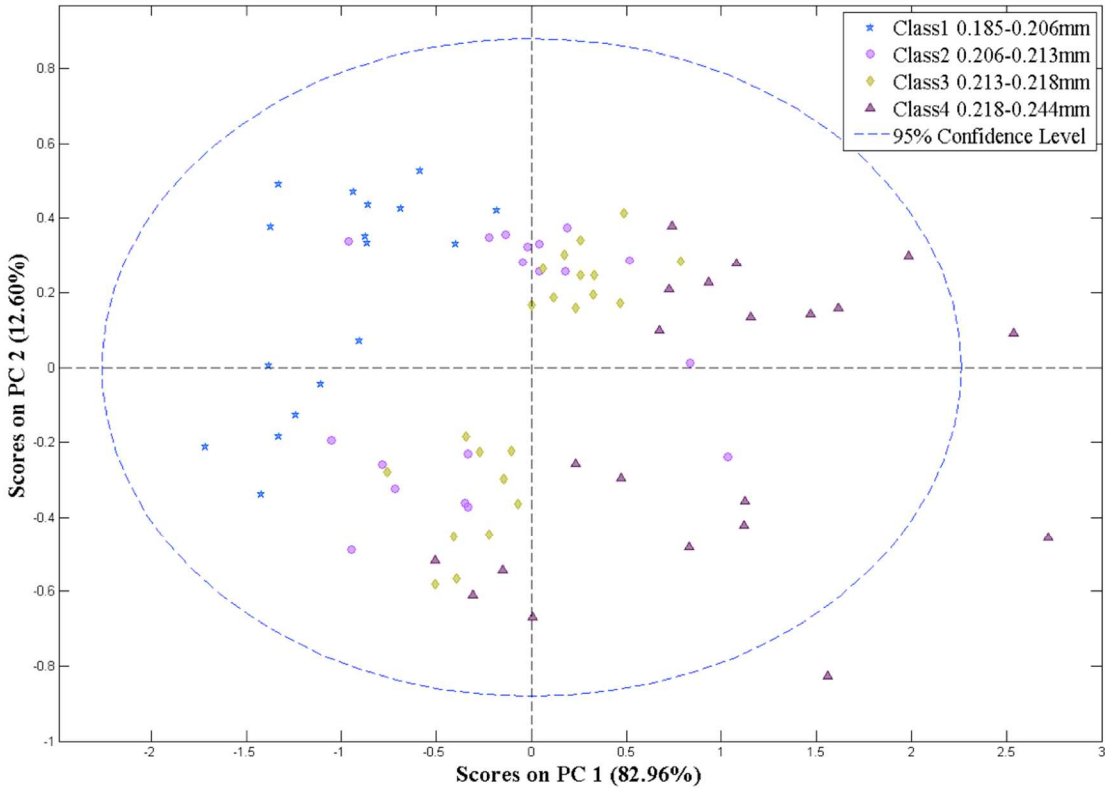

Fig 4.2, the PCA plot of raw spectra values with colors indicating different groups of thickness the principle component (PC) 1 and 2 were shown with PC1 accounted for 83% of the variability of the data set. The thickness were seen to be organized along the principle component (PC)1, demonstrating a high possibility PC1 reflects changes in films' thickness.

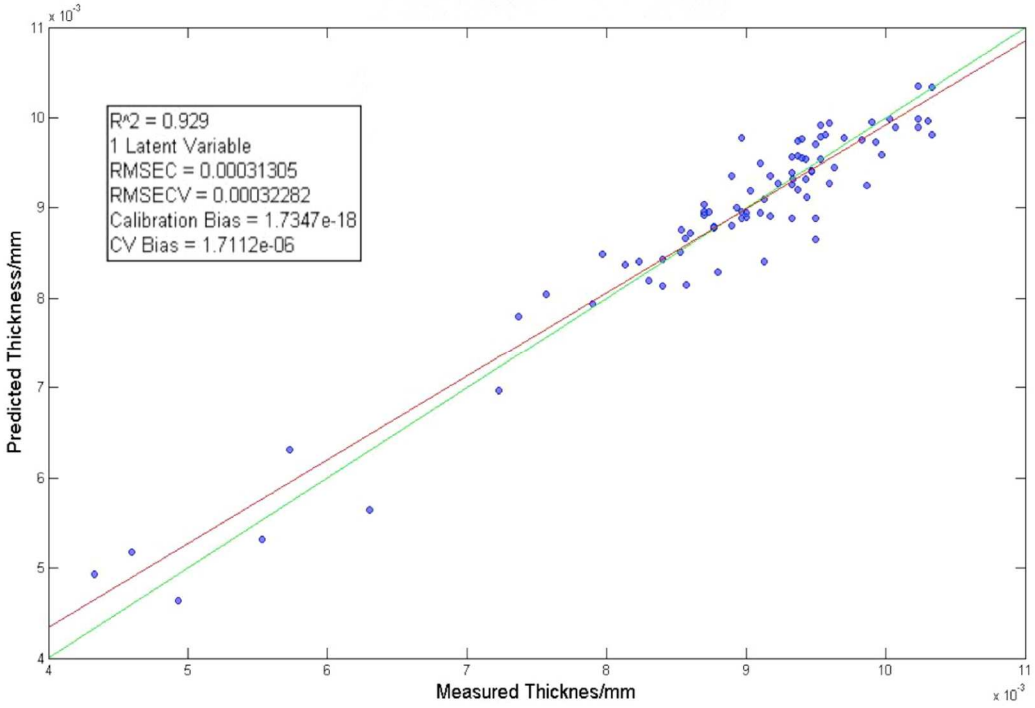

Fig 4.3: The PLS regression model using the raw spectra to predict thickness with correlation coefficient of 0.93, the NIR region was 400-2500nm and no pretreatment was used other than mean centering. The strong relationship indicated the NIR spectra were greatly governed by thickness of samples. The green line is the ideal 1:1 line and the red line is the fitted line for the data.

The effect of thickness was a major issue in the beginning for establishing PLS regression of spectral data to physical-mechanical quantities, using the many preprocessing treatment had been carried out and the highest R^2 for $\frac{TS}{YM}$ and WVP was around 0.5. In order to obtain the physical and chemical information about curing that is buried in the overwhelming effect of thickness, we needed to remove the effects of thickness by normalizing the spectra. The method carried out was for each film sample's absorbance in every wavelength to divide by its thickness, by doing so, the effect of the thickness would be minimized but we still maintained all the features of the original NIR spectra.

NIR Modeling of Physical-Mechanical Properties

After the normalization of thickness, then with the second derivative preprocessing treatment, two PLS models were established with the tensile property: $\frac{TS}{YM}$ and the vapor permeability WVP across the free films (Fig4.4a, b). The R^2 for $\frac{TS}{YM}$ regression was 0.87 with RMSEC of 6.5×10^{-3}; the cross validation method was venetian blind with data split of 8; and RMSECV was 8.14×10^{-3}. The R^2 for WVP was 0.91 with RMSEC of 1.8×10^{-5} and RMSECV was 2.0×10^{-5}; the cross validation method was venetian blind with data split of 10. Hence, both PLS models demonstrated a strong linear relationship to the physical-mechanical properties of interest.

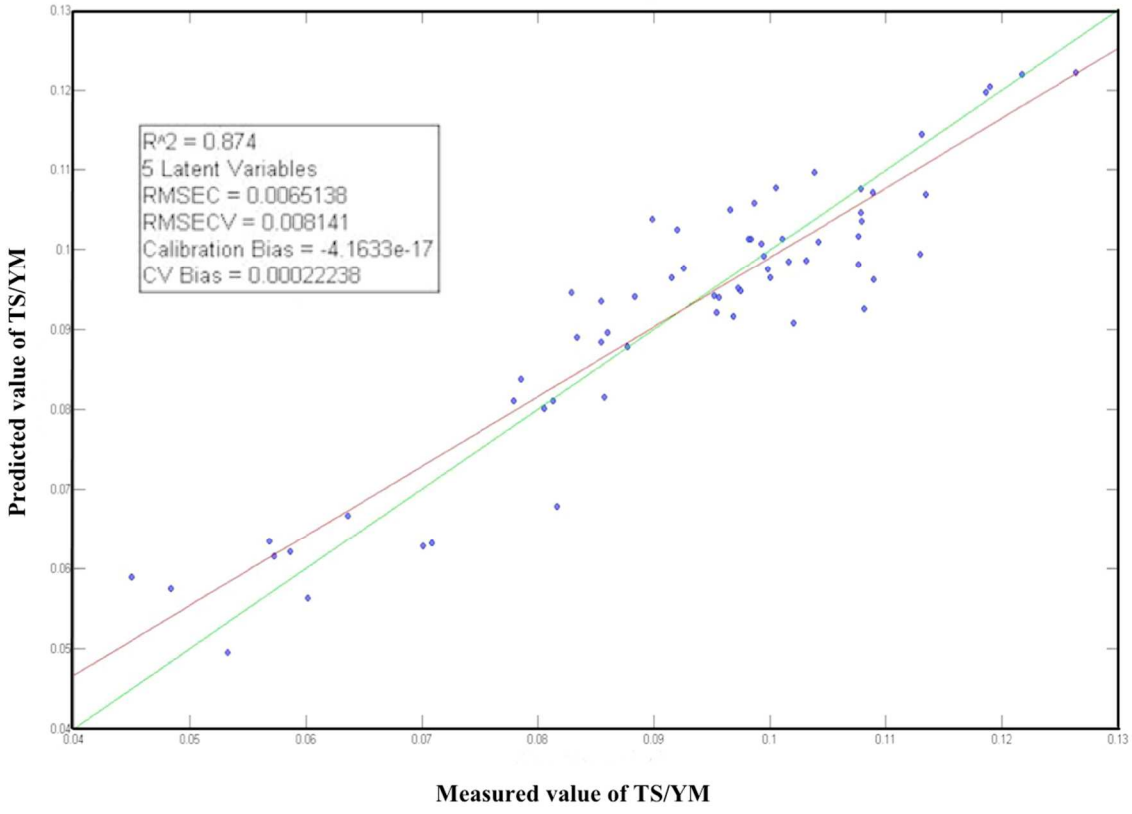

Fig.4.4a The PLS model for TS/YM prediction with correlation coefficient of 0.87, the NIR region selected for calibration was 1100-2200nm and the pretreatment was mean centering with second derivative. The green line is the ideal 1:1 line and the red line is the fitted line for the data.

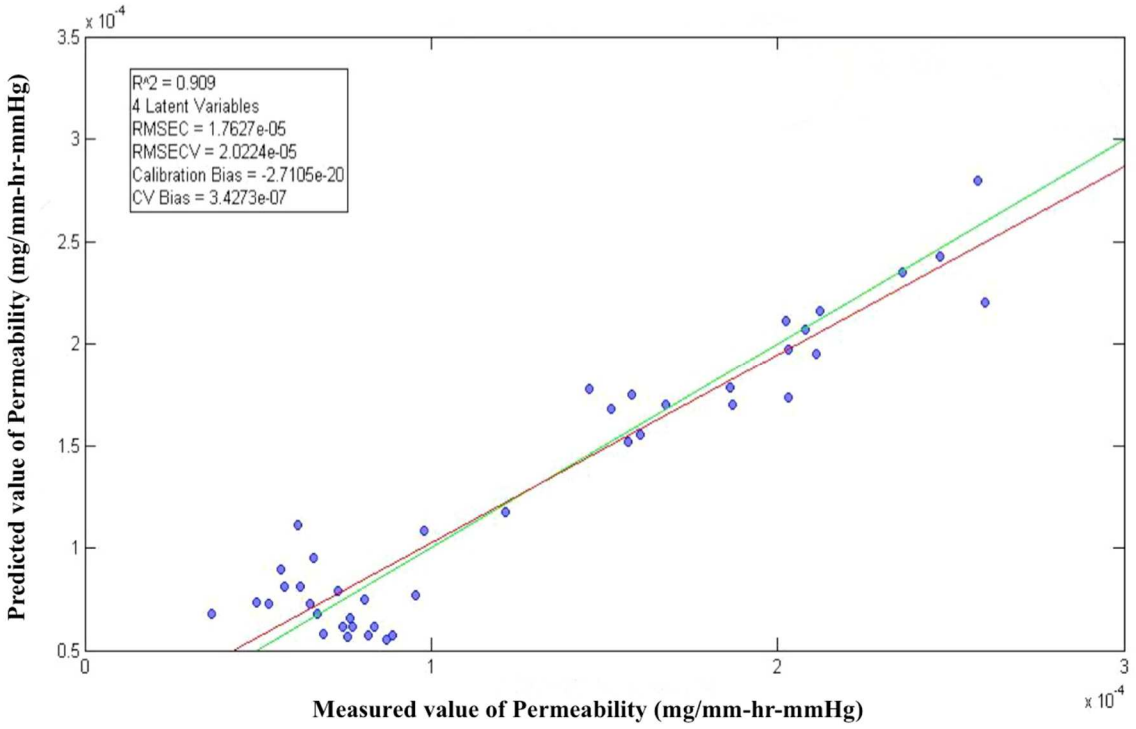

Fig.4.4b The PLS model for vapor permeability prediction with regression coefficient of 0.91. The NIR region selected for calibration was 1100-2200nm and the pretreatment was mean centering with second derivative. The green line is the ideal 1:1 line and the red line is the fitted line for the data.

The PLS regression models for both properties: $\frac{\mathrm{TS}}{\mathrm{YM}}$ and WVP showed promising predictability of the quantities of interest. From both cases, the regression coefficient R^2 is around 0.90, and the RMSECV values were close to the RMSEC values. The regression coefficient was not very high can be due to two reasons: 1. The mechanical measurements or permeability contained large variation due to the nature of the measurements; 2. There were large variations involved during sample preparation.

Despite the relatively low correlation coefficients R^2 for the PLS models, the linear relationship is clearly visible. For both quantities $\frac{\mathrm{TS}}{\mathrm{YM}}$ and WVP, it was the first time in literature they could be modeled with spectral data calibration. From previous results in

Chapter 3, it was shown that curing under higher moisture levels will provide higher plasticization power for EC pseudolatex films to obtain higher extent of coalescence. The two quantities $\frac{\mathrm{TS}}{\mathrm{YM}}$ and WVP had also been shown to directly tie with the extent of coalescence: both $\frac{\mathrm{TS}}{\mathrm{YM}}$ and WVP values increase as the extent of coalescence increase and $\frac{\mathrm{TS}}{\mathrm{YM}}$ can be used for directly quantifying the extent of coalescence. It demonstrated the NIR spectroscopy is able to analyze the effect of moisture on cured EC films through the measurements of the physical-mechanical properties. Therefore, by measuring these quantities can allow the direct measurement of the extent of coalescence without invasive or destructive tests. With the establishment of these relationships, it is therefore possible for future investigations to directly estimate extent of coalescence as a control of detection of the end of the curing for better quality control purposes[21].

Despite the success of using NIR to predict the physical-mechanical properties, this NIR calibration method works best with the free films rather than tablet or beads coating because in a coating process, the thickness of the film is constantly changing and there is not an easy way to normalize this effect of thickness. However, if the NIR was used for monitoring the increase of the thickness in the coating process, it can easily be done because the high influence of the thickness on the NIR spectra.

4.4.2 Analysis of Coated Beads

Dynamic Vapor Sorption (DVS) Properties of Coated Beads

The previous water vapor permeability (WVP) measurements on the free EC film showed a surprising findings that EC dispersion films, after highest temperature and curing

conditions, ie 60°C 75% RH for 4 h had the most water vapor permeability. ie, under the same condition and time interval, the more coalesced film allowed more moisture to go across. To further investigate this phenomenon, DVS was carried out on the 15% coated beads (Fig 4.5).

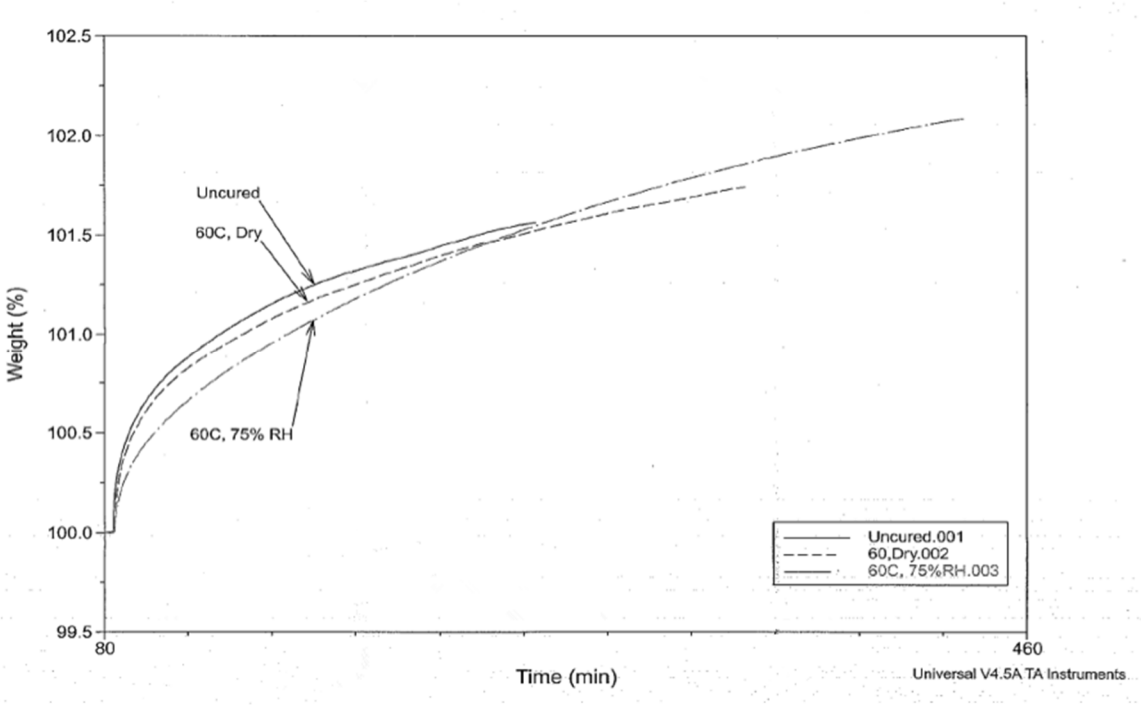

Fig 4.5: DVS curve for coated beads with 15% EC weight gain (Gp47-49) levels. Curing conditions were dry (no curing), cured for 4 hr at 60°C, ambient humidity and cured for 4 hr at 60°C75% RH. The time before 80min were not shown because the beads were being equilibrated and dried at 60°C. The experiment was carried out at constant 50% RH.

The measurements started by drying the beads in 60°C for at least an hour, making sure the beads were all dry (the time before the 80 min). The results showed by DVS plot was in good agreement with the free film: despite being the slowest absorbing initially, the 60°C 75% RH 4h (Gp49) treated beads rapidly increased its rate and overtook the other two curing treatment groups, which are uncured and cured at 60°C LH for 4 h (Gp47 and 48). The rate for moisture absorption for the other two treatment groups, Gp47 and the uncured and 60°C LH were similar. The water vapor permeability study was kept for

longer time for more than 24 hours because the measurements were done by weighing and at least 5 measurements were needed; nevertheless, the same results can be obtained with two different techniques.

The behavior of moisture absorption agreed with the surprising observations earlier on the WVP where the film had higher degree of coalescence would tend to have the higher rate for vapor transmission across the film. Since the experiments were done by pre-drying the samples for 1 hour, then there should not be any residual water in the beads specimen that can potentially affect the results. It revealed an important fact: the films with higher extent of coalescence are more prone to vapor absorption, and therefore, we could deduce that the films had a higher extent of coalescence would have more free volumes for diffusion, same as what we have observed previously. Through curing, the polymer particles move and break the particle-particle boundaries, during this process, such movement causes the free volume in the film to increase.

Particle Size Analysis

A summary of the particle sizes of EC coated colored beads is given in Fig 4.6. The original colored beads core (prepared according to the method in section 3.3) were determined to have had an average diameter of 850.4 μm. Then the EC coated beads reached a maximum coating thickness of 60 μm for a 20% weight gain level. The thickness of beads and the volume of EC coatings were highly correlated with different levels of weight gain levels demonstrated with high coefficient of regression R^2. Beside, the coated beads had no agglomerations. This demonstrated a reliable coating capability of the Bosch Mycrolab fluid bed coater and showed the experiments were well controlled.

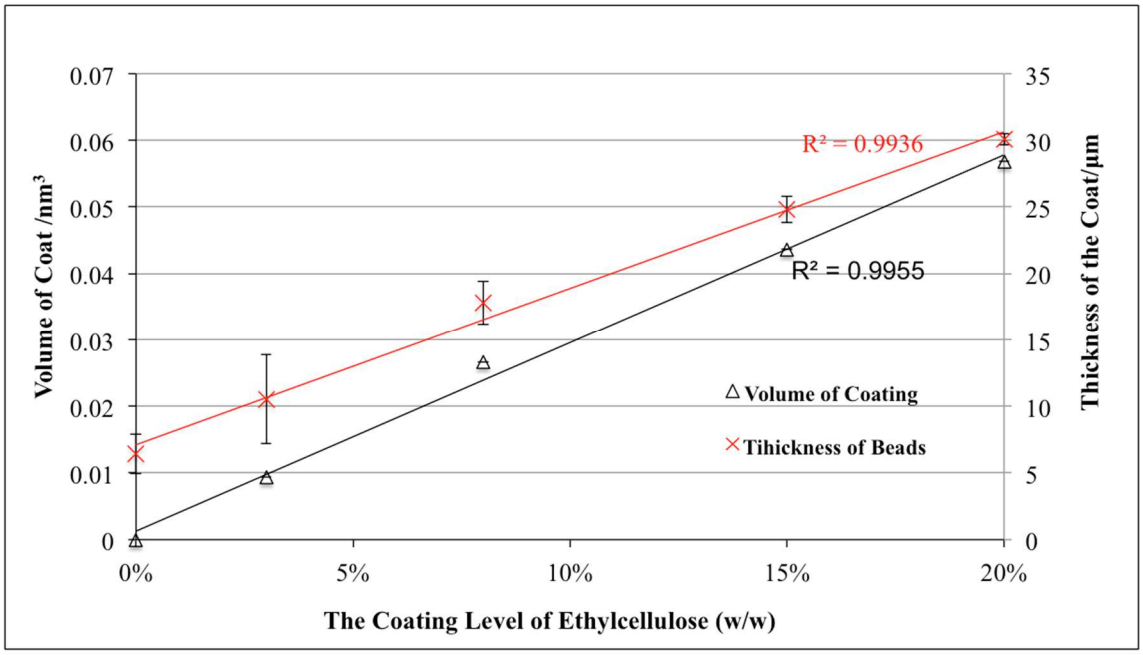

Fig 4.6: The Particle size analysis of Coated beads Core Beads (0%) and different EC coating levels with different weight gain levels of 3%, 8%, 15% and 20%. The volume of the coating were estimated from the thickness of the beads and showed an almost straight line demonstrating good coating capability of the instrument.

Release Performances

The release of coated colored beads with different amount EC levels (3%-20%) were summarized in the Figures 4.7-4.10. The readily soluble dye was used as model drug because it can instantaneous solubilize hence the amount released only governed by the extended release coating. For coating levels at 3% (Gp41-43, Fig 4.7), we did not see a significant differences among the three curing conditions, with nearly all the drug released in the first 20 mins; hence at the 3% w/w coating levels using aqueous EC dispersion, the coating did not perform the function of extended release as it supposed to. The release of 8% w/w coated beads (Gp44-47, Fig 4.8) started to show the difference among the three curing groups. The dry control group (Gp44) without the further curing had the fastest release among the three with over 90% release under half an hour; the group cured at 60°C but LH (Gp45) had the intermediate release rate, with over 90%

released under one hour; the group cured at 60°C 75% RH (Gp46) was the slowest releasing group, it required over 4 hours to reach over 90% release.

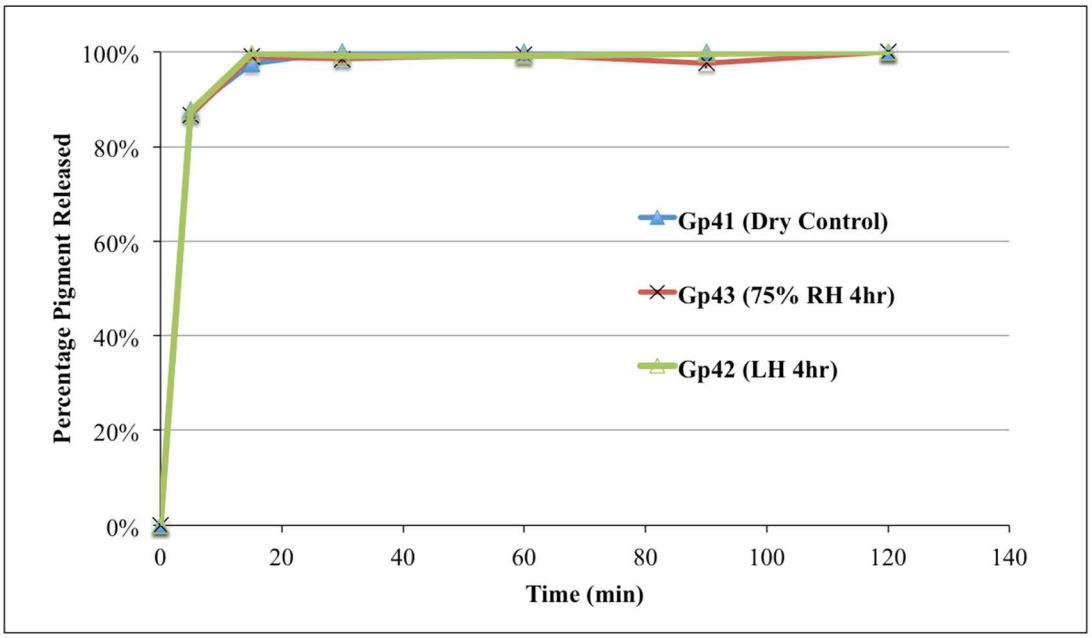

Fig 4.7 The drug release of the 3% EC coated beads with 3 different curing conditions (Gp 41-43); n=6 for each group

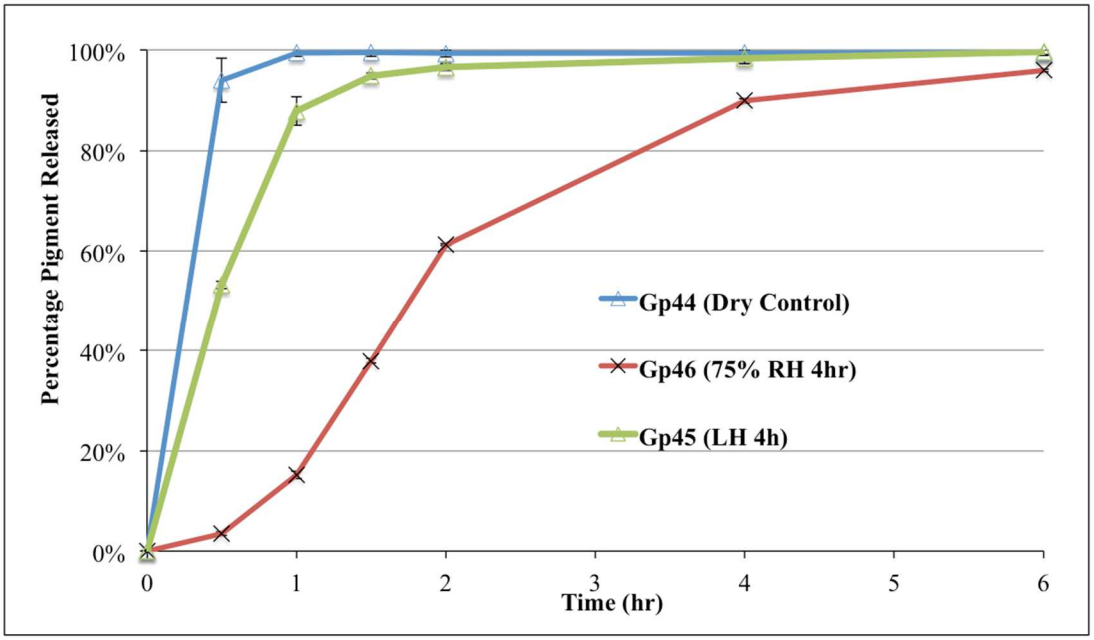

Fig 4.8 The drug release of the 8% EC coated beads (Gp 44-46) with 3 different curing conditions; n=6 for each group

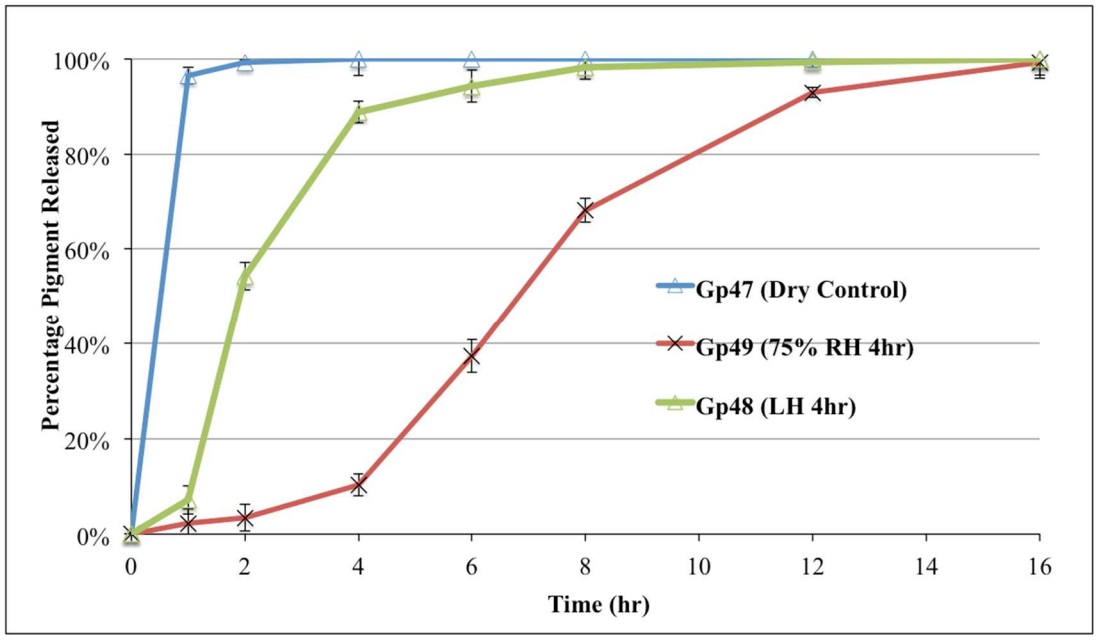

Fig 4.9 The drug release of the 15% EC coated beads (Gp 47-49) with 3 different curing conditions; n=6 for each group

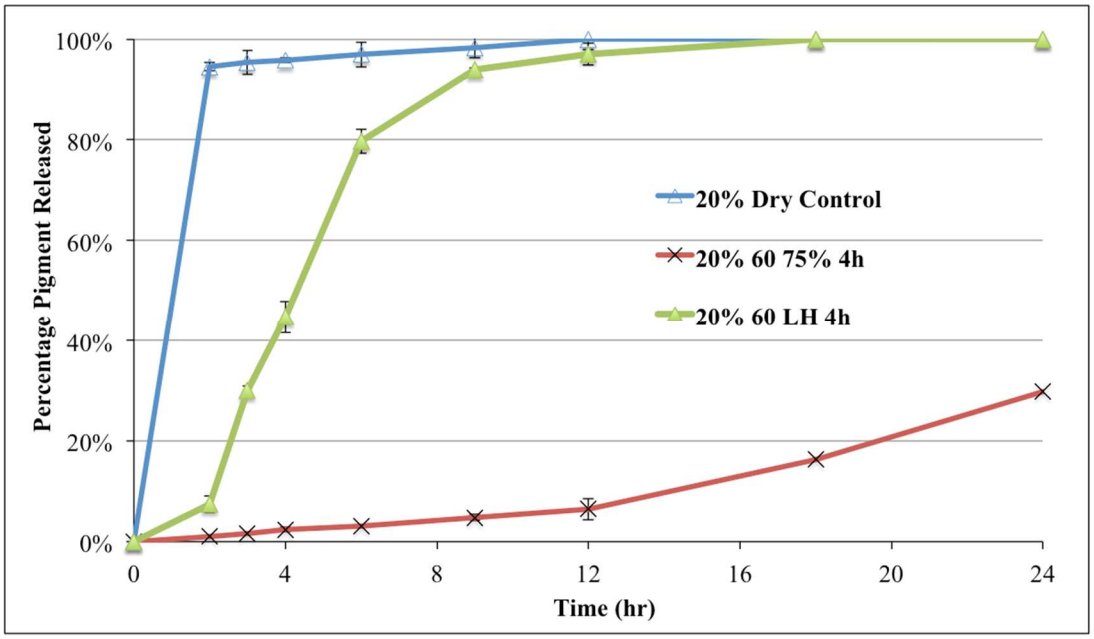

Fig 4.10 The drug release of the 20% EC coated beads (Gp 50-52) with 3 different curing conditions; n=6 for each group

The releases for the beads with coating levels 15% and 20% (Gp47-49, Gp50-52) were increasingly slower compared to the 8% level. However, the order of release with the

same coating level remained the same, the dry controlled beads (Gp47 and 50) among the two coating level still had much faster release rate than the beads that were further cured. It is worth noting that, the release cannot reach 50% for beads coated at 20% w/w level, after cured for 60°C, 75% RH.

SEM Analysis of Beads

The photos taken by SEM for beads coated with 20% EC w/w were listed in Fig 4.11(a-c) and Fig 4.12 (a-d). The beads before dissolution for Gp50-52 were listed in Fig 4.11, the beads before dissolution all had no cracks on the surface; the coating was all uniformly dispersed and homogenous. The sample cured at 60°C 75% (Group 52) had the most smooth surface and the surface of Group 51 (curing at 60°C LH) being the most coarse. The beads after 4 hours of dissolution testing showed cracking of the beads on both Group 50 and 51. The Group 51 (4.12a-b) had cracks started to develop and Group 50 (4.12c-d) had a much higher extent of cracking as the entire coat started to peel off.

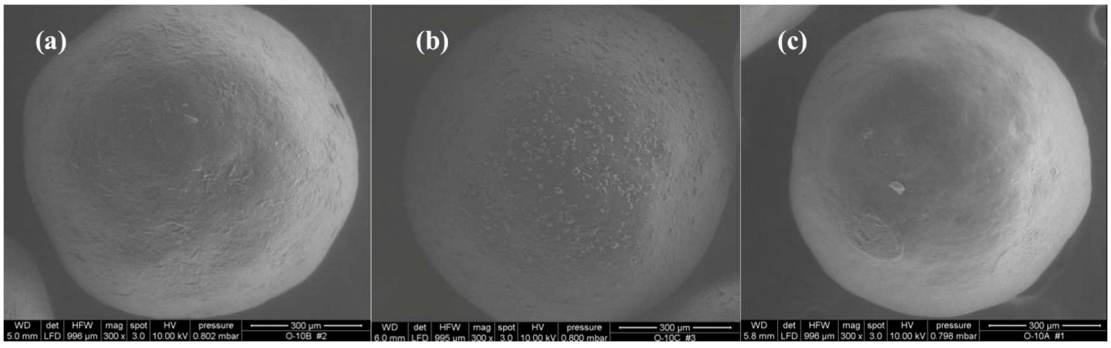

Fig 4.11 SEM picture of coated EC beads 20% w/w before dissolution (a) Group 50 dry beads, (b) Group 51, cured at 60°C LH (c) Group 52, cured at 60°C 75% RH

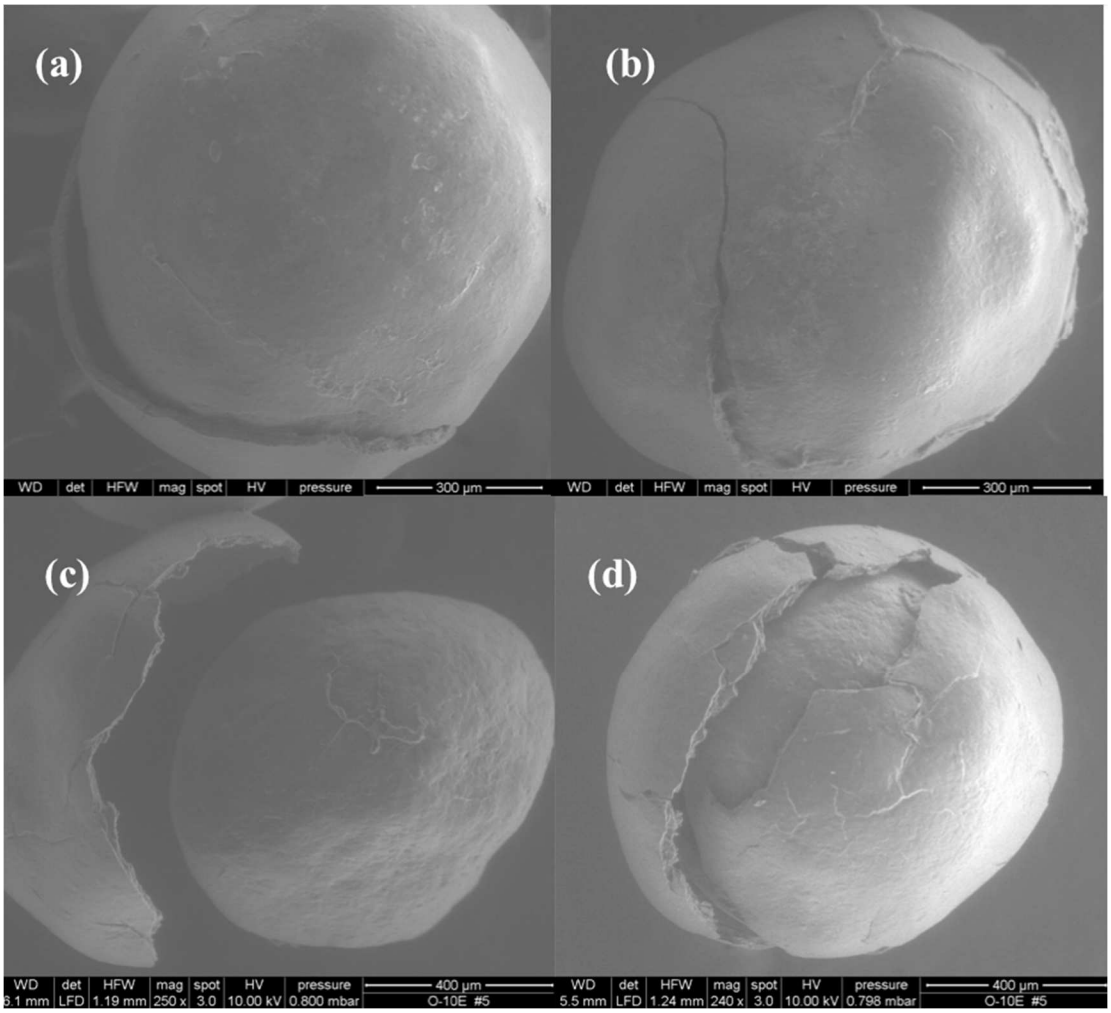

Fig 4.12 SEM picture of coated EC beads 20% W/W after dissolution testing for 4 hours (a)&(b) Group 51, cured at 60°C ambient showed small crack started to develop on surfaces of the beads, (c)&(d) Group 50, no curing, showed large cracked appeared and coating films fell off the center core.

Fig 4.12 showed the SEM photos of beads after 4 hours of dissolution. The beads after 4 hours of dissolution testing showed cracking of the beads on both Group 50 and 51. The Group 51 (4.12a-b) had cracks started to develop whereas Group 50 (4.12c-d) had a much higher extent of cracking as the entire coat started to peel off.

4.4.3 Understanding the Factors Affecting Drug Release

From Fig 4.8-4.10 (EC coating levels for 8%, 15% and 20% w/w), it was clear that the release results were in agreement with the literature measurements using EC coated films, that for all the coating levels, films cured at high humidity environments had the slowest release rate[18]. What had not been noticed was, for uncured, dry beads, the release was much faster so that it cannot be used to fulfill the role of extended release coating. These results proved again that the curing cannot be completed without sufficient presence of environmental moisture. Only elevated temperature is not enough to reach a stable release profile. Another important fact that we learned from the release figure is from the 3% w/w EC coated colored beads (Fig 4.7, Gp 41-43), there was no difference between the three release curves for 3 different curing groups, and there is no extended release slowing down for even the most highest coalesced coating in the Gp43. Hence, it is safe to say that in order for the EC coating to perform its extended release functions, the amount of coating must not be less than 3% w/w. Equal or below the 3% coating level cannot have the extended release function it supposed to have, any extended release curve seen with 3% EC coating can only mean the active pharmaceutical ingredient (API) is hard to solubilize in the dissolution media, the release curves would actually be the API dissolution curve.

From previous study on the pseudolatex EC cast free films, it was revealed that films with higher extent of coalescence were much stronger and flexible than dry film or under cured films; but at the same time, films with higher extent of coalescence had higher water vapor permeability across the film. Similarly, in the current DVS study on coated

beads (15% w/w group) using the same EC pseudolatex dispersion, the most coalesced films (Gp 49) had the most water vapor absorption hence making it the most permeable films out of the same coating level. Based on the DVS observations, the diffusion of API through the free volume across EC coating film cannot be a governing mechanism of release of EC coated beads; otherwise we would have observed the fastest release from the groups with the highest permeability in the coating films (Gp 47, 49 52) in their respective coating levels of 8%, 15% and 20% w/w. By examinning drug release curves, it further demonstrated the importance of film strength in governing the drug release: the Group 51 had about 40% release and Group 50 had almost 100% release (Fig 4.10) after 4 hours in dissolution testing; this was reflected on SEM pictures that Group 51 beads had cracks started appearing(Fig 4.12a, b); whereas the EC coating in Group 50 beads had already fallen off the beads' inner surface (Fig 4.12c,d). The difference in Gp50 and Gp51 was that Gp51 had been cured under 60°C, LH for 4 hours and Gp50 had no curing treatment; despite the curing conditions for Gp51 cannot obtain high coalescence like Gp52 (cured at 75%), the polymer chains can still undergo limited coalescence above the Tg of the system which is about 35°C so making the films a little stronger and hence more resistant to break. From the DVS results of the 15% w/w coating groups, we can deduce the DVS values out of the three 20% w/w coating level groups (Gp 50-52), Group 52 (cured at 60°C 75% RH for 4 hr) would have the highest permeability among them; however, despite this anticipated higher permeability, the release after 4 hours for this highly coalesced coating beads was much slower at only 10%. Hence it can be concluded with confidence that the main factor governing EC coating release and the extended release function provide by EC coating is the film strength after curing, the resistance to

film crack/break is the cause of the slowing down of release. The diffusion of API due to permeability can only contribute a small proportion to the drug release. Since the film strength is greatly impacted by the film thickness, for the cured groups in 3% w/w coating level (Gp42 and 43), although there was a great increase of the coalescence of EC coating on the beads, the coating was too thin to resist the hydrodynamic motions in dissolution tests so there is no difference between the Gp41-43. The other possible reason for this no change of release can be due to inhomogeneous coating, since the beads only gained 3% of coatings, the coating dispersions may not effectively cover all the surfaces of the beads during the spraying stages. Nevertheless, in order to use Aquacoat EC pseudolatex dispersion for extended release coating, one must apply more than 3% w/w coating level.

4.4.4 The Mechanism of Drug Release

Based on the understanding of the drug release described, we therefore would like to propose a mathematical description that can be used to, at least partially to generally account for the drug release of multiparticulate beads coated with EC dispersion. As state before, the drug release is primarily governed by film coat breakage or cracking hence leading to the drug API release; on the other hand, the diffusion through the free volume of the films can contribute partially to the total drug release. Since this two mechanisms work differently, we assume the release is the addition of these two mechanisms. From the previous free film water permeability data, and the DVS data present in earlier sections, although for the same coating thickness (ie, same coating level w/w) the higher coalesced films have higher permeability that can potentially leads to a high diffusion rate, the difference is small; hence we also assume the diffusion rate is constant for a

given coating thickness. Therefore, for the diffusion part, the amount of drug dissolved M_d, can be estimated be like Equation 1, assuming the constant diffusion rate of the drug out of the beads when beads were intact. Where the k is the rate of drug diffuse out of the EC film coat at a specific dissolution media.

$$M_d = k \cdot t \qquad \text{Eq.1}$$

Now turn to the part of the drug release that is governed by film breakage. In order to gain an inside look at the drug released due to the breakage along, the total drug release need to get rid of the contribution of the diffusion part (Eq.1). Careful examination of the release curves of the Gp50-52 (Fig4.10) revealed an interesting fact: for the curve of Gp51, the curve before and after 2 hr had a change of slopes with the part of curve after 2 hours significantly higher; same phenomenon was observed in the release curve of Gp52, the increase in the slope of the release curve occurred around 12 hr mark. Assuming only two mechanism contributing to the drug release, it is not hard to figure out the increase of the slope was due to the additional drug release caused by the film breakage. The film breakage for different strength of the films starts at different time point t_0, such as Gp51, t_0 is around 2 hr and Gp52, t_0 is at 12 hr; this can be understood by the fact that the beads of Gp52 had been cured to have higher extent of coalescence so the film had higher strength and hence more resistant to break. For the Fig 4.10, the 3 groups (Gp50-52) can be regarded to have similar permeability; therefore the drug release contributed by the diffusion can be calculated according to the amount released in the first 12 hours of Gp52 (Depicted in Table 4.2).

Table 4.2: Estimation of the release due to breakage

Time (h)	Release of Gp 51	Release of Gp 52	Difference (Release Due to Breakage)
2	7.4%	1.0%	6%
3	30%	1.6%	28%
4	45%	2.4%	42%
6	80%	3.1%	77%
9	94%	4.8%	89%
12	97%	6%	91%

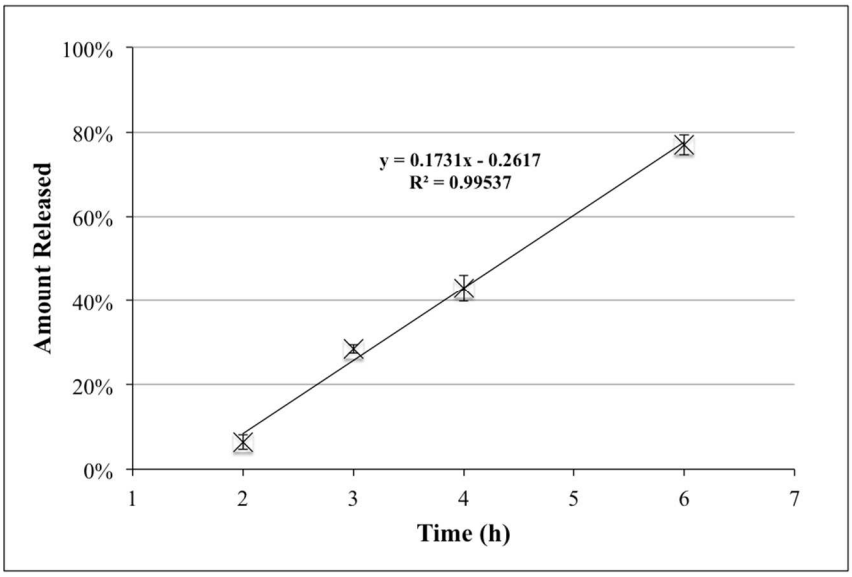

Fig 4.13 Plot of estimated release due to breakage against dissolution time. It was a linear relationship (zero order kinetics) with high regression coefficient of 0.99.

The plot of the release due to breakage (the third column in Table 4.2) for Gp51 was shown in Fig 4.13. The first 4 points showing the release in the first 6 hours were effectively zero order release with R2> 0.99, and it showed that the release between 2 and 6 hours the mechanism of the release is primarily due to the film breakage. If the plot were involved the last 2 time points the 9 and 12 hours, the amount released would not be a straight line with R2 almost equal to 1 for two reasons: 1) the drug release due to the film coat breakage cannot go on the same rate forever, it has to level off near 100%

release; 2) the contribution of the diffusion is no longer equal to the Gp52 release at the same time point since majority of the beads had already broken. The important message from the Fig 4.13 was that the mechanism due to film coat breakage is zero order kinetics, hence we proposed for the amount released due film breakage Mb with Equation 2. Where the δ is the rate of film breakage, measured in percentages, started at time t0 and M0 is the amount of drugs still not dissolved at time t0, also measured in percentages.

$$M_b = \delta \cdot M_0 \cdot (t\text{-}t_0) \qquad \text{Eq.2}$$

Combining the Eq.1 and 2, we then have the Equation 3 for the final description for the amount of drug released M of multiparticulate beads coated with pseudolatex EC dispersion.

$$M = k \cdot t + \delta \cdot M_0 \cdot (t\text{-}t_0) \qquad \text{Eq.3}$$

In this Equation, t0 is the time taken for the breakage to occur. This quantity is reflected by the film strength and is affected by many factors demonstrated throughout this work: t0 is larger when the coating thickness is higher, curing temperature is higher, curing humidity is higher and if stirring speed of the dissolution is lower. Taking the data in Table 4.2, it can be estimated k is 0.53%h-1 and δ is 17.3% h-1 and substitute into the Eq 3, we obtain M_0 is 1.01(101%) and t0 is 1.634 hr. The estimate of M_0 is a little off because the maximum drug remained to be dissolved can only be less than 100%, we are confident that if with more repeats, the estimation would be more accurate. Then the values were substituted back to Eq.3 to estimate the total release of the Gp51 (Table 4.3), it was shown the prediction was very reasonably accurate up to the time of 6 hr.

Table 4.3 The estimated release M compared to the measured release of Gp51

Time (h)	Release of Gp 51	Estimate of Release
2	7.4%	7%
3	30%	26%
4	45%	44%
6	80%	80%
9	94%	134%
12	97%	188%

One major limitation of using the Eq.3 is when the release approaching 100%, the model is incapable of taking into account the case when the amount of beads left unbroken is less than the rate of film breakage at a later stage of the dissolution; furthermore, the time t has to be greater or equal to t0. Hence, for this model to work, the criterion is therefore the amount of beads left unbroken should be larger than the amount of breakage would happen in an hour (Eq.4).

$$M(t) = \begin{cases} k \cdot t; (\text{ if } t < t_0) \\ k \cdot t + \delta \cdot M_0 \cdot (t\text{-}t_0); (\text{if } t \geq t_0) \end{cases} \quad \text{Eq.4}$$

Despite the limitation, one potential usage for such model is it would be able to predict the time it required to reach certain drug release, using the data again in Gp51, in Table 4.2, for 70% release, the time required to reach it can be calculated accurately to be 5.5 hr; which is what we can expect from the release curve. The same method was utilized for the beads with coating levels of 15% w/w. The diffusion rate k for the Gp47-49, was estimated from Gp49 to be 1.71% h-1 and δ for the Gp48 (cured at 60°C LH for 4 hr) was estimated to be 45.3% h-1, t0 is 0.88 hr and M0 is 100%. The method was used to estimate the 8% coating level w/w also, but it was not successful because the film broke

in the 8% too fast it was not possible to obtain a reasonable estimate on the release due to diffusion.

4.5 Conclusions

In this work, we continued the research on free cast psueolatex EC films, the NIR spectral data of the free films can be used to establish models to predict important physical-mechanical properties: $\frac{\mathrm{TS}}{\mathrm{YM}}$ and WVP accurately with the help of chemometrics statistical softwares. Then the same pseudolatex dispersion was coated onto MCC beads containing a layer of dye as a model drug. Beads with four coating levels were prepared and different curing conditions were applied to each coating levels. Then the beads were tested under dissolution. With the help of DVS and SEM measurements in addition to the dissolution tests, the release mechanism of the beads were studied in depth and a mathematical formula (Eq.4) was proposed to account for the drug release of EC coated beads. The formula has one limitation in predicting drug release close to 100%, however, with the more data in future works; the mathematical model would be further perfected and become more generalized.

4.6 References for Chapter 4

1. Keddie, J.L., *Film Formation of Latex.* Materials Science and Engineering, R Reports, 1997. **21**: p. 101-170.
2. Tabasi, S.H., et al., *Quality by design, part III: study of curing process of sustained release coated products using NIR spectroscopy.* Journal of pharmaceutical sciences, 2008. **97**(9): p. 4067-86.

3. *Aqueous Polymeric Coatings for Pharmaceutical Dosage Forms*. 3rd ed. DRUGS AND PHARMACEUTICAL SCIENCES, ed. J.W.M. Linda A. Felton. 2008: Dekker.

4. HARMONISATION, I.C.O., *PHARMACEUTICAL DEVELOPMENT Q8(R2)* 2009.

5. *Handbook of Near-Infrared Analysis*. Third Edition ed. PRACTICAL SPECTROSCOPY SERIES, ed. D.A. Burns and E.W. Ciurczak. 2008: CRC Press.

6. Kramer, K. and S. Ebel, *Application of NIR reflectance spectroscopy for the identification of pharmaceutical excipients.* Anal. Chim. Acta, 2000. **420**: p. 155-161.

7. Ulmschneider, M., et al., *Transferable basic library for the identification of active substances using near-infrared spectroscopy.* Pharm. Ind., 2000. **62**: p. 301-304.

8. Sinsheimer, J.E. and A.M. Keuhnelian, *Near-infrared spectroscopy of amine salts.* Journal of Pharmaceutical Sciences, 1966. **55**(11): p. 1240-1244.

9. Lodder, R.A., M. Selby, and G.M. Hieftje, *Detection of capsule tampering by near-infrared reflectance analysis.* Analytical Chemistry, 1987. **59**(15): p. 1921-1930.

10. Duan, J., K. Riviere, and P. Marroum, *In Vivo Bioequivalence and In Vitro Similarity Factor (f2) for Dissolution Profile Comparisons of Extended Release Formulations: How and When Do They Match?* Pharmaceutical Research, 2011. **28**(5): p. 1144-1156.

11. Ciurczak, E.W., *Pharmaceutical mixing studies using nearinfrared spectroscopy.* Pharm. Technol., 1991. **15**: p. 140-145.

12. El-Hagrasy, et al., *Near-infrared spectroscopy and imaging for the monitoring of powder blend homogeneity.* J. Pharm. Sci., 2001. **90**: p. 1298-1307.

13. Tabasi, S.H., et al., *Quality by design, part II: application of NIR spectroscopy to monitor the coating process for a pharmaceutical sustained release product.* Journal of pharmaceutical sciences, 2008. **97**(9): p. 4052-66.

14. Howland, H. and S.W. Hoag, *Analysis of curing of a sustained release coating formulation by application of NIR spectroscopy to monitor changes physical–mechanical properties.* International Journal of Pharmaceutics, 2013. **452**(1–2): p. 82-91.

15. Guo, J.-H., R.E. Robertson, and G.L. Amidon, *An Investigation into the Mechanical and Transport Properties of Aqueous Latex Films: A New Hypothesis for the Film-Forming Mechanism of Aqueous Dispersion System.* Pharmaceutical Research, 1993. **10**(3): p. 405-410.

16. Bodmeier, R. and O. Paeratakul, *Mechanical Properties of Dry and Wet Cellulosic and Acrylic Films Prepared from Aqueous Colloidal Polymer Dispersions Used in the Coating of Solid Dosage Forms.* Pharmaceutical Research, 1994. **11**(6): p. 882-888.

17. Ozturk, A.G., et al., *Mechanism of release from pellets coated with an ethylcellulose-based film.* Journal of Controlled Release, 1990. **14**(3): p. 203-213.

18. Korber, M., et al., *Effect of unconventional curing conditions and storage on pellets coated with Aquacoat ECD.* Drug development and industrial pharmacy, 2010. **36**(2): p. 190-199.

19. Corti, P., et al., *Application of NIRS to the control of pharmaceuticals identification and assay of several primary materials.* Pharm. Acta Helv., 1992. **67**: p. 57-61.

20. Brereton, R.G., *Chemometrics: Data Analysis for the Laboratory and Chemical Plant*. 2003: John Wiley & Sons, Ltd.

21. Reich, G., *Near-infrared spectroscopy and imaging: Basic principles and pharmaceutical applications.* Advanced Drug Delivery Reviews, 2005. **57**(8): p. 1109-1143.

22. Biopolymer, F. *Aquacoat ECD Product Brochure*. N/A.

Chapter 5 Using Fluorescence Anisotropy For Investigation on Ethylcellulose Pseudolatex Films Curing

5.1 Abstract

Fluorescence anisotropy technique has been excessively used in Chemistry for structural analysis or in biology for assessing binding for biological molecules such as proteins. Few examples have been seen in the literature for solid samples. In this investigation, one anisotropy rotating probe DMA-DPH was incorporated into the solid ethylcellulose pseudolatex cast films in order to study the curing process under different conditions. One reference fluorescence molecule Erythrosin B was used as the reference for the feasibility study for our experimental set up. A new technology that allows the real-time measurement for temperature and humidity inside the testing cuvette was also utilized. The results of fluorescence anisotropy investigation gained more insight into the curing process the was not able to detect previously and provided another way of detecting the extent of coalescence of ethylcellulose molecules in curing.

Keywrods: Fluoresnce Anisotropy, DSC, Ethylcellulose Curing, Relative Humidity Real Time Monitoring, Cetyl Aocohol

5.2 Introduction

Nowadays, pseudolatex dispersions have been used extensively to replace the conventional solvent coating systems. Uses of the aqueous based pseudolatex dispersion avoid using the harmful and often environmentally unfriendly solvent systems such as ethanol or dicholoromethane. The challenge of using pseudolatex dispersion lies in the

curing step where the water insoluble polymer particles need to coalesce in order to form a strong, stable film. This is particularly important for pharmaceutical products that have controlled release coating. The under cured products can potentially have the further gradual coalescence during storage that ultimate leads to slowing down of the release rate when patients take the medication.

In the previous work for curing investigation, we demonstrated using ethanol cast ethylcellulose (EC) films and tensile testing can establish a method of quantifying the extent of coalescence during curing for pseudolatex ethylcellulose(Chapter 3) and by using near infrared spectroscopy (NIR) and chemomestric tools, we were able to predict the tensile properties and water vapor permeability (Chapter 4). Here, we explore the possibility of using fluorescence anisotropy to study the curing process and with the aim of gaining more insight knowledge of the curing process.

Fluorescence anisotropy is extensively studied in the field of solution biochemistry to measure the kinetics of protein binding. When a fluorescence labeled protein binds to another large molecule, its tumbling speed greatly reduced, this leads to an increase in anisotropy r and hence can be quantified with the amount bind[1]. In our case, we hope to expand this usage into the solid phase: fluorescence probes were added into the EC pseudolatex dispersion and the probes can then participate into the polymeric films after drying. By Perrin's Equation (Eq1), the depolarization by rotational diffusion of spherical rotors can be described[2, 3]; where the r is anisotropy θ is the rotational correlation time; r_0 is fundamental anisotropy, τ is fluorescence life time. In the same system, r_0 and τ can

be regarded as constant, anisotropy r is therefore dependent on θ. From Eq. 2, θ is proportional to the molecular rotating volume V. Therefore the larger the V leading to larger θ and eventually lead to the larger of r. For the fluorescence rotating probe that incorporate into the solid films, the more restriction on the probe's rotational motion, the larger of its rotating volume V and then results in the higher value of anisotropy r.

$$r = \frac{r_0}{1+\frac{\tau}{\theta}} \qquad \text{Eq.1}$$

$$\theta = \frac{\eta V}{RT} \qquad \text{Eq.2}$$

Therefore, with such incorporation, it is able to detect the microenviromental changes inside polymer film during curing by monitoring the changes to the fluorescence anisotropy. Because of the measurements require complete films be held in the cuvette, only dry films will be used. By these measurements, we were able to study the changes of free volume directly impacting the free volume inside the EC pseudolatex films and gained more in-depth knowledge regarding the curing mechanism. It also allowed us to be able to further interpret the data obtained earlier such as tensile or permeability. We began this investigation with a common fluorescence benchmark Erythrosin B to check the calibration and reproducibility of our test methods and equipment[4]. Then dry pseudolatex EC films with the fluorescence rotating probe 1-(4-dimethylaminophenyl)-6-phenylhexatriene (DMA-DPH) were prepared. These films were treated with different curing conditions and these effects were assessed by fluorescence anisotropy. Also thanks to the newly developed, custom-made probe "Pyrocuvette", which provided real time readings of the temperature and humidity inside the fluorescence cuvette. Our equipment allowed the observation onto the coalescence process become possible for the first time.

Based on the information above, we hypothesized if the probe DMA-DPH can reflect the local environmental changes during curing around the probe, then such change can be obtained through fluorescence anisotropy and eventually leading to better understanding of the cuing mechanism.

5.3 Materials and Methods

5.3.1 Materials

Ethylcellulose (EC) pseudolatex dispersion (30% solid content) Aquacoat ECD 30D (FMC Biopolymer, Ewing, NJ. Lot: JN11823341). Triethyl citrate was (Vertellus Indianapolis, IN, lot: 116266). 70 mm round aluminum crinkle dishes (VWR Cat.No. 25433-085). The fluorescence DMA-DPH probe (Marker Gene Technology, Lot # 091JJN083). The fluorescence bench mark Erythrosin B (E.B) (Aldrich, Milwaukee, WI, lot: EQ 02101CG). Glycerin USP (Sigma Aldirch, Lot: 32896EM)

Equipments used were: K2 Multifrequency Phase Fluorometer (ISS, Champaign, IL); RTE-111 water heater (NESLAB, Thermo Scientific), 2920 Modulated DSC (TA Instrument, New Castle, DE); PyrroCuvette humidity and temperature data monitoring system (Opulus, Philadelphia, PA).

5.3.2 Methods

Fluorescence labeled Film Preparation

DMA-DPH solution (50ppm) was first prepared by dissolving the probe in ethanol solution. Then required amount of the solution for 10ppm final dispersion was added first to a beaker and let the ethanol to evaporate first so that the fluorescence molecules were deposited on the beaker wall. Then the Aquacoat dispersion and water was added to the beaker and the mixed solution was kept stirring for 48 hours to enable a complete incorporation of the fluorescence probes into the EC chains. Finally, plasticizer TEC (25% of Aquacoat Solid) was added to the dispersion and continue to stir for at least 3h to make the final dispersion (15% solid). The dispersion was then dried in 40°C convection oven to obtain the dried fluorescence labeled film samples which were slightly yellow. The fluorescence labeled dry films were then cut in to rectangular strips with dimension 2.6 x 1cm. And were treated under the curing conditions at 60°C with ambient humidity which measured to be 3-4% relative humidity and 75% RH. The 75% RH environment was obtained with saturated NaCl solution inside a sealed desiccator.

Key Equipment and Set Up

Fluorescence anisotropy measurements took place in an ISS K2 Multifrequency Phase Fluorometer. The anisotropy measurements were set up in an L-format. A water heater (NESLAB, Model: RTE-111) was connected to the chamber of the fluorometer to allow the temperature control of the sampling cuvette. To measure dry, solid films, a modified fluorescence cuvette that houses a glass cover slip (2.6×1cm) holder was utilized (Fig 5.1). Films specimens were fixed in-between the glass cover slip and the vertical central holder inside the cuvette. The vertical black holder attaching to the cord on top of the

cuvette were a custom made probe made by Opulus Inc called “PyrroCuvette”; this measures the temperature and humidity inside this fluorescence cuvette during measurements. The benchmark probe E.B was first evaluated in water inside a regular fluorescence cuvette by dissolving trace amount of E.B in DI water. Then mixture of trace E.B and glycerin were applied to the surface of the glass slips, and held in-between two glass slips vertically for fluorescence anisotropy measurements.

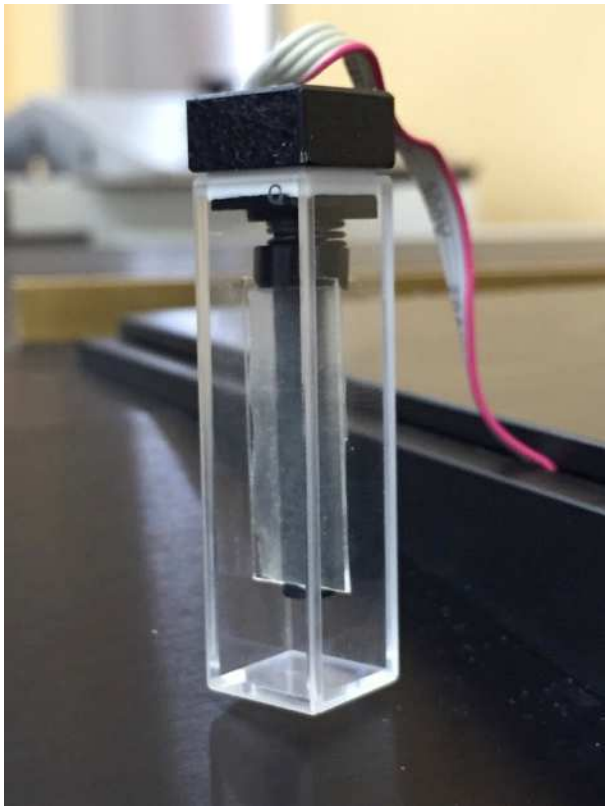

Fig 5.1: The Cuvette for the fluorescence anisotropy measurements showing the hanging of the vertical glass plate holding the film specimen. The cord runs on the top of the vial is part of the humidity temperature data logger system that can record the temperature and humidity inside cuvette during measurements.

Film Sample Measurements

All tested groups (including the benchmarks and the solid films) were organized in Table 5. 1. “Low RH (LH)” curing conditions for Gp4 was used to represent the almost no moisture in the curing for Gp4. Groups1-5 were measured with a single point

fluorescence anisotropy. Additionally, the last 2 groups (Gp6 and 7) of the curing films were measured via kinetic methods where the films were cured inside the cuvette under specific conditions. For the Gp6, the humidity was uncontrolled, the temperature was gradually increased from RT to 43°C and then to 60°C. Gp7 had the same profile for the temperature, but filled with water to the level it just touching the end of the plastic holder. This is to simulate high RH (75% RH) environment inside the cuvette The reason cannot use saturated NaCl solution inside the cuvette because the solid would condense on to the inner surface of cuvette. Fluorescence anisotropy measurements were recorded at 400 nm for excitation and 467 nm for the DMA-DPH films. For the Gp1 and Gp2 containing E.B, the specimen was excited at 2 wavelengths of 350 and 400nm and record emission at 550nm.

Table 5.1. The Materials and curing conditions for the tested samples

Groups	Materials	Curing Condition
Gp 1	E.B in Water	NA
Gp 2	E.B in Glycerin	NA
Gp 3	Dry Labeled EC Film	Dry (No Curing)
Gp 4	Cured Labeled EC Film	60°C Ambient RH 4h
Gp 5	Cured Labeled EC Film	60°C 75% RH 4h
Gp 6	Dry Labeled EC Film	Cured inside cuvette at Ambient RH
Gp 7	Dry Labeled EC Film	Cured inside cuvette at High RH

The thermal properties of the pseudolatex films were recorded by the techniques of differential scanning calorimetry (DSC) to confirm the events in the values of fluorescence anisotropy. The DSC the test method used was: heating ramp 5°C/min from -50°C to 90°C.

5.4 Results

5.4.1 The Reference Checking with Benchmark Material

Table 5.2: The results of the reference fluorescence materials E.B

Groups	Materials	Excitation/nm	Emission/nm	Anisotropy
Gp 1	E.B in Water	350	550	0.018±0.001
Gp 1	E.B in Water	400	550	0.19±0.03
Gp 2	E.B in Glycerin	350	550	0.016±0.001
Gp 2	E.B in Glycerin	400	550	0.23±0.02

The results of the reference fluorescence material E.B was provided in Table 5.2. The benchmark data for the fluorescence anisotropy readings for E.B measured in water from literature was around 0 when excitation at 350 and 0.2 with excitation at 400nm. The measured anisotropy values with the Gp1 showed the equipment was in good agreement with the literature value. The Gp2 measurements were carried out with the glass slips with the E.B and glycerine in-between 2 parallel vertical slips. The measured anisotropy values were almost identical to the Gp1.

5.4.2 Fluorescence Anisotropy of Pseudolatex Films

The one-time measurements of the three groups (Gp3-5) showed in Fig 5.2. The fluorescence anisotropy were small compared to previous cases of E.B. But we saw a significant increase on the reading from Gp3 to Gp4 and then surprisingly decrease from Gp4 to Gp, when curing at 60°C 75% RH (Gp5), there is little change on the fluorescence anisotropy compared the dry films (Gp3).

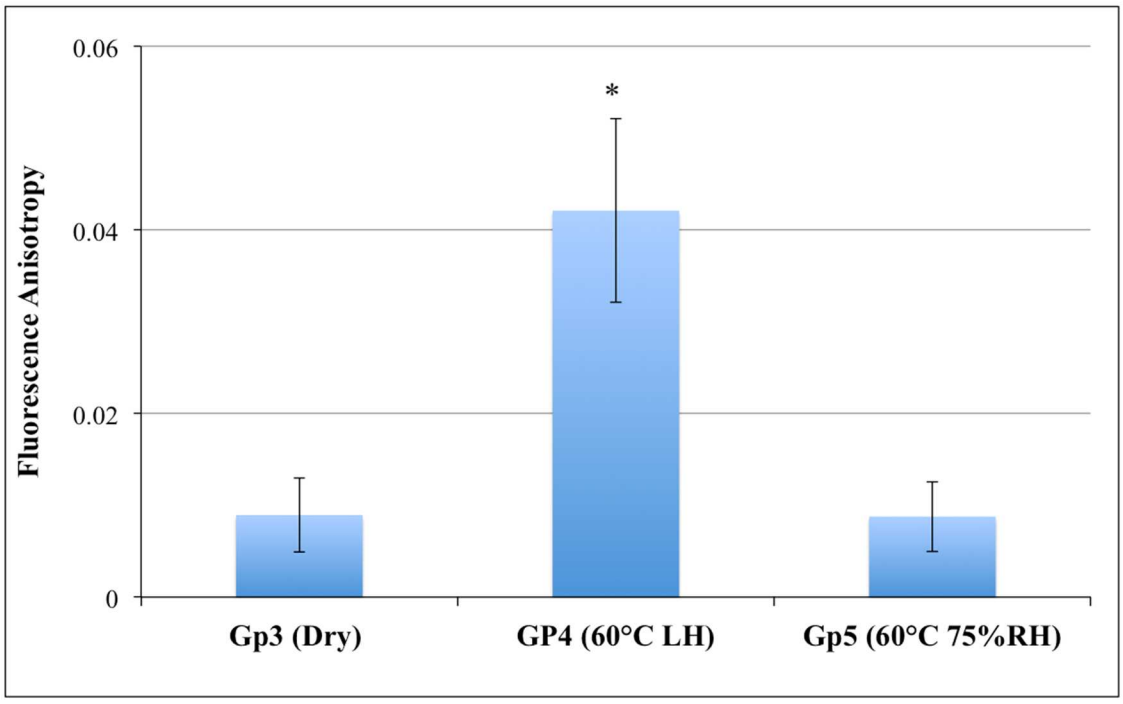

Fig 5.2 The anisotropy of films after curing with three curing conditions The values shown were mean ±SD with n in the range of 7-10 for test groups. The * indicates the statistical significance ($p<0.05$) compared to the Gp3 (Dry) group. The statistical analysis was carried out by One-way ANOVA test with post Dunnett's multiple comparison test with the Gp3 (Dry) group with GraphPad Prism 6.0.

Results of the continuous monitoring of the Gp6 were showed in the Fig 5.3 and 5.4 for a selected specimen to further investigate the event going on throughout the curing process. Three quantities: anisotropy, relative humidity and temperature were monitored throughout the full process and two of each was showed in each figure with temperature data showed twice as a reference.

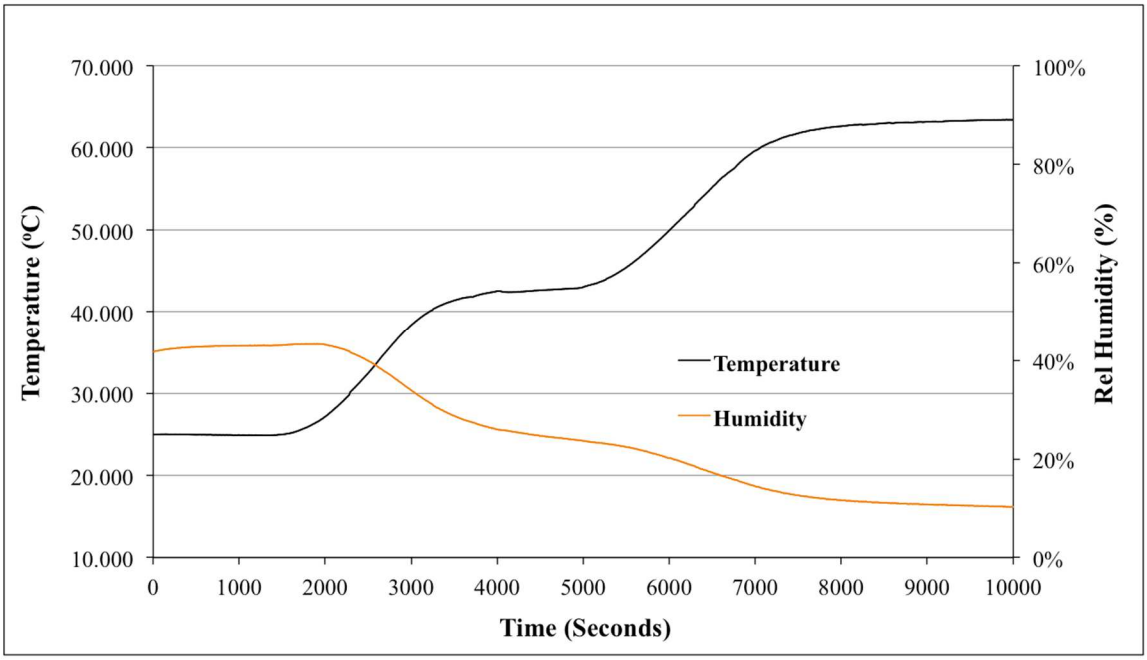

Fig 5.3: The relative humidity and temperature monitoring of the Gp6 curing. The temperature started at RT of 25°C and were then increased twice and held constant at 43 and 63°C to investigate fluorescence anisotropy response, the relative humidity was also recorded. It decreased as temperature increased.

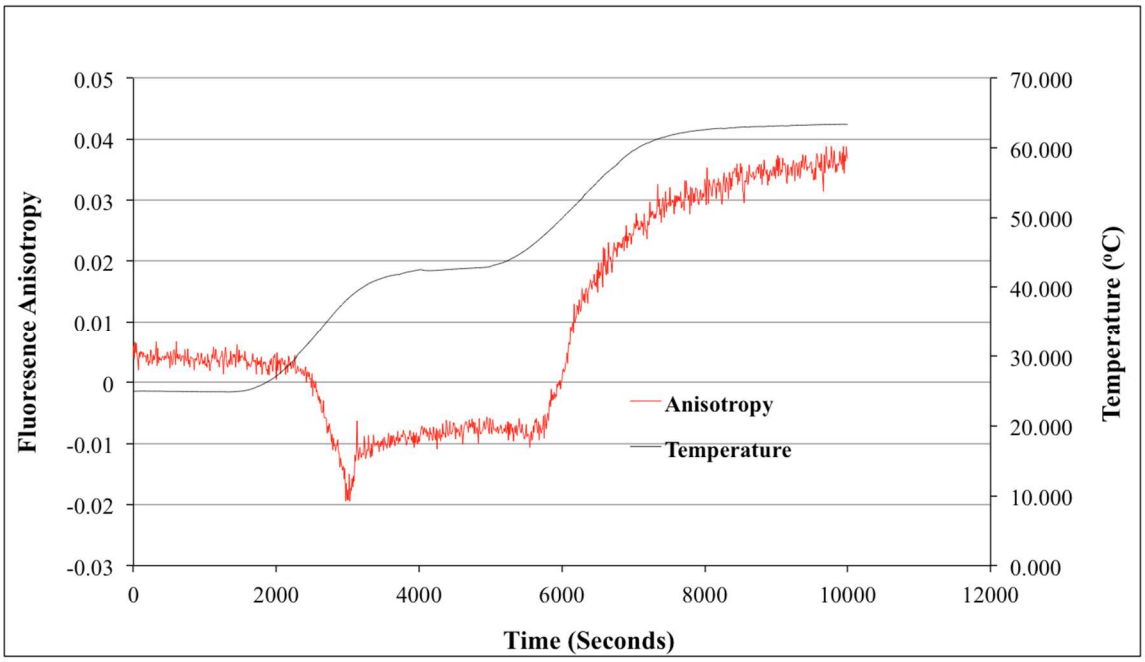

Fig 5.4: The anisotropy and temperature monitoring of the Gp6 curing, where the fluorescence cuvette contained film specimen only. The same temperature profile as Fig 5.3 was shown to compare the anisotropy change. It was shown the anisotropy started to decrease due to polymer softening when temperature increased to 43°C and the

anisotropy increased when temperature increased further to 63°C which is due to the cetyl alcohol melting.

From the figures shown, the relative humidity was gradually decreasing as expected since higher temperatures result in higher saturated vapor pressure[5]. The moisture was very low and from previous investigations, it is known that at this set of conditions, the extent of coalescence can be minimal. However, the anisotropy values were more responsive towards the change of the temperature: there were two abrupt changes during the heating process: the first was the drop around 35°C and the second was the increase at temperature of around 50°C.

The same set of figures of Gp7 monitoring were shown in Fig 5.5 and 5.6. Because the difficulty of using saturated salt solution mentioned earlier, the high humidity environment was created by filling water in the cuvette. As can be seen from Fig 5.5, this time round, the humidity was much higher than Gp6. At this extremely high humidity, anisotropy behaved differently: after a short decrease initially, the anisotropy went up significantly like in Gp6, then over time, it gradually came back down.

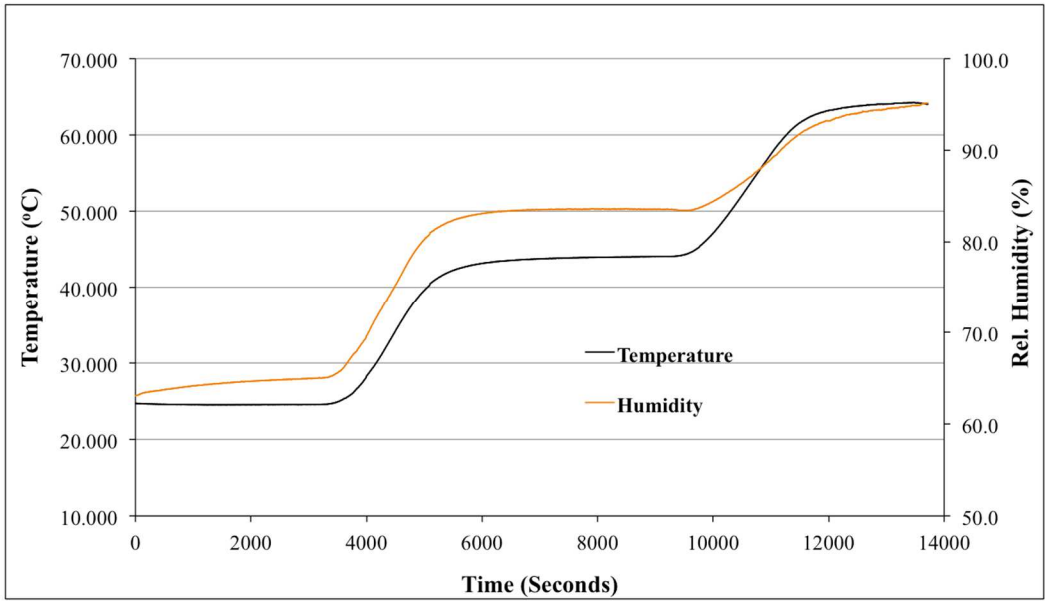

Fig 5.5: The temperature and relative humidity monitoring of the Gp7 curing, where the cuvette containing not only the film specimen, but also contained small amount of water. The temperature started at RT of 25°C and were then increased twice and held constant at 43 and 63°C to investigate fluorescence anisotropy response, the relative humidity was also recorded. Because the water presence, the relative humidity increased with the increase of the temperature.

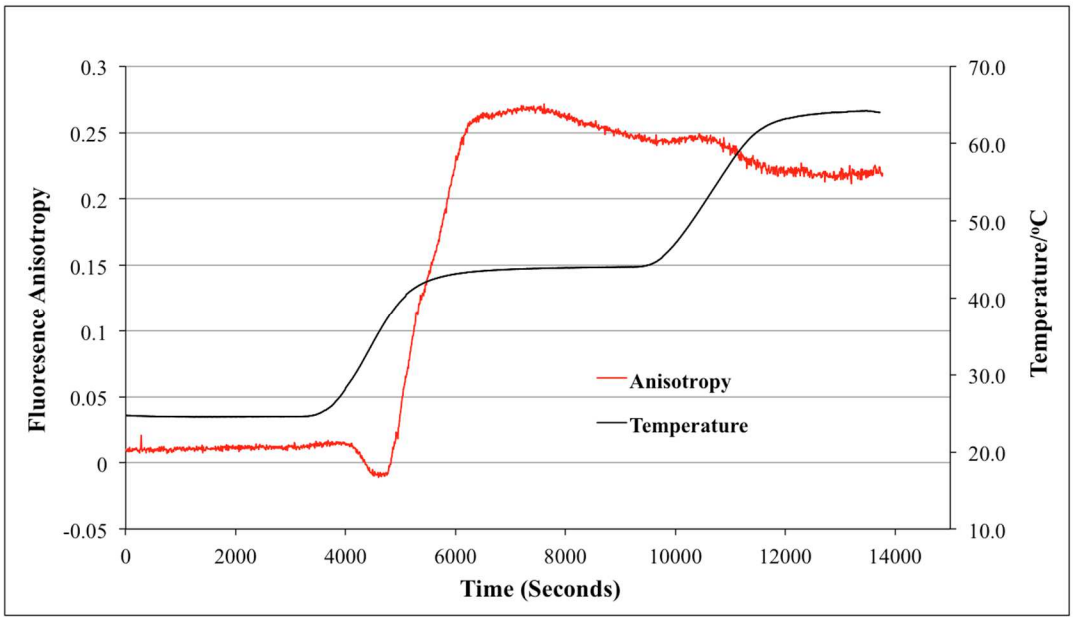

Fig 5.6: The anisotropy and temperature monitoring of the Gp7 curing, where the fluorescence cuvette contained both film specimen and water. The same temperature profile as Fig 5.5 was shown to compare the anisotropy change. It was shown the anisotropy started to decrease a little before increased dramatically due melting of cetyl

alcohol during temperature was increased from RT to 43°C, when the temperature was heated further, the anisotropy gradually decreased due to the relax and EC particle coalescence.

The DSC profiles for the dry films showed in the Figure 5.7, the Tg of the polymer were relatively week, but it was still visible at 34.9°C, there is also a clear endothermic peaks at 67°C. Cetyl alcohol is the 2nd most abundant materials in the Aquacoat system, comprising of 8.7% of the solid content, therefore it is also important for the behavior of the system. Its DSC profile was shown in Fig 5.8. The DSC cycle started from 0°C and then cooled down back to 10°C. The large endothermic peak at 52.8°C indicated the melting point for the cetyl alcohol and the 2 exothermic peaks on the cooling cycle showed there were possible 2 crystalline forms generated for this material.

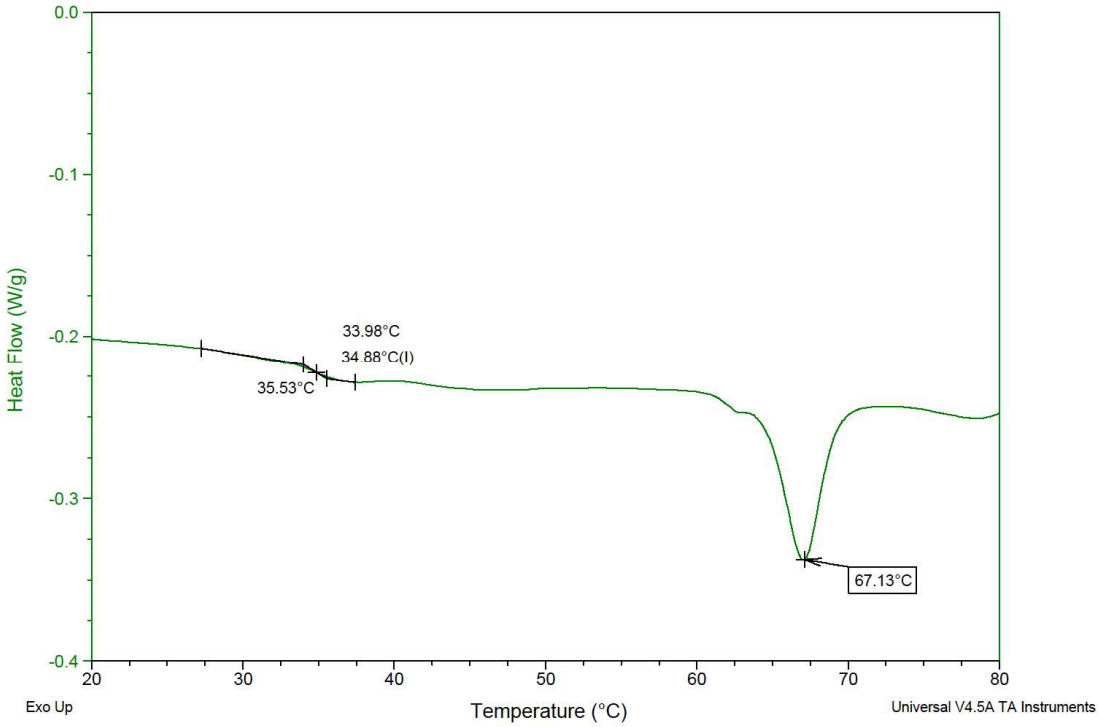

Fig 5.7. The DSC profile of sample pseudolatex dry film when heating up. The Tg were determined to be around 35°C determined when the film samples were during first heating up cycle.

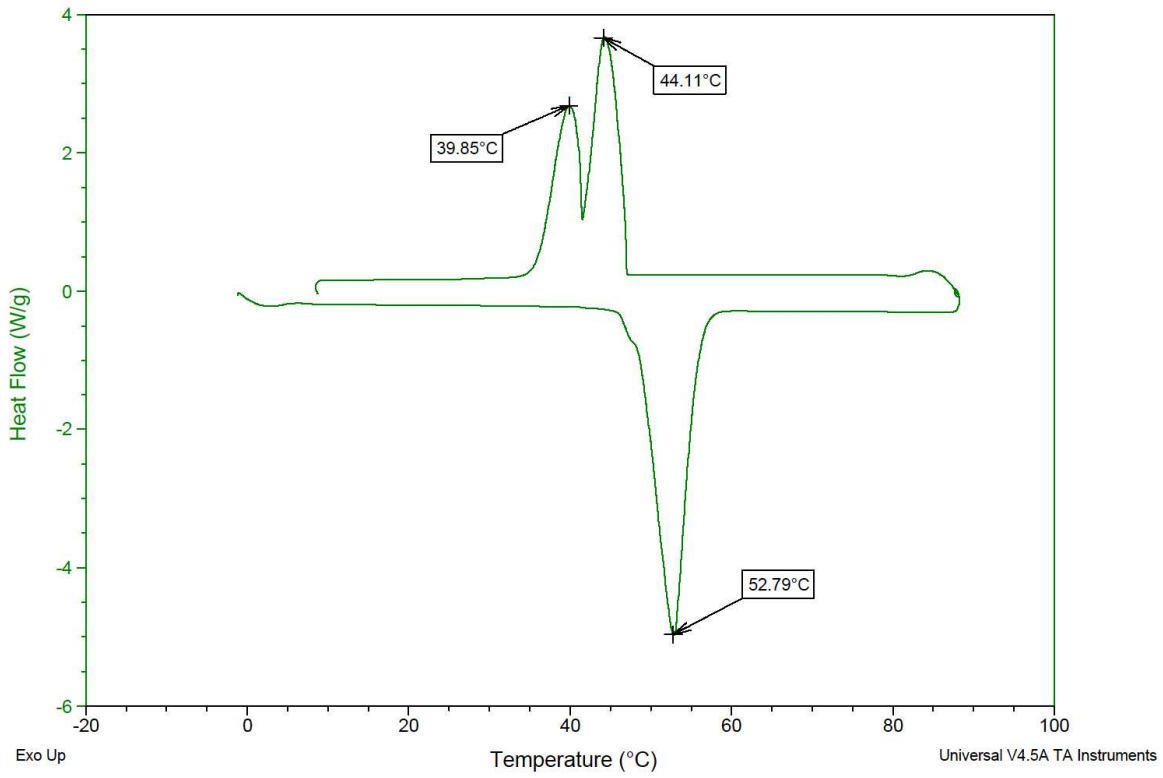

Fig 5.8. The DSC profile of the heating and cooling cycle of the pure cetyl alcohol. The melting of the cetyl alcohol was determined through the first heating cycle to be around 52.8°C. On the cooling cycle, two crystallization peak was also observed.

5.5 Discussions

The reference checking using the Erythrosin B (E.B) as the benchmark material provided consistent results with the reported reference values for both measuring the solution anisotropy in water and using our innovative experimental set up. Therefore, it provided a confidence for using this experiment set up for the evaluations.

The Gp3-5 showed interesting results of the fluorescence anisotropy, although the absolute change in anisotropy was small, the changes were significant. The film specimens cured at 60°C ambient humidity (also can be regarded as low RH) showed significant increase in anisotropy can therefore by explained by the increase in the local

constrained environments for fluorescence probes. This increase of constraint were new discovery because in the previous investigations, the curing at 60°C, ambient humidity had no changes in either tensile testing or permeability. After examining the anisotropy and temperature curve of Gp6 (Fig 5.4), the increase at around 6000 second, 50°C is the reason why the anisotropy ended up high. This transition is the melting point of the cetyl alcohol at 52.8°C, indicated with DSC profiles for pure cetyl alcohol (DSC Fig 5.8). More mobile cetyl alcohol molecules upon melting can therefore move to the vicinity of the fluorescence probe; the mobile cetyl alcohol molecules therefore impeded the rotation of the DMA-DPH and resulted in this large increase of the anisotropy. The other noticeable feature of the Gp6 anisotropy behavior was it had an initial reduction of at around 35°C, 3000 second. From the DSC curves of the EC film (Fig 5.7), this initial decrease happened exactly at the glass transition temperature (Tg) of the ethylcellulose. It is well understood that when polymer molecules were above their Tg, the polymer chains would become more mobile and easier to move. This improved mobility for polymers reduced the initial constraints on the DMA-DPH rotations, hence decreased the anisotropy initially. The drop in anisotropy was noticed before by Thulborn et al[6]: in micelles formed with phospholipid dipalmitoylphosphatidylcholine (DPPC), the fluorescence probes 12-anthroyloxy stearate (12-AS) and 1,6-diphenyl-1,3,5-hexatriene (DPH) were found to have a temperature –dependent polarization where the anisotropy dropped significantly when the temperature is above the lipid phase transition temperature. Above this temperature, because the lipid bilayer structure will no longer hold, the probes become almost free. As in our case here, above the glass transition

temperature, the polymers had a greater mobility, and this increased mobility reduced the restriction on the DMA-DPH so a decrease of the anisotropy was observed.

The Gp7 anisotropy of pseudolatex EC films was quite different compared to that of Gp6. From the previous study (Chapter 3), it was clear the high humidity can dramatically increase the extent of coalescence of EC polymers in curing. This impact of high humidity had a different impact on the Gp7: the previous abrupt change at 50°C (Gp6) was now expedited to lower temperature at around 40°C (Fig 5.6), this is likely due to the reduction of the air pressure inside the cuvette. Assuming the cuvette was originally at 1atm, the increase of vapor pressure reduced the air pressure inside the cuvette. By Clausius-Clapeyron equation, this reduction of the pressure will lead to the decrease of melting point[7]. Further more, when the anisotropy reached plateau, the anisotropy kept decreasing: this is the process of the coalescence that provided the EC polymers with a much higher mobility. The increase of extent of coalescence at high moisture provided a constraint-relieving role for the DMA-DPH, which can rotate with less local crowdness and reflected on the decrease on this anisotropy value. These two effects offset each other, and brought an almost identical value of the anisotropy in Gp5 compared to the dry film of Gp3.

5.6 Conclusions

An innovative approach using fluorescence anisotropy for studying the film curing of ethylcellulose was carried out. The experimental set up was first evaluated using existing benchmark of fluorescence probes and proved to be in good agreement. Then fluorescence probes containing EC pseudolatex films were tested using both one-time

and continuous measuring techniques. The tests results, along with the thermal testing using DSC, revealed subtle internal changes during the curing and provided us a more in-depth understanding of the events occurring during EC curing and will serve as a great starting point for future researchers that want to use the fluorescence anisotropy techniques to study in latex/pseudolatex systems.

5.7 References for Chapter 5

1. Lakowicz, J.R., *Principles of Fluorescence Spectroscopy*. 3rd ed. 2006: Springer.
2. Weber, G., *Polarization of the fluorescence of macromolecules. II. Fluorescent conjugates of ovalbumin and bovine serum albumin.* Biochem J, 1952. **51**: p. 573-590.
3. DJR, L., *A study of the adsorption of dyes on bovine serum albumin by the method of polarization of fluorescence.* Biochem J, 1952. **51**: p. 168-180.
4. Thompson, R.B., I. Gryczynski, and J. Malicka, *Fluorescence Polarization Standatds for High-Throughput Screening and Imaging.* BioTechniques, 2002. **32**(1): p. 36-41.
5. Oyj, V. *HUMIDITY CONVERSION FORMULAS Calculation formulas for humidity*.
6. Thulborn, K.R. and G.S. Beddard, *The effects of cholesterol on the time-resolved emission anisotropy of 12-(9-anthroyloxy)stearic acid in dipalmitoylphosphatidylcholine bilayers.* Biochimica et Biophysica Acta (BBA) - Biomembranes, 1982. **693**(1): p. 246-252.
7. EB, S., *Basic chemical thermodynamics*. 1990: Oxford University Press.

Chapter 6 Understanding the Influence of Drug Properties and Product Design on In Vitro Drug Release, Its Potential Link to In Vivo Performance and Implication on Biowaiver Regulation of Oral Extended Release Dosage Forms

6.1 Abstract

Purpose: Bioequivalence (BE) studies are often required to ensure therapeutic equivalence for major product and manufacturing changes. Waiver of a BE study (biowaiver) is highly desired such changes. . Current regulatory guidelines allow for biowaiver of proportionally similar lower strengths of an extended-release (ER) product provided it exhibits similar dissolution to the higher strength in multimedia. The objective of this study is to demonstrate that (1) proportionally similar strengths of ER tablets exhibiting similar *in vitro* dissolution profiles do not always assure BE; (2) different strengths that do not meet the criteria for dissolution profile similarity may still be bioequivalent. **Methods and Results:** Four marketed ER tablets were used as model drug products. Higher and lower (half) strength tablets were prepared or obtained from commercial source. *In vitro* drug release was compared using multi-pH media (pH 1.2, 4.5, 6.8) per regulatory guidance. *In vivo* performance was assessed based on the available *in vivo* BE data or established *in vitro-in vivo* relationships. This study demonstrated that relationship between *in vitro* dissolution and *in vivo* performance is complex and dependent on the characteristics of specific drug molecules, product design

and *in vitro* test conditions. As a result, proportionally similar strengths of ER dosage forms that meet biowaiver requirements per current regulatory guidelines cannot ensure bioequivalence in all cases. Thus, without an established relationship between *in vitro* and *in vivo* performance, granting biowaiver based on passing *in vitro* tests may result in approval of certain bio-inequivalent products, presenting risks to patients. **Conclusions:** To justify any biowaiver using *in vitro* test, it is essential to understand effects of drug properties, formulation design, product characteristics, test method and its *in vivo* relevance. Therefore, biowaiver requirements of different strengths of ER dosage forms specified in the current regulatory guidance should be careffully examined for possible revisions.

Keywords: *In vitro* drug release, *in vivo* evaluations, bioequivalence, biowaiver, extended-release

6.2 Introduction

In vitro drug release is one of the most critical quality attributes currently used for product quality assessment and process control, for assuring sameness after making product/process changes and for supporting waiver of *in vivo* bioequivalence studies (biowaiver) under certain conditions. Over the last two decades, *in vitro* release and its application in supporting biowaivers have received increased attention from the regulators, industry and academia, particularly for products with release rate-limited absorption, such as extended release (ER) dosage forms, because of its likely link to *in vivo* performance. For oral ER drug products, *in vitro* drug release test can be used as a

surrogate for *in vivo* bioequivalence when an *in vitro-in vivo* correlation (IVIVC) is established and validated according to the regulatory guidance issued by US Food and Drug Administration (FDA) and European Medicine Agency (EMA) (1-3). Current regulation also allows the use of *in vitro* release test to support biowaiver between the proportionally similar higher and lower strengths of the same drug product regardless of the type of ER dosage forms or whether there is a qualitative or quantitative *in vitro-in vivo* relationship (IVIVR). As a result, the lower strengths and, in some cases, higher strengths of many oral ER products have been approved without conducting bioequivalence studies.

Oral ER products are generally single-unit or multiple-unit dosage forms (pellets, tablets or capsules) that involve one or more of the drug release mechanisms, such as diffusion, erosion, dissolution and osmotic pressure (4). It is well established in the scientific field that *in vitro* drug release from an ER system usually depends on drug properties, type of delivery technology, formulation composition, size and geometry of the dosage form, manufacturing process as well as test method and conditions. However, how the above-mentioned variables and their interplays may impact the association between *in vitro* drug release in multimedia and *in vivo* absorption has not been well understood. More importantly, a quantitative link between the *in vitro* and *in vivo* performance that can be generalized for any types of drugs and dosage forms does not exist. As a result, it is often challenging to determine whether or how a change in dissolution observed during product development, post-approval changes or routine commercial production may impact *in vivo* performance in the absence of an IVIVR. For example, a formulation or

manufacturing change that results in passing or failing similarity factor (f_2) criteria may or may not have direct *in vivo* implication depending on the characteristics of the API and product design, nature of the change, and the test method. Except for the multiple-unit dosage forms where various strengths differ only in the number of units, a lower strength of an ER drug product made either by making proportional change in composition or by only matching *in vitro* drug release may or may not be bioequivalent to the higher strength. Hence, allowing biowaiver for lower strengths of ER products based on *in vitro* drug release in the absence of an IVIVC or IVIVR by current regulatory guidelines can result in compromised product performance and increased risks to the patients. This is of particular concern for products containing active pharmaceutical ingredients (API) with narrow therapeutic index (NTI). Therefore, an improved understanding of the drug release in relation to API, drug product and test method is urgently needed to provide sound scientific basis for regulatory requirements of biowaiver and to assure product quality.

In the present study, the *in vitro* release of proportionally similar higher and lower strengths of ER tablets were evaluated and compared with the corresponding *in vivo* performance. Four model drug products, namely extended-release drug A, drug B, drug C and verapamil hydrochloride, were chosen to show four possible scenarios illustrated in Fig 6.1, The findings can have significant scientific, business and regulatory implications with respect to regulatory clearance of proportionally similar strengths of an ER product that are only required to exhibit similar *in vitro* drug release in multimedia.

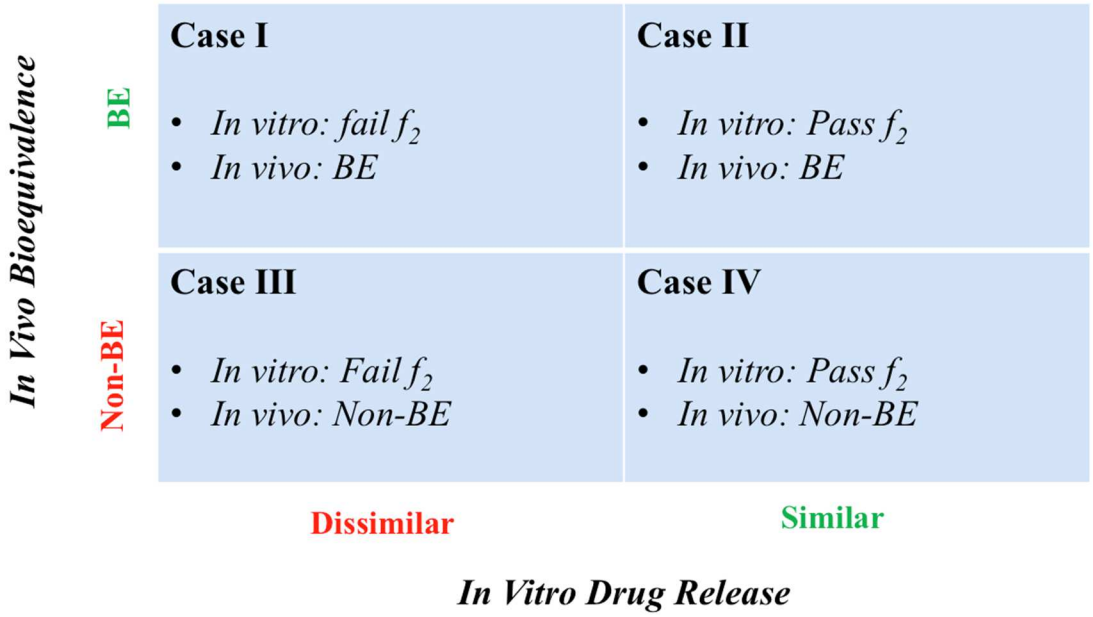

Fig 6.3 Four possible scenarios linking in vitro drug release to in vivo performance between the proportionally similar strengths of an ER product

6.3 Experimentals

6.3.1 Materials and Equipment

The following materials and equipment were used in the study: compound A (AbbVie, North Chicago, IL), compound B (AbbVie, North Chicago, IL), compund C (AbbVie, North Chicago, IL); Isoptin® SR tablets (120 mg Lot #316168D, 240 mg lot #286628D; Abbott Laboratories, Limited. Québec, Canada), Methocel K15MP CR, (Dow Chemical Co., Midland, MI), Methocel E10M (Dow Chemical Co., Midland, Michigan), Methocel K100LV CR (Colorcon, West Point, PA).

Equipment used were: KG5 high shear granulator (Key International, Englishtown, NJ); Fitzpatrick L1A Comminutor (The Fitzpatrick Company, Elmhurst, IL); Strea-1™ fluid-bed dryer (Aeromatic-Fielder AG, Bubendorf, Switzerland); Twin Shell Dry Blender

(Patterson-Kelley Co., East Stroudsburg, PA); Carver laboratory press (Model: 88881DI0A00, Carver, INC Wabash, IN), VK7000 dissolution testing stations (Varian Inc., Palo Alto, CA), Perkin Elmer 200 HPLC (Waltham , MA).

6.3.2 Methods

Preparation of Tablets

Low and high strengths of Isoptin® SR tablets that are proportionally similar in composition were obtained from commercial source. Proportionally similar low and high strengths of extended release drug A, drug B and drug C were prepared by using the same formulations and manufacturing processes of the corresponding commercial tablets, Drug A ER, Drug B ER, and Drug C ER tablets respectively. All three products were made using wet granulation in a high shear mixer granulator followed by fluid bed drying, milling, blending and compression using Carver press.

6.3.3 Evaluation of Tablets

In the present study, the higher strength of marketed dosage form was used as the reference for evaluation of *in vitro* and *in vivo* performance of the proportionally similar lower strength of each product. Specifically, extended-release tablets of drug A, 500 mg, drug B, 500 mg, drug C, 1000 mg and verapamil hydrochloride, 240 mg, were compared with the corresponding half-strength tablets, 250 mg, 250 mg, 500 mg and 120 mg, respectively.

Evaluation of In Vitro Drug Release

In vitro dissolution test conditions of all four drug products are provided in Table 6.1. The higher strengths were first tested using the method approved by the FDA to ensure that the *in vitro* performance is the same as the clinical batches used in the *in vivo* bioavailability studies during product development. Subsequently, drug release profiles of both the lower and higher strengths were generated using three USP buffer media at pH 1.2, pH 4.5, and pH 6.8 (5). When testing dissolution of drug A ER tablets at pH 1.2 and drug B ER tablets at pH 6.8, two 250 mg tablets were used to compare with a single 500 mg tablet, in order to match the effect of non-sink condition on drug release of the higher strength resulting from limited drug solubility under the testing conditions. To facilitate evaluation of their *in-vivo* performance, *in vitro* dissolution of the lower and higher strengths was also tested using the IVIVC- or IVIVR-based methods that are available for drug A and drug B ER tablets, respectively.

All test samples were assayed for drug concentrations using analytical methods described in USP–NF for each product (6-8). Six or twelve *replicates* were tested to generate each profile. The drug release profiles of the higher and lower strengths were compared using the similarity factor f_2 (Eq.1). The release profiles of the two strengths are considered similar if $f_2 \geq 50$ and dissimilar if $f_2 < 50$.

$$f_2 = 50 \times \log\left\{\left[1 + \frac{1}{n}\sum_{j=1}^{n}\left|R_j\text{-}T_j\right|^2\right]^{-0.5} \times 100\right\} \qquad \text{(Eq.1)}$$

Table 6.1 *In Vitro* Drug Release Test Methods

Product	**Multimedia Methods**	**NDA* and/or USP method**
Drug A ER	USP II, pH = 1.2, 4.5 and 6.8; 100 rpm, 37°C in 900 mL media with wire helical sinkers	USP II, 100 rpm, 0.1 N HCl for 0.75 hour followed by 0.05 M phosphate buffer containing 75 mM sodium dodecyl sulfate (SDS) at pH 5.5 with wire helical sinkers
Drug B ER	USP II, pH = 4.5 and 6.8; 75 rpm, 37°C in 900 mL media with wire helical sinkers	USP II, 50 rpm, 0.21 M Phosphate buffer at pH 4.0 with wire helical sinkers
Drug C ER	USP I, 40 mesh, pH = 1.2, 4.5 and 6.8; 100 rpm, 37°C in 900 mL media	USP I, basket 40 mesh; 100 rpm, water
Isoptin® SR	USP II, pH = 1.2, 4.5 and 6.8; 50 rpm, 37°C in 900 mL media	USP II, 50 rpm, pH 1.0 for 1h followed by phosphate buffer at pH 7.5

*http://www.accessdata.fda.gov/scripts/cder/dissolution/dsp_SearchResults_Dissolutions.cfm?PrintAll=1

The HPLC assay of the above test for each individual drug product was strictly followed by the USP assay methods(6-9). For every drug product, standard curves for each HPLC test for each pH value were evaluated by dissolving pure API in that specific media. The standard curves were established at 6 concentrations, for every concentration, 5 determinations were made. The coefficient of variation (CV) for every concentration level was ensured to be below 10% to ensure the precision for concentration measurements. And all standard curves had regression coefficient above 0.999.

In Vivo Evaluation

The *in vivo* performance of the high and low strengths of the four drug products were evaluated and compared using data obtained from either bioequivalence studies or dissolution test based on a IVIVR or IVIVC model. Specific test methods for comparing *in vivo* performance of each drug product are summarized in Table 6.2.

Table 6.2 Methods for evaluating in vivo performance of high and low strengths

Produt	Method used for comparing *in vivo* performance	Source
Drug A ER	IVIVC	(1, 10)
Drug B ER	IVIVR	(11)
Drug C ER	Bioequivalence studies	(12, 13)
Isoptin® SR	Bioequivalence studies	(14, 15)

ER Tablets of Drug A

The approved *in vitro* dissolution method for extended release hydrophilic matrix tablets of drug A (Table 6.1) is based on a validated IVIVC model. Thus, it was used as a surrogate test to compare *in vivo* performance of the drug A ER tablets, 500 mg and 250 mg. Bioequivalence between the two strengths were evaluated based on drug release specification established using the IVIVC model.

ER Tablets of Drug B

The *in vitro* dissolution method provided in Table 6.1 for testing extended release hydrophilic matrix tablets of drug B, 500 mg and 250 mg, is an IVIVR-based dissolution test. A dissolution range with demonstrated bioequivalence has been mapped out in a 3-way crossover single-dose study and confirmed in a multiple-dose bioavailability study (11). In the present study, the two strengths were considered bioequivalent when their dissolution profiles fall within the drug release space with proven bioequivalence.

ER Tablets of Drug C

No qualitative or quantitative relationship has been established between the approved *in vitro* dissolution test described in Table 6.1 and *in vivo* performance of extended release hydrophilic matrix tablets of drug C. Thus, comparison of *in vivo* performance between

the 1000 mg and 500 mg Drug C ER tablets was based on bioequivalence studies of the two strengths (Table 6.2).

Isoptin SR® Tablets

A quantitative relationship between the approved *in vitro* dissolution test method (Table 6.1) and *in vivo* performance of extended release hydrophilic matrix tablets of verapamil hydrochloride was explored in the original regulatory submission. However, it could not be validated due to a single release rate. Therefore, relative bioavailability studies of the 240 mg and 120 mg Isotin SR® tablets available in the literature and regulatory filing documents were used to compare the *in vivo* performance of the two strengths.

6.4 Results and Discussions

For ER tablets of drug A, B and C, the *in vitro* performance of the higher strength tablets prepared in this study was tested and confirmed to match that of the clinical batch of each product before being used as the reference for evaluation of the proportionally similar lower strengths. For Isoptin SR® tablets, both higher and lower strengths were commercial products obtained directly from Pharmacy.

6.4.1 Comparing In Vitro and In Vivo Performances

ER Tablets of Drug A

Dissolution profiles of the compositionally proportional lower strength drug A ER tablets (250mg) are compared with the higher strength (500 mg) in Fig 6.2. Considering complete *in vivo* drug release/absorption of drug A ER tablets occurs within approximately 20 hours, test duration in all media was limited to 24 hours despite of the inherently slow dissolution of drug A ER tablets in the standard multi-pH media. Data

analysis shows that the lower strength meets the similarity factor (f_2) criteria in all three media over the pH range of 1.2 - 6.8 using the conventional USP test method. Thus, according to the regulatory guidelines, a bioequivalence study for proportionally similar lower strength can be waived based on: both strengths (1) have the same dosage form design, (2) have the same drug release mechanism, and (3) are within the ranges of linear disposition and therapeutic dose.

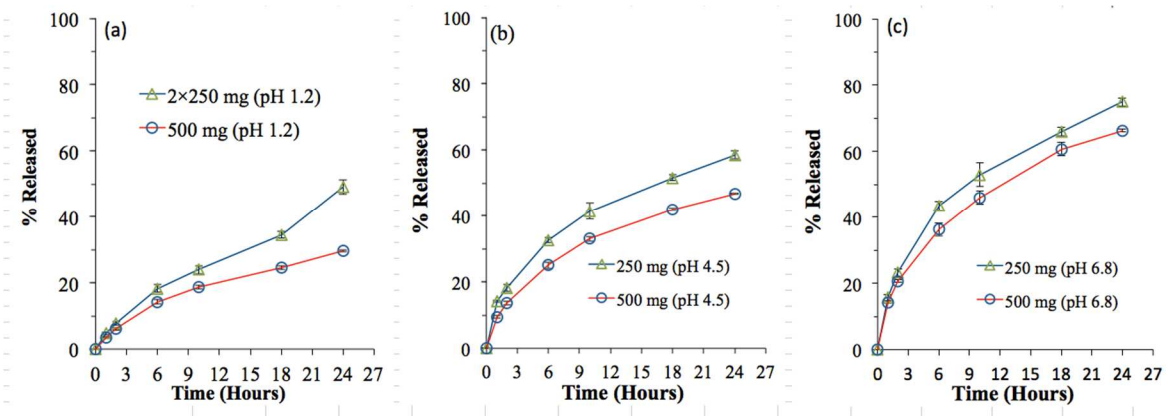

Fig 6.2 In vitro dissolution of Drug A ER tablets, 250 and 500 mg, in multi-pH media. (a) pH 1.2 (f2 = 51.2); (b) pH 4.5 (f2 = 54.1); (c) pH 6.8 (f2 = 61.0); n=6 for every product

However, dissolution data generated using the IVIVC-based test method in Fig 6.3 show a more rapid drug release for the proportionally similar 250 mg tablets that would fail to meet the dissolution specification established using IVIVC model, resulting in bio-inequivalent C_{max}. It was based on this finding that a decision was made to develop a new formulation for the 250 mg tablet in spite of the acceptable multimedia testing results of the proportionally similar formulation. Through formulation screening studies, the currently marketed 250 mg tablet was identified and found to exhibit similar dissolution profile to the 500 mg strength when tested by the IVIVC dissolution method (Fig 6.3b). The reformulated 250 mg tablet represents a 50% and 30% increase in both HPMC content and surface area/volume ratio (S/V), respectively, relative to the

proportionally similar 500 mg tablets. A subsequent single-dose pilot bioequivalence study not only further confirmed the IVIVC-based prediction, but also indirectly inferred different *in vivo* performance of the proportionally similar formulation.

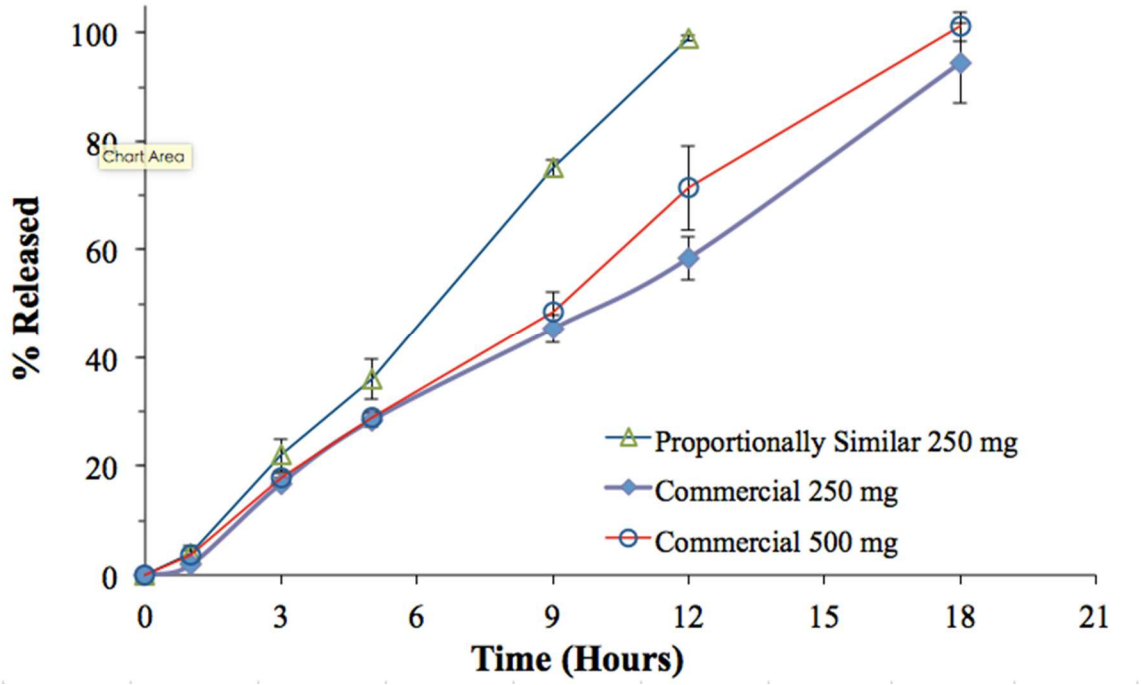

Fig 6.3 In vitro dissolution of proportionally similar (f2 = 39.7) and reformulated (f2 = 60.2) commercial 250 mg ER tablets of Drug A compared with the 500 mg ER tablets using an IVIVC-based test method ; n=6 for each product

ER Tablets of Drug B

Fig 6.4 shows that dissolution profiles of the proportionally similar lower strength tablets (250 mg) meet the similarity factor criteria in media over the pH range of 4.5 -6.8 using conventional USP test method. Data in pH 1.2 dissolution medium are unavailable because of the rapid degradation of drug B at low pH (16).

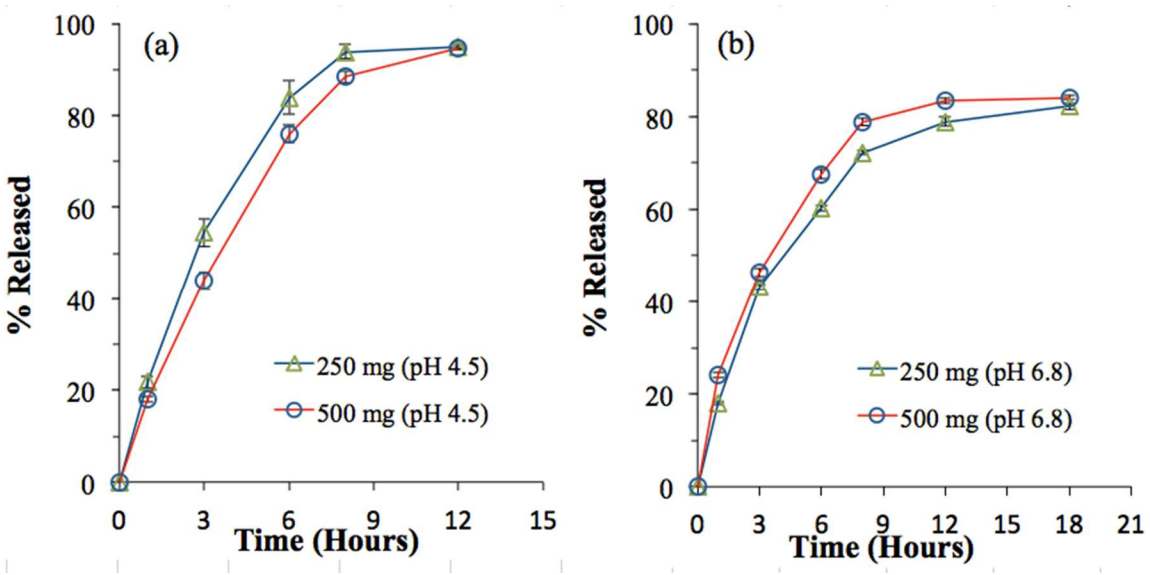

Fig 6.4 In vitro dissolution of drug B ER tablets, 250 and 500 mg in multi-pH media. (a) pH 4.5 (f_2 = 60.8); (b) pH 6.8 (f_2 = 63.2); n=6 for every product

To compare *in vivo* performance of the two strengths, a different dissolution test previously used to *map in vitro and in vivo* performance of extended release drug B hydrophilic matrix tablets during product development was utilized (Table 6.1). Specifically, a dissolution range with demonstrated bioequivalence of three ER formulations, where the levels of the HPMC rate-controlling polymer differed, was established in a single-dose and a multiple-dose crossover bioavailability studies (11) (Fig 6.5a). Dissolution profiles of the two strengths generated using this test method shown in Fig 6.5b not only are similar (f_2 = 61.0) but also fall well within the space with proven bioequivalence, indicating similar *in vivo* performances between the proportionally similar 250 and 500 mg tablets.

3Fig 6.5b not only are similar (f_2 = 61.0) but also fall well within the space with proven bioequivalence, indicating similar *in vivo* performances between the proportionally similar 250 and 500 mg tablets.

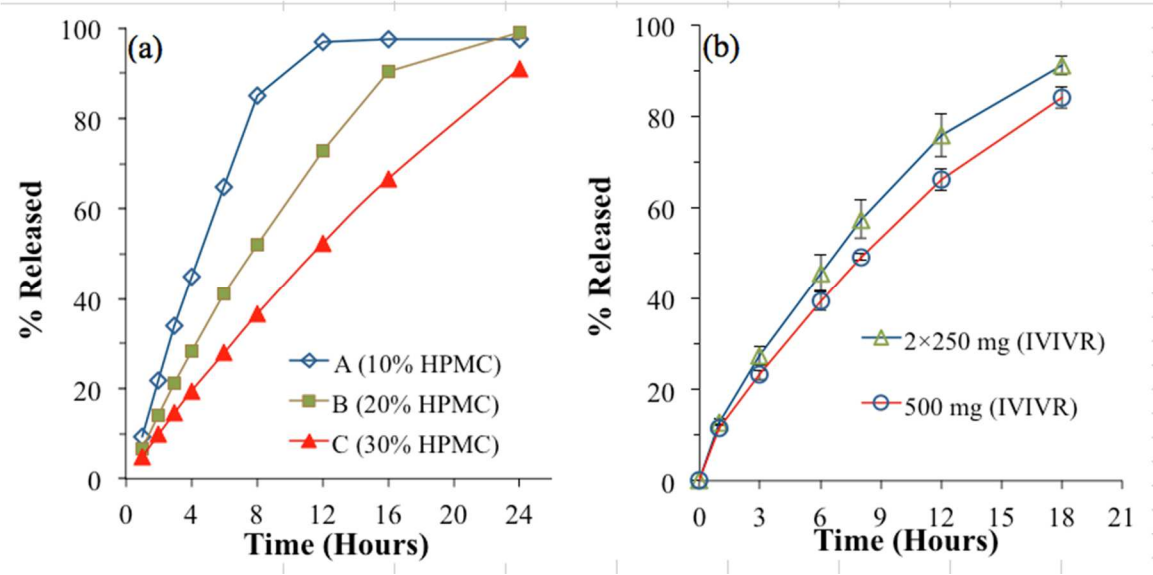

Fig 6.5 In vitro dissolution profiles of (a) three bioequivalent drug B ER tablets containing different levels of HPMC and (b) proportionally similar ER tablets, 250 and 500 mg, using the IVIVR method (n=6 for both products)

ER Tablets of Drug C

In vitro dissolution testing of the two proportionally similar strengths of drug C ER tablets (500 mg and 1000 mg) was carried out using a USP Apparatus I at different pH values of 1.2, 4.5 and 6.8. The data provided in Fig 6.6 indicate dissimilar dissolution profiles under all test conditions except at pH 1.2.

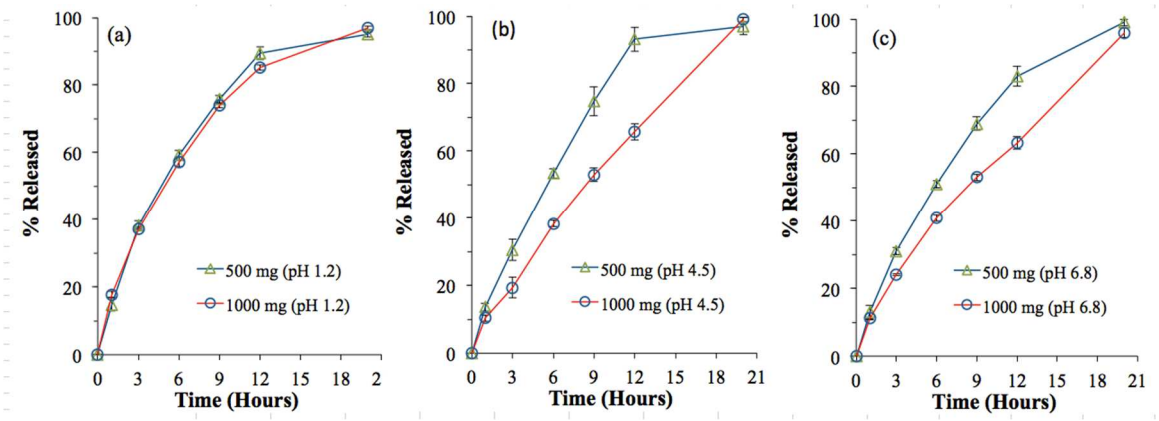

Fig 6.6 In vitro dissolution of drug C ER tablets, 500 and 1000 mg in multi-pH media. (a) pH 1.2 (f2 = 78.5); (b) pH 4.5 (f2 = 39.3); (c) pH 6.8 (f2 = 47.1); n=6 for each product

Since there is no established relationship between the *in vitro* and *in vivo* data, comparison of the *in vivo* performance of the two strengths are carried out using bioavailability studies that are available in the literature. It was found that the proportionally similar 500 mg and 1000 mg strengths of Drug C ER tablets are not interchangeable based on a single-dose bioavailability studies (12). The 1000 mg strength was found to be absorbed more slowly than the 500 mg tablets. As a result, the 1000 mg strength of commercial Drug C ER was later reformulated to achieve bioequivalence to the 500 mg strength (13).

Isoptin® SR tablets

In vitro dissolution data of compositionally proportional 120 and 240 mg Isoptin® SR tablets were generated using three media of pH 1.2, 4.5 and 6.8. Fig 6.7 shows that the two strengths exhibit similar dissolution behaviors only at pH 1.2 and failed similarity criteria at both pH 4.5 and 6.8.

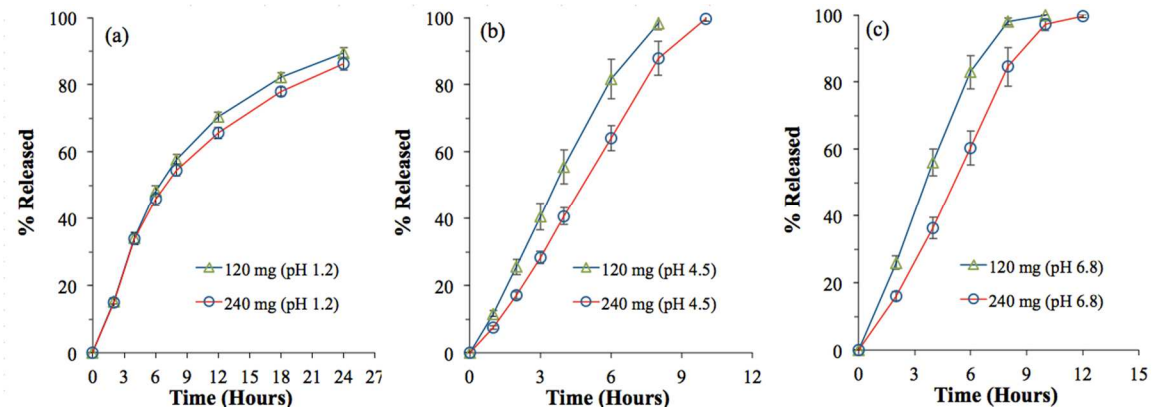

Fig 6.7 In vitro dissolution of Isoptin® SR tablets, 120 and 240 mg in multi-pH media. (a) pH 1.2 (f2 = 73.4); (b) pH 4.5(f2 = 45.8); (c) pH 6.8 (f2 = 44.1); n=6 for each product

Due to a lack of qualitative or quantitative relationship between *in vitro* dissolution test and *in vivo* performance for this product, the *in vivo* performance of the two strengths is evaluated based on a review of bioavailability studies reported in the literature, regulatory filing and the product label. For instance, there were no significant differences in mean C_{max}, T_{max} and AUC values after dosing two 120 mg tablets and one 240 mg tablet in a crossover multiple-dose study in 10 healthy subjects (14). The average C_{max} and AUC values were 116 and 122 ng/ml, and 1523 and 1416 ng hr/ml for the two dosing regimens, respectively. Similar results were found for the metabolite, norverapamil. In a separate study comparing two half-240 mg tablets and a single 240 mg tablet, similar results were also obtained, which is consistent with the product label of Isoptin SR (14, 15) that allows patients to split the 240 mg tablet in half when necessary. These findings indicate similar *in vivo* performance between the two proportionally similar strengths despite of the observed differences in i*n vitro* dissolution and tablet sizes.

In summary, investigation of *in vitro* and *in vivo* data of four marketed ER products containing different API's, rate-controlling polymers and product designs has shown that all four outcomes illustrated in Fig 6.1 are possible. Therefore, in the absence of any

known *in vitro-in vivo* relationship, biowaiver decision of proportionally similar strengths of an ER product based on the *in vitro* dissolution tests in multi-media needs to be supported by further sound scientific evidences. It may (1) be acceptable for products that fall within Cases II and III, such as Drug B ER and Drug C ER, (2) lead to unnecessary *in vivo* bioequivalence study for Case I, i.e., products with dissolution behaviors similar to Isoptin® SR, or (3) result in approval of certain bio-inequivalent products as described in Case IV such as proportionally similar lower strength of Drug A ER tablet. Thus, establishing *in vitro* and *in vivo* relationship of an ER product is critical for any decision involving the need for conducting bioequivalence studies. In addition, gaining enhanced understanding of how drug properties, product design and their interplay with test condition influence *in vitro* dissolution is also important.

6.4.2 Understanding the Influence of Drug Properties and Product Design on Drug Release in Multi-pH Media

Oral extended-release systems typically fall into three broad categories: matrix, reservoir and osmotic systems (4). Depending on drug property and formulation design, drug release from these systems generally involves one or a combination of the following mechanisms: drug diffusion through pores of a barrier, through tortuous channels or through a viscous gel layer formed by entangled polymer chains, system swelling followed by diffusion and/or erosion and dissolution, or osmotic pressure-induced drug release. For a monolithic dosage form, smaller dosage unit size of the proportionally similar lower strength generally results in a shorter diffusional pathlength and/or time for complete hydration in a matrix system, thinner coating film in the membrane-controlled reservoir, or semipermeable membrane in the osmotic devices because higher S/V

provides larger normalized surface. As a result, drug release is usually faster than that of the higher strength counterpart.

The design of four ER products in the current study is based on hydrophilic matrix technology which is utilized in over 75% of the ER products on the market (17) due to its applicability across a broad range of therapeutic drugs and ease of manufacture. They are all single-unit tablets, hence, one might expect similar release rate change between the proportionally similar lower and higher strength across all four products because of their similar increase in S/V. However, unlike an inert hydrophobic matrix system that usually involves negligible dimensional changes throughout drug release, drug release from the swellable and erodible matrix system is more complex where the relative contribution of diffusion and polymer erosion to the total drug release not only depends on the properties of specific drug and rate-controlling polymer, product composition, processing and dissolution test conditions, but also is constantly changing with time. For drug molecules with negligible solubility, diffusion plays a minimum role and drug release from the matrix is expected to be primarily determined by the rate of surface erosion. Therefore, the increase in drug release rate in this case is generally proportional to the increase in the normalized surface area. For spherical geometry, the increase in S/V of a proportionally similar half-strength tablet is approximately 26%. Thus, *in vitro* drug release from this type of half-strength tablet is not expected to pass the dissolution similarity criteria. For soluble drugs or drugs with intermediate solubility, the drug release is much more complex due to the interplay between drug diffusion, particle dissolution, water penetration, polymer hydration that leads to glass-rubber transition (i.e. gel formation and

swelling), and the subsequent polymer disentanglement and dissolution from the matrix surface. An added complication is the dynamic aspect of the above processes that changes constantly with time.

The gel layer formation and development is important for drug release from swellable hydrophilic matrices because the gel regulates both diffusion and polymer erosion processes. During dissolution, polymer starts to hydrate when in contact with water, where polymer and water can be considered as a solid solution. With the continuous influx of water, concentration of the polymer in this solid solution decreases over time, and eventually reaches a critical point where the glass-rubber transition occurs, leading to the formation of a rubbery gel. This critical point corresponds to polymer/water composition where the glass transition temperature is the same as the environmental temperature (i.e., 37°C). As more water ingresses through the existing gel, the gel layer thickness would increase over time, leading to an inward movement of the glass-rubber boundary. An outer-to-inner concentration gradient of water and inner-to-outer concentration gradient of the polymer are hence created within the gel and the glassy regions. At the gel-water interface, polymer concentration is lowered to a critical point where chain disentanglement occurs and polymer starts to dissolve (i.e. erosion). Therefore, gel layer thickness does not increase indefinitely and a steady state may be reached where polymer erosion balances with water ingression. The development of the gel layer thickness depends on the rate of water diffusion and the rate of polymer erosion. While the rate of water diffusion in the same type of polymeric gel is similar (18), the rate of erosion does change appreciably with molecular weight/viscosity grade (19),

polymer chemistry (20) and solubility of the API and other excipients in the matrix . The disentanglement concentration ($C_{p,dis}$) of hydroxyl propyl methocellulose (HPMC) was found to scale up with molecular weight (M_w) as: $C_{p,dis}$ (g/mL) = $0.05(M_w/96000)^{-0.8}$. For example, Methocel K100LV (M_w = 30 kDa) is a lower viscosity grade HPMC and its disentanglement concentration was measured as 0.13 g/mL, which is much higher than the 0.05 g/mL for Methocel® K4M (M_w = 100 kDa). Therefore, insignificant gel layer formation is often visually observed for matrix tablets made with low viscosity grade of HPMC such as K100LV, reflecting a small gel layer thickness that reaches steady state more quickly due to faster polymer erosion. On the contrary, thick gel layer and significant swelling are noticeable with matrix tablet prepared using high viscosity grade HPMC such as K15M and K100M. The slower polymer erosion rate also indicate that gel layer development is more gradual before reaching the steady state, as shown in the simulation in Fig 6.8 based on the work of Harland et al (21).

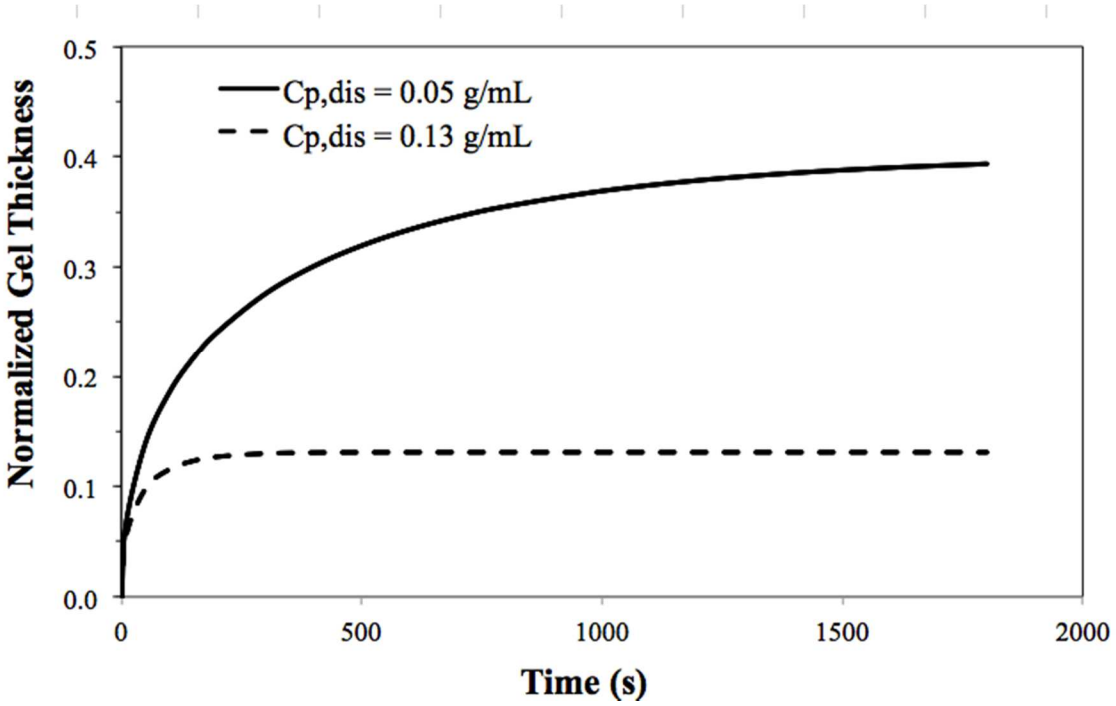

Fig 6.8 Impact on gel layer thickness development by the polymer erosion rate

The gel layer of slowly eroding polymer matrix increases significantly over duration of the dissolution testing. The increase in the diffusion pathlength over this period results in decreasing overall drug release if the driving force for drug release remains constant (i.e. similar drug concentration at the glass-rubber boundary). This is in essentially similar to drug release from a hydrophobic matrix, where the increasing diffusion pathlength and decreasing surface area over time lead to the square-root time behavior of the overall drug release. For proportionally similar lower and higher strengths, the gel layer thickness is expected to be similar due to the same composition, except at later stage when complete hydration is reached earlier for the lower strength. Hence drug release is relatively faster for the lower strength due to its increased S/V. However, when drug solubility is high, the drug molecules will be fully dissolved at the glass-rubbery interface and throughout the gel layer. The drug concentration gradient in the gel layer will gradually decrease, reducing release rate over time. Therefore, the overall drug release

tends to be affected less by the difference in S/V. In other words, for slowly erodible matrix tablets of soluble drugs, proportionally similar lower and high strengths will more likely to have similar dissolution profiles. However, if the drug solubility is low such that most of the drug molecules are not solubilized in the gel layer, drug diffusion will play a decreased role and the concentration gradient of the drug will be more similar between proportionally lower and higher strengths. In this case, the difference in the overall drug release rate will more closely align with the difference in S/V.

Similar analysis can be applied to matrices prepared using fast eroding polymers. Because of the fast rate of polymer erosion, a thin and steady state gel layer is developed quickly and maintained throughout the dissolution process until complete hydration of the tablet core. If drug is fully solubilized, drug release from proportionally similar lower and higher strengths has a higher chance to dissolve similarly, depending on the dose difference between the strengths. For drugs where diffusion is limited by solubility, release rate may be governed by the difference in S/V. However, the requirement on drug solubility may not be as high as in the cases of slowly eroding polymer in order to compensate for the disparity in S/V, because the concentration gradient is over a thinner gel layer (diffusion pathlength).

The above analysis indicates that, for high solubility drugs, release from proportionally similar lower and higher strength hydrophilic matrices tend to be less sensitive to S/V than low solubility drugs. In addition, we postulate that the ratio of drug solubility/gel layer thickness is likely a critical parameter impacting the contribution of diffusion to

overall drug release. A high solubility/gel thickness ratio will compensate more for the difference in S/V between the proportionally similar lower and higher strengths. In addition, whether a lower and a higher strength may have similar dissolution profiles is also dependent on the dose difference which determines the extent of S/V difference. Generally, half-strength tablets result in approximately 20-30% increase in S/V over its full strength counterpart of the same geometry. Therefore, lower and higher strength of soluble drugs, in particular, drug with high solubility/gel layer thickness ratio, will likely pass dissolution similarity test. It should be noted that properties of other excipients present in significant quantity, and the potential interactions among formulation components usually also plays a role during the drug release process, such is the case with Isoptin® SR, making the system more complicated.

To help understand how API properties, product design and *in vitro* test condition may influence the linkage between *in vitro* and *in vivo* performance, characteristics of the API and formulation relevant to drug release control and behaviors was evaluated. Information provided in Table 6.3 shows that percent change of S/V of the lower to higher strengths are rather similar across the four tested products (22-34%), even though the tablet geometry between Isoptin SR 120 mg and 240 mg are different. Thus, the observed different *in vitro* behaviors in multimedia dissolution testing across four products are compared based on an integrated analysis of (1) drug pK_a and solubility, (2) type, grade and content of polymer and (3) drug loading and other excipients. To derive the apparent release controlling mechanism under different test conditions, a well-known

semi-empirical approach was used by fitting of the release data to a simple exponential equation (Eq.2) (22) and the results are provided in Table 6.4.

$$M_t/M_\infty = kt^n \qquad \text{(Eq. 2)}$$

M_t and M_∞ are the absolute cumulative amount of drug released at time t and infinite time, respectively; k is a constant incorporating structural and geometric characteristics of the device, and n is the release exponent, indicative of the apparent mechanism of drug release.

It has established that an n value of 0.5 (i.e., square root of time) is indicative a diffusional mechanism and an n value of 1.0 suggests an erosion mechanism, assuming a film/slab geometry, whereas an n value of 0.5–1.0 indicates a combination thereof. The critical values of the exponents are somewhat different for other geometries (22). For example, the critical diffusional exponents are 0.45 and 0.43 for Fickian diffusion from cylinders and spheres, respectively. The corresponding limiting values for erosion-based release are 0.89 and 0.85, respectively. The critical values are not available for geometries other than the cylinder and sphere (such as the oval tablet in this study). However, they are expected to lie in between those values obtained from cylinder and spheres, given their intermediate aspect ratios.

Table 6.3. Characteristics of Drug Substances and Product Design

Drug product	**Drug A ER**	**Drug B ER**	**Drug C ER**	**Isoptin® SR**
	Drug Properties			
pK_a	4.8 (acidic)	8.76 (basic)	4.86 (acidic); 2.19 (basic)	8.8 (basic)
Solubility at pH 1.2	Slightly Soluble (1.3 mg/mL) (c)	N/A	Freely soluble (180 mg/mL) (c)	Soluble (60-70 mg/mL)
Solubility at pH 4.5	Slightly soluble (2.1 mg/mL) (c)	Freely soluble (230 mg/mL) (c)	Soluble (24 mg/mL) (c)	Soluble (60-70 mg/mL)
Solubility at pH 6.8	Freely soluble (165 mg/mL) (c)	Slightly soluble (1.2 mg/mL) (c)	Very soluble (1.4 g/mL) (c)	Sparingly soluble (~13 mg/mL)
	Product Design			
Tablet shape	Oval	Oval	Oval	Oval (240mg) Round (120mg)
% S/V (a)	122	132	134	128
Drug Loading	53%	50%	83%	35%
Polymer	HPMC	HPMC	HPMC	Alginate
Viscosity grade	High	Low	High	low
Polymer level	High	Medium	Low	High
Soluble filler	Low	High	None	None

(a) S/V: Surface area-to-volume ratio of lower strength normalized to that of the higher strength

(b) Multimedia dissolution testing compared with *in vivo* absorption

(c) Estimated based on pH-solubility profile, intrinsic solubility, and pKa

Table 6.4 Fitting Of Multimedia Dissolution Testing Data

Drug product	**Drug A ER**		**Drug B ER**		**Drug C ER**		**Isoptin® SR**	
Strength	**500 mg**	**250 mg**	**500 mg**	**250 mg**	**1000 mg**	**500 mg**	**240 mg**	**120 mg**
pH 1.2								
n	0.66	0.71	-	-	0.65	0.74	0.83	0.86
k	0.58	0.68	-	-	1.25	1.19	0.97	0.97
R^2	0.99	1.00	-		1.00	0.99	0.96	0.97
f_2	51.4		-		78.5		73.4	
pH 4.5								
n	0.51	0.46	0.80	0.76	0.76	0.77	1.20	1.13
k	0.99	1.14	1.26	1.35	0.98	1.13	0.97	0.97
R^2	1.00	1.00	1.00	0.99	0.99	1.00	0.96	0.97
f_2	54.1		60.8		39.3		45.8	
pH 6.8								
n	0.49	0.49	0.58	0.69	0.71	0.76	1.20	1.06
k	1.16	1.22	1.38	1.27	1.05	1.12	0.84	1.10
R^2	1.00	0.99	1.00	0.98	1.00	1.00	1.00	1.00
f_2	61.0		63.2		47.1		44.1	

Case I: Isoptin® SR tablets

The rate-controlling polymer of Isoptin® SR is a low viscosity grade sodium alginate, a pH-dependent, natural water-soluble linear unbranched polysaccharides consisting of different proportions of β-D-mannuronic acid (M) and α-L-guluronic acid (G) units. At acidic pH below the pK_a of M (3.38) and G (3.65) monomers, sodium alginate is converted to insoluble and non-swellable alginic acid (23), resulting in altered release-controlling characteristics.

At pH 1.2, the *in vitro* release from Isoptin® SR tablets is slow and mainly controlled by diffusion because of high solubility of the API and the formation of the inert alginic acid. In addition, surface area available for drug release also increases over time due to tablet

cracking and lamination at acidic pH (24, 25). Hence, a 28% change in S/V of the 120 mg strength showed negligible influence on drug release rate compared with the 240 mg strength. At pH 4.5 and 6.8, sodium alginate hydrates and swells rapidly, forming a gel layer surrounding the tablet. Unlike matrices consisting of low viscosity grade HPMC, the gel layer development of alginate is significant (24, 25). However, it is interesting to note that drug release at pH 4.5 was essentially governed by polymer erosion in spite of high drug solubility. In addition, drug release profiles are essentially the same as those at pH 6.8 even though drug solubility is drastically lower at high pH. These observations can be attributed to the interaction between the protonated tertiary amine cation of verapamil and the carboxyl anion of sodium alginate, resulting in erosion-controlled drug release and a decrease in free drug concentration in the gel. As a result, the release rate at pH 4.5 and 6.8 is influenced by the difference in S/V between the two proportionally similar strengths, resulting in dissimilar dissolution profiles at both pHs. Therefore, in assessing proportionally similar Isoptin® SR tablets, *in vitro* multimedia dissolution testing are found to be over-discriminating with respect to their *in vivo* performance because the two strengths have been shown to be bioequivalent.

Case II: ER Tablets of Drug B

Drug B is freely soluble at pH 4.5. The rate controlling polymer is low viscosity grade HPMC, Methocel 100LV. Because of the fast erosion rate, a thin, steady-state gel layer is established quickly and maintained throughout the drug release. Therefore, the release profile is mostly linear, reflecting an apparent mechanism of polymer erosion (n = 0.76 and 0.80 for the 250 mg and 500 mg strengths, respectively) even though drug release is

primarily via diffusion. As discussed previously, high solubility tend to compensate for the difference in S/V, and in this case, the two strengths exhibit similar dissolution profiles (f_2 = 60.8). The solubility is much lower at pH 6.8 (~1.2 mg/mL), which generally suggests increased influence by S/V for drug release. However, because the gel layer is very thin due to the presence of high levels of both Methocel100LV and highly water soluble lactose, the drug solubility/gel thickness ratio is moderate. The fitted release exponents of 0.69 and 0.58 for the 250 mg and 500 mg strengths, respectively, indicate an increased contribution of apparent diffusion-control. The observed curvature at pH 6.8 is a result of non-sink conditions and incomplete drug release due to lower solubility. The change in release mechanism and the moderate ratio of solubility/gel thickness may have partially negated the 32% increase in S/V, resulting in a similar dissolution profile at pH 6.8 nevertheless. In addition, the highly soluble filler in the formulation can also create pockets in the weakened gel layer, making the drug release a more complex process.

When utilizing the test method developed for mapping *in vitro* and *in vivo performance*, the 250 mg and 500 mg strengths exhibit similar drug release (Fig 6.5b), suggesting similar *in vivo* performance. Thus, for ER tablets of drug B, the *in vitro* multimedia dissolution testing fortuitously turns out to be useful for comparing the proportionally similar strengths.

Case III: ER Tablets of Drug C

A high viscosity grade HPMC, Methocel E10M is employed in drug C ER tablet. During dissolution, the gel layer thickness development is very pronounced. Drug C is a zwitterion with an acidic pK_a of 4.75 and a basic pK_a of 1.2, and has a U-shaped pH-solubility profile over the pH range 1.2–6.8. Solubility at pH 1.2 is very high (~180 mg/mL) and drug release is predominantly diffusion through the gel layer. The high solubility and slower polymer erosion compensated for the 34% difference in S/V between the two proportionally similar strengths and resulted in similar dissolution profiles (f_2 = 78.5). At pH 4.5, erosion is the predominant mechanism due to low solubility (Fig 6.6b). However, it is surprising to observe that at pH 6.8, the apparent drug release not only follows a near-zero-order kinetics, but also is slower than that at pH 1.2 despite of higher drug solubility (~1.4 g/mL). For example, release of the 1000 mg tablet at 6 hours is about 60% at pH 1.2 and but only about 40% at pH 6.8. Additionally, the differences in release rates between pH 4.5 and 6.8 media are insignificant even though drug solubility is significantly higher at pH 6.8. These observations suggest a likely interaction between the drug C and HPMC at pH around and above its acidic pK_a where the carboxylic anion is the dominant species. The interaction may lead to the formation of certain type of drug/HPMC complex, significantly reducing free drug concentration in the gel layer for diffusion. Therefore, drug release is dictated by polymer matrix erosion. Although the exact mechanism is unknown, hydrophobic interactions between HPMC and certain drug molecules containing carboxylic group such as ibuprofen sodium have been reported in the literature (26). Consequently, when compared with the 1000 mg strength, a 34% increase in S/V of the 500 mg strength led to significant increase (30-

40%) in release rate at pH 4.5 hours and 6.8, presumably due to decreased free drug concentration in the gel layer. Therefore, in evaluating proportionally similar ER drug C tablets, the dissolution profiles happened to be dissimilar at pH 4.5 and 6.8, leading to the coincidental agreement with the *in vivo* data.

Case IV: ER Tablets of Drug A

Drug A ER tablets contain high content of high viscosity grade HPMC that erodes slowly and exhibits a significant gel layer development phase. During dissolution, there is a very higher degree of polymer swelling. At pH 1.2, *the in vitro* drug release of the proportionally similar strengths is extremely slow primarily due to low solubility and non-sink condition. The apparent increase of the release rate from 18 to 24 hours observed for the 250 mg strength (Fig 6.2a) may result from earlier completion of tablet hydration due to its smaller size. Drug solubility increases at pH 4.5 and much more significantly at pH 6.8. But it is still inadequate to allow complete dissolution of the solid API in the gel layer. Hence, diffusion through the gel layer is the predominant drug release mechanism as indicated by release exponent values of approximately 0.5. The increasing gel layer thickness over time due to rapidly swelling and slowly eroding polymer compensated for the 34% difference in S/V between the two proportionally similar strengths and resulted in similar dissolution profiles.

The *in vitro* results in multimedia differ significantly in both release rate and kinetics from the *in vivo* apparent absorption profiles obtained by deconvolution (1, 10). Using IVIVC-based test method, the proportionally similar strengths exhibited not only dissimilar profiles, but also a more rapid and predominantly erosion-controlled release

mechanism, consistent with the in vivo observation (Fig 6.3). Consequently, a change in S/V ratio resulted in different release rate between the two strengths. The results of the current study indicate that *in vitro* multimedia dissolution testing is unable to discriminate between formulations with acceptable and unacceptable *in vivo* behavior of drug A ER tablets, which is consistent with previous studies involving formulations with different release rates during the development of IVIVC (10).

6.4.3 Evaluating Implications of the Study Findings on Biowaiver Requirement

Four cases shown in Fig 6.1 are represented by four model ER products used in the study. Among them, only Case II (Drug B ER) and Case III (Drug C ER) comply with the biowaiver requirements stipulated in regulation from the perspective of assured product quality and performance. Case I (Isoptin SR) presents a scenario where biowaiver of proportionally similar strengths that are bioequivalent would be rejected because *in vitro* testing using multi-pH media is over-discriminating. This case would generally result in a bioequivalence study without presenting risk to patients except for unnecessary exposure of the trial subjects to the test drug and cost and resources associated with the study. However, Case IV (Drug A ER) represents a situation that could have the most serious impact on product efficacy and safety or could even cause patient harm, particularly for ER dosage forms containing drugs with narrow therapeutic index (NTI). For instance, bio-inequivalent strengths of antiepileptic products, such as, Depakote ER, Keppra XR and Tegretol XR, could lead to the increased risk of adverse events and even breakthrough seizures due to incorrect dose titration. A recent example

of Case IV was related to the withdrawal of regulatory approval in 2012 by the FDA of the 300 mg strength of Budeprion XL, a bupropion hydrochloride ER tablet. Since it was first approved in 2006, the product had been the subject of many reports of reduced efficacy when switch was made from the innovator's Wellbutrin XL 300 mg tablets. The 300 mg strength was originally approved through a biowaiver based on comparative *in vitro* study with the 150 mg strength. It was later determined to be not bioequivalent in both the rate and extent of absorption to the reference product in a study commissioned by the FDA (27). Subsequently, four other generic ER tablets of bupropion hydrochloride were subject to *in vivo* bioequivalence studies per request from the FDA because all of them were originally granted waivers of *in vivo* BE testing on the 300 mg strength (28). As a result, one additional 300 mg strength product was withdrawn from the market due to bio-inequivalence. A review of ER technologies utilized in four branded and five generic ER tablets of bupropion HCl indicates a diverse mechanisms for controlling drug release that include hydrophilic and hydrophobic matrices, reservoir system and matrix-reservoir combination. Bupropion is a weak base with pH-dependent solubility. Mechanistically, difference in S/V between the single-unit compositionally proportional strengths is likely to affect drug release from all types of ER systems employed in these products as discussed in previous section. Whether changes in drug release are manifested in the *in vitro* multimedia testing or *in vivo* absorption are primarily determined by the drug properties, formulation design, dosage form geometry and their interplays with *in vitro* test condition and *in vivo* absorption environment. This is why strength-specific formulations are required to achieve bioequivalence for certain products

while proportionally similar formulations are bioequivalent between different strengths for others.

For over two decades, guidelines issued by the leading regulatory agencies and organizations, such as FDA, EMA and World Health Organization (WHO), have been allowing biowaiver of proportionally similar lower strengths of extended-release drug products based on *in vitro* multimedia dissolution testing. The present study has shown that scientific rationale for this specific part of regulation is not sufficient. First of all, there is no known evidence that similar *in vitro* drug release obtained in the multi-pH media using standard USP apparatus has the general ability to reliably predict or assure equivalent *in vivo* performance for any type of proportionally similar ER products containing any API's, particularly for single-unit dosage forms. Additionally, for formulations containing API and rate-controlling materials of which solubility is pH-independent, multi-media dissolution testing is not different from testing in single medium because drug release profiles usually remain unchanged within biological pH range. Secondly, the *in vitro* drug release behaviors of ER dosage forms are highly dependent on characteristics of specific API, rate-controlling polymer used, delivery technology and dosage form designs as well as the interplays between these variables and the dissolution test method and conditions. Thus, possible impact of S/V change of proportionally similar ER dosage forms on product performance *in vitro* and *in vivo* should be evaluated based on the understanding of the drug substance, drug product, specific test method and condition on a case-by-case basis. To assure consistent *in vivo* performance, current regulation regarding biowaiver of proportionally similar strengths

of any ER products solely based on the *in vitro* tests should be changed. In the absence of a proven relationship between the *in vitro* and *in vivo* data, bioequivalence study should be required for approving different strengths of any monolithic ER dosage forms except for multiple-unit dosage forms where strengths differ only in the number of dosage unit.

6.5 Conclusions

Existing guidelines issued by the major regulatory bodies accept biowaiver of proportionally similar strengths of ER drug products based on matching *in vitro* release profiles generated in multimedia provided different strengths are of the same dosage form with the same release mechanism and linear pharmacokinetics. However, the relationship between *in vitro* behaviors and *in vivo* performance of ER drug products is complex and dependent highly on many variables related to drug substance, product design, test method and their interplays. There is no general link between the *in vivo* apparent drug absorption taking place in the dynamic environment of the gastrointestinal tract and *in vitro* data generated under the static condition of the standard USP dissolution apparatus. Through the investigation of *in vitro* and *in vivo* performances of four marketed ER dosage forms, this study (1) offers insight into how interplays among the API, formulation and dissolution media may affect *in vitro* behavior and its uncertain link to *in vivo* performance, and (2) shows that the current regulation that permits biowaiver of proportionally similar strengths of ER drug products had insufficient scientific evidences. Therefore, this biowaiver requirements is best to apply to multiple-unit dosage forms, such as pellets, beads or mini-tablets. For other types of ER dosage forms, careful considerations and examinations would be required; and in some particular cases, a

bioequivalence study should be required to assure product quality, efficacy and safety when there is no *in vitro in vivo* relationship available.

6.6 References for Chapter 6

1. Dutta S, Qiu Y, Samara E, Cao G, Granneman GR. Once-a-day extended-release dosage form of divalproex sodium III: Development and validation of a Level A in vitro–in vivo correlation (IVIVC). Journal of Pharmaceutical Sciences. 2005;94(9):1949-56.

2. Guidance for Industry Bioavailability and Bioequivalence Studies Submitted in NDAs or INDs —General Considerations DRAFT GUIDANCE. In: CDER, FDA, editors. 2014.

3. Guidance for Industry Bioavailability and Bioequivalence Studies for Orally Administered Drug Products — General Considerations Rev 1. In: CDER, FDA, editors. Mar 2003.

4. Yihong Qiu YC, Geoff G. Z. Zhang. Developing Solid Oral Dosage Forms: Pharmaceutical Theory and Practice: ELSEVIER; 2009.

5. Pharmacopeia US. Buffer Solutions. USP Official Monograph 36: USP Official Monigraph 36; 2013.

6. Pharmacopeia US. Divaproex Sodium Extended-Release Tablets. USP Official Monograph 362013.

7. Pharmacopeia US. Niacin Extended-Release Tablets. USP Official Monograph 36: USP Official Monigraph 36; 2013.

8. Pharmacopeia US. Verapamil Hydrochloride Extended Release Tablets. USP Official Monigraph 36; 2014.

9. Pharmacopeia US. Clarithromycin Extended-Release Tabelts. USP Official Monograph 36: USP Official Monigraph 36; 2013.

10. QIU Y, GARREN J, SAMARA E, CAO G, ABRAHAM C, CHESKIN HS, et al. Once-a-day controlled-release dosage form of divalproex sodium II: development of a predictive in vitro drug release method. Journal of Pharmaceutical Sciences. 2003;92(11):2317-25.

11. Notario GF, Palmer RN, Hom RC, Zhang J, Devcich KJ, Semla SJ, inventors; Abbott Laboratories, assignee. Extended Release Formulations of Erythromycin Derivatives. USA patent US006551616B1. 2003.

12. FDA. Niaspan Labelling Revision Letter. http://www.accessdata.fda.gov/drugsatfda_docs/label/2005/020381s020lbl.pdf2005.

13. Rocca JG, Cefali E, Zhu Y, inventors; Abbott Laboratories, assignee. LOW FLUSH NIACIN FORMULATION. USA patent US20090069275A1. 2008.

14. McEwen J, Durnin C, M.E.McMurdo, Moreland TA. Sustained-Release Verapamil: Multiple-Dose Pharmacokinetic Comparison of 120-mg and 240-mg Tablets and the Effect of Halving a 240-mg tablet. J Cardiovasc Pharmacol. 1989;13 (Suppl 4):S57-9:S57-9.

15. Abbott Laboratories L. Product Monograph: ISOPTIN SR verapamil hydrochloride sustained-release tablets 120 mg, 180 mg and 240 mg2014.

16. Erah PO, Goddard AF, Barrett DA, Shaw PN, Spiller RC. The Stability of Amoxycillin, Clarithromycin and Metronidazole in Gastric Juice: Relevance to the Treatment of Helicobacter Pylori Infection. Journal of Antimicrobial Chemotherapy. 1997;39(1):5-12.

17. Colorcon. Hydrophilic Matrix Tablets http://www.colorcon.com/products-formulation/all-products/polymers-controlled-release/hydrophilic-matrix-tablets.

18. Gao P, Fagerness PE. Diffusion in HPMC Gels. I. Determination of Drug and Water Diffusivity by Pulsed-Field-Gradient Spin-Echo NMR. Pharm Res-Dordr. 1995;12(7):955-64.

19. Ju RTC, Nixon PR, Patel MV, Tong DM. Drug release from hydrophilic matrices. 2. A mathematical model based on the polymer disentanglement concentration and the diffusion layer. Journal of Pharmaceutical Sciences. 1995;84(12):1464-77.

20. Zhou D, Law D, Reynolds J, Davis L, Smith C, Torres JL, et al. Understanding and Managing the Impact of HPMC Variability on Drug Release from Controlled Release Formulations. Journal of Pharmaceutical Sciences. 2014;103(6):1664-72.

21. Harland R, Gazzaniga A, Sangalli ME, Colombo P, Peppas N. Drug/Polymer Matrix Swelling and Dissolution. Pharm Res-Dordr. 1988;5(8):488-94.

22. Siepmann J, Peppas NA. Modeling of drug release from delivery systems based on hydroxypropyl methylcellulose (HPMC). Advanced Drug Delivery Reviews. 2001;48(2–3):139-57.

23. Chan LW, Ching AL, Liew CV, Heng PWS. Mechanistic Study on Hydration and Drug Release Behavior of Sodium Alginate Compacts. Drug Development and Industrial Pharmacy. 2007;33(6):667-76.

24. Ching AL, Liew CV, Heng PWS, Chan LW. Impact of cross-linker on alginate matrix integrity and drug release. Int J Pharmaceut. 2008;355(1–2):259-68.

25. Mandal S, Basu S, Sa B. Sustained Release of a Water-Soluble Drug from Alginate Matrix Tablets Prepared by Wet Granulation Method. Aaps Pharmscitech. 2009;10(4):1348-56.

26. Wells ML, Williams SO, Sanftleben RA, Balik SB, Evans BA. Investigation into the dissolution rate increase on storage of Wellbutrin SR 100 mg tablets. Aaps Pharmscitech. 2010;11:113-9.

27. FDA. Update: Bupropion Hydrochloride Extended-Release 300 mg Bioequivalence Studies: FDA; 2013 [updated 10-10-2013

]. Available from: http://www.fda.gov/drugs/drugsafety/postmarketdrugsafetyinformationforpatientsandproviders/ucm322161.htm.

28. FDA. FDA/CDER to Valeant Pharmaceuticals International, Inc. (Covington & Burling) - Partial Approved and Denied Docket No. FDA-2012-P-1091. http://www.regulations.gov/ - !documentDetail;D=FDA-2012-P-1091-00042013.

Chapter 7 Overall Summary and Future Directions

The extended release formulation is an important field in the pharmaceutical realm; the ER medications provide patients with improved convenience and better experiences of taking medications, whereas at the same time, the formulation became more challenging in terms of stability, reliability and safety. In this current research, we addressed issues that arise in the ER formulations, the curing for ethylcellulose and the in vitro in vivo relationship for ER tablets.

Curing of pseudolatex ethylcellulose (EC) films caused problems in stability and release profiles for extended release coated formulations, and there is an urgent need in the pharmaceutical industry to find a way so that the extent of coalescence in curing can be quantified. In **Chapter 3**, the effects of environment moisture, residual moisture temperature and time were examined during EC curing, to create various extent of coalescence for pseudolatex EC films. Based on ethanol cast EC films, it was found the ratio of two tensile properties $\frac{\mathrm{TS}}{\mathrm{YM}}$ formed a linear relationship with the films' thickness. Based on this observation, it allowed us to be able to quantify the extent of coalescence in the percentages so that provided a direct, straightforward measurement of such difficult quantity. This estimate was reliable based on the agreement with the other quantity commonly used to describe the curing process, the percent elongation at break (PEB). The water vapor permeability (WVP) across the EC dispersion films were also measured,

it was surprised to find out that the higher extent of coalescence of curing caused the films to become more permeable to water vapor.

The Near Infrared (NIR) spectroscopy was used to scan the free pseudolatex EC films, with the help of the chemometrics tools; tensile property $\frac{\mathrm{TS}}{\mathrm{YM}}$ and WVP can be accurately predicted by partial least square (PLS) linear models (**Chapter 4**). Because of these two properties is direct reflection of curing; the NIR can be model the extent of coalescence as well. Besides free films, microcrystalline cellulose (MCC) beads and a model drug was used for EC coating. The coated beads were cured at different curing conditions with respect to temperature, humidity time and coating thickness. Then the coated beads were evaluated by dynamic vapor sorption techniques to confirm the trend of WVP and revealed the same outcome. The beads were subjected to dissolution tests and by analyzing the dissolution results, a general mathematical equation was proposed for describing the curing effects on multiparticulate coating.

The fluorescence anisotropy has been extensively used to track the progress of the protein binding but has only seen extended usages in solid systems. In **Chapter 5**, the possibility of using fluorescence anisotropy as a monitoring tool has was explored with the fluorescence anisotropy spectrometer and custom made probe that was able to measure temperature and humidity in real time (Pyro Cuvette). The results was promising: using a reference benchmark material Erythrosin B demonstrated the reliability of using the experimental set up for performing solid sample monitoring. Then with fluorescence labeled DMA-DPH EC films, fluorescence anisotropy was able to detect the change

when the EC polymers started to coalescence. With the help of DSC, it further revealed the thermal event of cetyl alcohol melting in curing.

The future study regarding the curing investigation in pharmaceutical coatings still lies plenty of opportunities: the tensile property $\frac{\mathrm{TS}}{\mathrm{YM}}$ was found useful on EC dispersion systems and whether it would be applicable for other polymer system remained to be explored. The fluorescence anisotropy was demonstrated to have great potential for monitoring the thermal event in curing, it could potentially has many other applications in other solid systems.

Existing guidelines issued by the regulators in the US, Europe and WHO allows for biowaiver of proportionally similar strengths of ER drug products based on matching *in vitro* release profiles generated in multimedia provided different strengths are of the same dosage form with the same release mechanism and linear pharmacokinetics. However, the relationship between *in vitro* behaviors and *in vivo* performance of ER drug products is complex and dependent highly on many variables related to drug substance, product design, test method and their interplays. In **Chapter 6**, four drug products were tested against their proportionally similar half strength counterpart to evaluate this claim. It was found out that only two out the four products had the same outcome expected from the guidance. There is no general link between the *in vivo* apparent drug absorption taking place in the dynamic environment of the gastrointestinal tract and *in vitro* data generated under the static condition of the standard USP dissolution apparatus. Through the investigation of *in vitro* and *in vivo* performances of four marketed ER dosage forms, this

study (1) offers insight into how interplays among the API, formulation and dissolution condition may affect *in vitro* behavior and its link to *in vivo* performance, and (2) shows that the current regulation that allows biowaiver of proportionally similar strengths of ER drug products lacks a solid scientific basis. Therefore, current biowaiver requirements for proportionally similar strengths of ER drug products should be carefully considered to address this potential issue.

Chapter 8 Comprehensive List of References

1 CDER, FDA, Guidance for Industry Waiver of In Vivo Bioavailability and Bioequivalence Studies for Immediate-Release Solid Oral Dosage Forms Based on a Biopharmaceutics Classification System. 2000.

2 CDER, FDA, Guidance for Industry Bioavailability and Bioequivalence Studies for Orally Administered Drug Products — General Considerations Rev 1,. Mar 2003.

3 CDER, FDA, Guidance for Industry Bioavailability and Bioequivalence Studies Submitted in NDAs or INDs —General Considerations DRAFT GUIDANCE. 2014.

4 Anand, O., et al., Dissolution testing for generic drugs: an FDA perspective. The AAPS Journal, 2011. 13(328-335).

5 Aqueous Polymeric Coatings for Pharmaceutical Dosage Forms. 3rd ed. DRUGS AND PHARMACEUTICAL SCIENCES, ed. J.W.M. Linda A. Felton. 2008: Dekker.

6 Aqueous Polymeric Coatings for Pharmaceutical Dosage Forms. DRUGS AND PHARMACEUTICAL SCIENCES, ed. J.W. McGinity. 1997: Dekker.

7 ASTM, Standard Definitions of Terms and Symbols Relating to Molecular Spectroscopy, in Vol.14.01, Standard E131-90.

8 ASTM, Standard Test Methods for Water Vapor Transmission of Materials. 2000.

9 Belaroui, F., et al., Distribution of water-soluble and surface-active low-molecular-weight species in acrylic latex films. Journal of Colloid and Interface Science, 2003. 261(2): p. 336-348.

10 Bhattacharjya S Fau - Bhattacharjya, S. and D.E. Wurster De Fau - Wurster, Investigation of the Drug Release and Surface Morphological Properties of Film-Coated

Pellets, and Physical, Thermal and Mechanical Properties of Free Films as a Function of Various Curing Conditions. AAPS PharmSciTech, 2008. 9(2).

11 Bhattacharjya, S. and D.E. Wurster, Investigation of the drug release and surface morphological properties of film-coated pellets, and physical, thermal and mechanical properties of free films as a function of various curing conditions. AAPS PharmSciTech, 2008. 9(2): p. 449-57.

12 Binnig, G. and C.F.Quate, Atomic force microscopy. Phys Rev Lett, 1986. 56: p. 930-933.

13 Biopolymer, F. Aquacoat ECD Product Brochure. N/A.

14 Biopolymer, F., Aqueous Coating Acuacoat ECD Sustained Release Moisture Barrier Taste Masking.

15 Birkett, D.J., Generics – equal or not? Australian Prescriber 2003. 26(4): p. 85-87.

16 Bodmeier, R. and O. Paeratakul, Mechanical Properties of Dry and Wet Cellulosic and Acrylic Films Prepared from Aqueous Colloidal Polymer Dispersions Used in the Coating of Solid Dosage Forms. Pharmaceutical Research, 1994. 11(6): p. 882-888.

17 Boehm, G., et al., Development of the generic drug industry in the US after the Hatch-Waxman Act of 1984. Acta Pharmaceutica Sinica B, 2013. 3(5): p. 297-311.

18 Brereton, R.G., Chemometrics: Data Analysis for the Laboratory and Chemical Plant. 2003: John Wiley & Sons, Ltd.

19 Cappella, B. and G. Dietler, Force-distance curves by atomic force microscopy. Surface Science Reports, 1999. 34(1–3): p. 1-104.

20 Chidambaram, A. Global Generic Pharmaceutical Market - Qualitative and Quantitative Analysis. 2014.

21 Ciurczak, E.W., Pharmaceutical mixing studies using nearinfrared spectroscopy. Pharm. Technol., 1991. 15: p. 140-145.

22 Corti, P., et al., Application of NIRS to the control of pharmaceuticals identification and assay of several primary materials. Pharm. Acta Helv., 1992. 67: p. 57-61.

23 Duan, J., K. Riviere, and P. Marroum, In Vivo Bioequivalence and In Vitro Similarity Factor (f2) for Dissolution Profile Comparisons of Extended Release Formulations: How and When Do They Match? Pharmaceutical Research, 2011. 28(5): p. 1144-1156.

24 Duan, J., K. Riviere, and P. Marroum, In Vivo Bioequivalence and In Vitro Similarity Factor (f2) for Dissolution Profile Comparisons of Extended Release Formulations: How and When Do They Match? Pharmaceutical Research, 2011. 28(5): p. 1144-1156.

25 El-Hagrasy, et al., Near-infrared spectroscopy and imaging for the monitoring of powder blend homogeneity. J. Pharm. Sci., 2001. 90: p. 1298-1307.

26 FDA, PHARMACEUTICAL CGMPS FOR THE 21ST CENTURY —A RISK-BASED APPROACH. 2004.

27 Felton, L.A. and J.W. McGinity, Aqueous Polymeric Coatings for Pharmaceutical Dosage Forms. 3rd ed. DRUGS AND PHARMACEUTICAL SCIENCES, ed. J.W.M. Linda A. Felton. 2008: Dekker.

28 Felton, L.A. and M.L. Baca, Influence of Curing on the Adhesive and Thermomechanical Properties of an Applied Acrylic Polymer. Pharmaceutical Development and Technology, 2001. 6(1): p. 53-59.

29 Feng, J. and M.A. Winnik, Effect of Water on Polymer Diffusion in Latex Films. Macromolecules, 1997. 30(15): p. 4324-4331.

30 Goudy, A., et al., Atomic Force Microscopy Study of Polystyrene Latex Film Morphology: Effects of Aging and Annealing. Langmuir, 1995. 11(11): p. 4454-4459.

31 Guo, J.-H., R.E. Robertson, and G.L. Amidon, An Investigation into the Mechanical and Transport Properties of Aqueous Latex Films: A New Hypothesis for the Film-Forming Mechanism of Aqueous Dispersion System. Pharmaceutical Research, 1993. 10(3): p. 405-410.

32 Handbook of Near-Infrared Analysis. Third Edition ed. PRACTICAL SPECTROSCOPY SERIES, ed. D.A. Burns and E.W. Ciurczak. 2008: CRC Press.

33 HARMONISATION, I.C.O., PHARMACEUTICAL DEVELOPMENT Q8(R2) 2009.

34 Higuchi, T., Mechanism of sustained-action medication. Theoretical analysis of rate of release of solid drugs dispersed in solid matrices. Journal of Pharmaceutical Sciences, 1963. 52(12): p. 1145-1149.

35 HortolÀ, P., SEM examination of human erythrocytes in uncoated bloodstains on stone: use of conventional as environmental-like SEM in a soft biological tissue (and hard inorganic material). Journal of Microscopy, 2005. 218(2): p. 94-103.

36 Howland, H. and S.W. Hoag, Analysis of curing of a sustained release coating formulation by application of NIR spectroscopy to monitor changes physical–mechanical properties. International Journal of Pharmaceutics, 2013. 452(1–2): p. 82-91.

37 Howland, H., Application of NIR Spectroscopy and Fluorescence Spectroscopy for Monitoring of Curing of Sustained Release Coatings, in School of Pharmacy. 2011, University of Maryland.

38 Hutchings, D., S. Clarson, and A. Sakr, Studies of the mechanical properties of free films prepared using an ethylcellulose pseudolatex coating system. International journal of pharmaceutics, 1994. 104(3): p. 203-213.

39 IMS, Declining medicine use and costs: for better or worse? A review of the use of medicines in the United States in 2012. 2013.

40 J. Duan, K. Riviere, and P. Marroum, In Vivo Bioequivalence and In Vitro Similarity Factor (f2) for Dissolution Profile Comparisons of Extended Release Formulations: How and When Do They Match? . Pharmaceutical Research, 2011. 28(5): p. 1144-1156.

41 John.E.Hogan, Pharmaceutical Coating Technology Ch 2: Film-coating materials and their properties, ed. G. Cole. 2002.

42 Joseph Keddie and A.F. Routh, Fundamentals of Latex Film Formation: Processes and Properties. First Edition ed. 2010: Springer Laboratory.

43 Kablitz, C.D. and N.A. Urbanetz, Characterization of the film formation of the dry coating process. European journal of pharmaceutics and biopharmaceutics : official journal of Arbeitsgemeinschaft fur Pharmazeutische Verfahrenstechnik e.V, 2007. 67(2): p. 449-57.

44 Keddie, J.L., Film Formation of Latex. Materials Science and Engineering, R Reports, 1997. 21: p. 101-170.

45 Kirsch, J. and J. Drennen, Near-Infrared Spectroscopic Monitoring of the Film Coating Process. Pharmaceutical Research, 1996. 13(2): p. 234-237.

46 Kona, R., et al., Application of in-line near infrared spectroscopy and multivariate batch modeling for process monitoring in fluid bed granulation. International Journal of Pharmaceutics, 2013. 452(1–2): p. 63-72.

47 Korber, M., et al., Effect of unconventional curing conditions and storage on pellets coated with Aquacoat ECD. Drug development and industrial pharmacy, 2010. 36(2): p. 190-199.

48 Kramer, K. and S. Ebel, Application of NIR reflectance spectroscopy for the identification of pharmaceutical excipients. Anal. Chim. Acta, 2000. 420: p. 155-161.

49 Lakowicz, J.R., Principles of Fluorescence Spectroscopy. 3rd ed. 2006: Springer.

50 Lang, K.M., et al., Conducting atomic force microscopy for nanoscale tunnel barrier characterization. Review of Scientific Instruments 2004. 75(8): p. 2726–2731.

51 Lodder, R.A., M. Selby, and G.M. Hieftje, Detection of capsule tampering by near-infrared reflectance analysis. Analytical Chemistry, 1987. 59(15): p. 1921-1930.

52 Lodin, S. Reply to citizen petition: Cardizem CD. Docket no.98P-0145/PRC 1. 2000; Available from: http://www.fda.gov/ohrms/dockets/dailys/00/mar00/032300/pdn0002.pdf.

53 M.A. Katzman, Did a switch to a generic antidepressant cause relapse? Journal of Family Practice, 2008. 57(2): p. 109-114.

54 M.R., H., G.-S. I, and N. R.U., A Water-Based Coating Process for Sustained Release. Pharmaceutical Technology, 1986.

55 McKinsey&Company, A Review of the Use of Medicines in the United States: Generating value in generics: Finding the next five years of growth. 2013.

56 MEHTA, A. Animation for the Principle of Fluorescence and UV-Visible Absorbance. 2013; Available from: http://pharmaxchange.info/press/2013/03/animation-for-the-principle-of-fluorescence-and-uv-visible-absorbance/.

57 Morisseau, K. and C. Rhodes, Near-Infrared Spectroscopy as a Nondestructive Alternative to Conventional Tablet Hardness Testing. Pharmaceutical Research, 1997. 14(1): p. 108-111.

58 Notario, G.F., et al., Extended Release Formulations of Erythromycin Derivatives. 2003, Abbott Laboratories: USA.

59 Ozturk, A.G., et al., Mechanism of release from pellets coated with an ethylcellulose-based film. Journal of Controlled Release, 1990. 14(3): p. 203-213.

60 P.Ratnaparkhi, M. and P.G. Jyoti, Sustained Release Oral Drug Delivery System - An Overview. International Journal of Pharma Research & Review, 2013. 2(3).

61 Reich, G., Near-infrared spectroscopy and imaging: Basic principles and pharmaceutical applications. Advanced Drug Delivery Reviews, 2005. 57(8): p. 1109-1143.

62 Rubinstein, M. and R.H. Colby, Polymer Physics 2003.

63 Sinsheimer, J.E. and A.M. Keuhnelian, Near-infrared spectroscopy of amine salts. Journal of Pharmaceutical Sciences, 1966. 55(11): p. 1240-1244.

64 Sinsheimer, J.E. and A.M. Keuhnelian, Near-infrared spectroscopy of amine salts. Journal of Pharmaceutical Sciences, 1966. 55(11): p. 1240-1244.

65 Suzuki, E., High-resolution scanning electron microscopy of immunogold-labelled cells by the use of thin plasma coating of osmium. Journal of Microscopy, 2002. 208(3): p. 153-157.

66 Tabasi, S.H., et al., Quality by design, part II: application of NIR spectroscopy to monitor the coating process for a pharmaceutical sustained release product. Journal of pharmaceutical sciences, 2008. 97(9): p. 4052-66.

67 Tabasi, S.H., et al., Quality by design, part III: study of curing process of sustained release coated products using NIR spectroscopy. Journal of pharmaceutical sciences, 2008. 97(9): p. 4067-86.

68 Tabasi, S.H., et al., Quality by design, part III: study of curing process of sustained release coated products using NIR spectroscopy. Journal of pharmaceutical sciences, 2008. 97(9): p. 4067-86.

69 Ulmschneider, M., et al., Transferable basic library for the identification of active substances using near-infrared spectroscopy. Pharm. Ind., 2000. 62: p. 301-304.

70 Update: Bupropion Hydrochloride Extended-Release 300 mg Bioequivalence Studies. 2013; Available from: http://www.fda.gov/drugs/drugsafety/postmarketdrugsafetyinformationforpatientsandproviders/ucm322161.htm.

71 Walker, R.B., Modified-Release Drug Delivery Technology. 2nd Edition ed. Vol. 1. 2008: Informa Healthcare.

72 Weber, G., Rotational Brownian motion and polarization of the fluorescence of solutions. Adv. Protein Chem, 1953. 8: p. 415-459.

73 White, J., On-Line Moisture Detection for a Microwave Vacuum Dryer. Pharmaceutical Research, 1994. 11(5): p. 728-732.

74 Wurster, D.E., S. Bhattacharjya, and D.R. Flanagan, Effect of Curing on Water Diffusivities in Acrylate Free Films as Measured via a Sorption Technique. AAPS PharmSciTech, 2007. 8(3).

75 Yihong Qiu, Y.C., Geoff G. Z. Zhang, Developing Solid Oral Dosage Forms Pharmaceutical Theory and practice. 2009: ELSEVIER.

76 Yu, Y. and S. Gupta, Pioneering advantage in generic drug competition. International Journal of Pharmaceutical and Healthcare Marketing, 2014. 8(2).